The role of exosomes and microRNA in astrocyte-mediated HIV-1 Tat neurotoxicity

Pejman Rahimian

Submitted to the faculty of the University Of North Texas Health Science Center

In partial fulfillment of the requirements for the

Doctor of Philosophy degree

In the Department of Cell Biology and Immunology

University of North Texas Health Science Center

June 2016

Accepted by the Faculty of University of North Texas Health Science Center, in partial fulfillment of the requirements for the degree of Doctor of Philosophy

Johnny J. He, Ph.D., Chair

Doctoral Committee

June 15, 2016

Anuja Ghorpade, Ph.D.

Kunlin Jin, Ph.D.

Shaohua Yang, Ph.D.

Porunellooe Mathew, Ph.D.

ACKNOWLEDGMENTS

I would like to express my sincere gratitude to my advisor Dr. Johnny He for his excellent mentorship and training in his laboratory during my graduate career. He provided selfless support, patience, and encouragement for my continued success in the completion of my research projects.

I would also like to thank the members of my committee: Dr. Anuja Ghorpade, Dr. Kunlin Jin, and Dr. Shaohua Yang for their valuable advice and constructive criticism during my career. I also thank Dr. Porunelloor Mathew for serving as the university member on my dissertation committee.

I also would like to thank the past and present members of Dr. He's laboratory for their support and guidance.

Finally, I would like to thank my wife for her love, patience, and support during my doctoral studies.

ABSTRACT

Pejman Rahimian

The role of exosomes and microRNA in Astrocyte-mediated HIV-1 Tat neurotoxicity

Human immunodeficiency virus invades the central nervous system (CNS) soon after the initial infection, often leading to neurological complications including cognitive and motor dysfunction, which have been collectively termed HIV/neuroAIDS. The introduction of combination antiretroviral therapy in the mid-1990's led to reduced viral replication, improved immune function and increased life expectancy among HIV-infected individuals. As a result, the incidence of the most severe form of cognitive impairment due to HIV, so called HIV-associated dementia, reduced dramatically. However, the treatment regimen was not successful in protecting the patients from neuroAIDS as more discrete forms of CNS dysfunction, so-called minor cognitive motor disorders, have become more common.

HIV-1 Tat protein is an indispensable factor for successful transcription and replication of the viral genome. Aside from nucleus-bound functions, Tat is diffusely and unconventionally secreted outside of infected cells and contributes immensely to the pathology of neuroAIDS as a potent neurotoxin. The presence of Tat in the CNS despite the implementation of combination anti-retroviral therapy and the strong correlation of pathological hallmarks of neuroAIDS with continued Tat expression in CNS cells warrant a thorough understanding of the partially explained unconventional secretion mechanism(s) by Tat. Exosomal secretion of cargo has been established as an extremely

efficient pathway of glia-neuron communications and astrocytes have been shown to utilize this delivery mechanism for the provision of neurotrophic factors and danger-associated molecular patterns to neurons.

My dissertation research consisted of two parts. In the first part, we investigated the possibility of exosomal association and distribution of Tat protein from astrocytes and its delivery to neurons. We demonstrated significant presence of HIV-1 Tat in exosomes derived from Tat-expressing primary astrocytes, astrocytoma cell lines, and HIV-infected T cells. We further showed that exosome-associated Tat from Tat-expressing astrocytes was capable of causing neurite shortening and neuron death, further supporting that this new form of extracellular Tat is biologically active. Lastly, we constructed a Tat mutant deleted of its basic domain and determined the role of the basic domain in Tat trafficking into exosomes. Basic domain-deleted Tat exhibited no apparent effects on Tat trafficking into exosomes, while maintained its dominant negative function in Tat-mediated LTR transactivation. Taken together, these results show a significant fraction of Tat is secreted and present in the form of exosomes and may contribute to the stability of extracellular Tat and broaden the spectrum of its target cells.

In the second part, we investigated the mechanism of neurite shortening by Tat. Dendritic pruning and synaptic loss of neurons are the most prominent pathological hallmarks of neuroAIDS in the cART era. Although Tat has been implicated in the synaptodendritic damage to neurons, the exact mechanisms of this injury by Tat have not yet been elucidated.

Several important controllers of dendritic plasticity have been shown to be post-transcriptionally regulated by a brain-enriched microRNA, miR-132, which is abundantly expressed in the brains of the HIV-infected individuals with cognitive impairment. We found significant induction of miR-132 in both astrocytic and neuronal cell lines following Tat transfection. Tat expression in primary astrocytes from our doxycycline-inducible Tat transgenic mice (iTat) and HIV-infected primary human astrocytes also led to significant upregulation of this microRNA. We confirmed the repression of miR-132 target genes involved in the regulation of dendritic length following Tat expression. Using a basic-domain-deletion mutant of Tat we further demonstrated that Tat-induced miR-132 expression involved CREB phosphorylation. Lastly, we showed that following Tat expression in astrocytes, exosome-associated miR-132 was significantly increased and caused neurite shortening in primary mouse cortical neurons. Taken together, these results demonstrate for the first time the role of miR-132 in Tat-induced damage of the dendritic arbor.

Table of Contents

List of Figures

LIST OF ABBREVIATIONS

ARV	Antiretrovirals
AIDS	Acquired immune deficiency syndrome
ANI	Asymptomatic neurocognitive impairment
ARS	Acute retroviral syndrome
AD	Alzheimer's disease
ART	Antiretroviral therapy
BBB	Blood-brain barrier
BMVEC	Brain microvascular endothelial cells
cART	Combination antiretroviral therapy
CSF	Cerebrospinal fluid
CNS	Central nervous system
DAPI	4',6'-diamidino-2-phenylindol
DMEM	Dulbecco's modified eagle's medium
Dox	Doxycycline
ECL	Enhanced chemiluminesence
GFP	Green fluorescence protein
GFAP	Glial fibrillary acidic protein
gp120	HIV-1 glycoprotein 120
HAD	HIV-associated dementia
HAND	HIV-associated neurocognitive disorders

HIV-1	Human immunodeficiency virus type 1
HRP	Horseradish peroxidase
HTLV-I	Human T cell leukemia virus type I
HIVE	HIV encephalitis
HAART	Highly active antiretroviral therapy
IF	Immunofluorescence
IL-1β	Interleukin-1 beta
LRP	Low-density lipoprotein receptor
MS	Multiple sclerosis
MCMD	Minor cognitive and motor disorder
Nef	Negative regulatory factor
NF-κB	Nuclear factor kappa-light-chain-enhancer of activated B cells
PCR	Polymerase chain reaction
Rev	Regulator of expression of virion proteins
ROS	Reactive oxygen species
RT	Reverse transcriptase
RT	Room temperature
SDS-PAGE	Sodium dodecyl sulfate-polyacrylamide gel electrophoresis
SOC	Super optimal broth with catabolite repression
TAR	Trans-activation response
Tat	Trans-activator of transcription
TCA	Trichloroacetic acid

TNFα	Tumor necrosis factor-α
VSV-G	Vesicular stomatitis virus envelope glycoprotein
WB	Western blotting
WT	Wild type
iTat	DOX-inducible astrocyte-specific Tat transgenic mice

INTRODUCTION

1. The epidemiology of HIV/AIDS

HIV-1, a member of the lentivirus family, is the virus that causes acquired immune deficiency syndrome (AIDS), a continued global threat to public health [1-4]. HIV-1, the predominant subtype of the virus, was initially called the lymphadenopathy-associated virus (LAV) and the human T-lymphotropic virus-III (HTLV-III). This subtype causes the majority of all infections globally while the HIV-2 subtype is only limited to West Africa [5]. According to the 2015 UNAIDS report, 36.9 million people are currently living with HIV worldwide and 2 million have been newly infected since 2014. Both new infections and AIDS-related deaths however have fallen dramatically (35% and 42% respectively) compared to the data from 2004. Access to combination anti-retroviral therapy (cART) has also improved from 23% in 2010 to 41% in 2014, reflecting the reason for the rise in life expectancy of people living with the virus [6].

Four classes of compounds have been effectively used to interfere with HIV life cycle and replication; these include: nucleotide reverse transcriptase inhibitors, non-nucleotide reverse transcriptase inhibitors, protease inhibitors, and integrase inhibitors. cART incorporates at least two classes of antiretroviral drugs to successfully suppress viral replication . Unfortunately, the success of cART in improving the length and quality of the infected population's life has not translated into a viable cure for this devastating disease and the aging HIV-infected individuals experience accelerated co-morbidities of aging and significant neurocognitive impairments associated with the HIV invasion of the CNS. Until

the complete identification and removal of latent reservoirs of the virus and a reliable vaccine, HIV remains an epidemic with colossal socio-economic consequences worldwide.

2. Clinical staging of HIV/AIDS

HIV-1 infection was categorized into three stages prior to the cART era: acute, clinical latency, and AIDS. The slow and progressive destruction of CD4+ T cells represents the hallmark of progression in HIV-1 infection (**Fig. 1**) [7]. The acute phase, also termed acute retroviral syndrome (ARS) represents following 2-4 weeks after the initial exposure as flu-like symptoms which include fever, enlarged lymph nodes, sore throat, rash, muscle and joint pain, and headache [8, 9]. In the acute stage, outburst of virion production in dendritic cells and their travel to lymphoid organs leads to the infection of CD4+ T cells [10], and reduction of CCR5+ subset of memory T cells. Consequently, the infected CD4+ T cells disseminate the virus by entering the systemic circulation, leading to initial viremic burst and high numbers of viral RNA. Following viremia, the CD8+ T cell response leads to sharp reduction in viral load and increase in CD4+ T cell numbers.

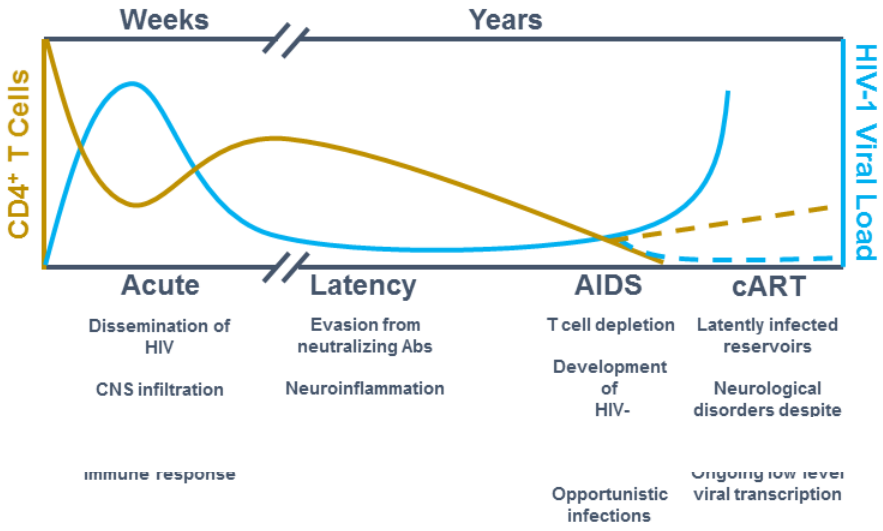
Weeks
Years
CD4+ T Cells
HIV-1 Viral Load
Acute
Latency
AIDS
cART
Dissemination of HIV
CNS infiltration
Evasion from neutralizing Abs
Neuroinflammation
T cell depletion
Development of HIV-
Opportunistic infections
Latently infected reservoirs
Neurological disorders despite
viral transcription

Figure 1. Clinical staging of HIV-1 infection. Clinical phases of HIV-1 infection is plotted as changes in $CD4^+$ T cell counts per mm^3 and plasma viral load (HIV RNA copies per ml in the plasma) against the duration of time after exposure. Clinical stages and their representative hallmarks are indicated at the bottom. Adapted from Maartens, G et al. 2014 [9].

[11]. This brings about the next stage of the disease which is the clinical latency phase. This period can last from 2 to over 20 years and bears minimum to no symptoms. Viral load measurements in this stage remain low or undetectable while CD4+ T cell numbers drop gradually [12]. cART has made it possible for patients to remain within the clinical latency phase for decades. Once CD4+ T cell depletion reaches to counts lower than 200 cells/mm3, the dramatic compromise in cellular immunity breaks the wall of protection against opportunistic infection and at this stage, progression to AIDS has been established [18].

3. Invasion of the CNS by HIV-1

3.1. HIV-1 entry into CNS

HIV-1 invades the CNS in the early phase following the systemic exposure [13]. In general, four different mechanisms have been proposed for virus entry into the CNS environment (**Fig. 2**) [14]. These include Trojan horse hypothesis, transcytosis of endothelial cells, infection of endothelial cells, and cell-free virus entry. Trojan horse hypothesis (**Fig. 2A-1**) is the most commonly accepted model which explains HIV-1 entry into the CNS through infiltration of virus-infected immune cells such as CD4+ T cells, monocytes and macrophages from systemic circulation [14-16]. This method of entry has been observed in other retroviruses including feline immunodeficiency virus (FIV), simian immunodeficiency virus (SIV) and human T cell leukemia virus type I (HTLV-I) [16]. Autopsy brain samples from AIDS patient and SIV-infected rhesus macaques has also shown the infiltration and accumulation both CD4+ and CD8+ T cells [17, 18]. Additional

enforcing evidence for this hypothesis comes from the fact that viral proteins of HIV-1 induce the secretion of cytokines and chemokines, which invite even greater numbers of immune cells into the CNS and facilitate HIV-1 traffic through the BBB [19]. The blood-brain barrier is composed of brain microvascular endothelial cells (BMVEC) connected to one another through tight junctions, pericytes located in the basal membrane of blood vessels, and the surrounding astrocytes which extend their projections to endothelial cells [20, 21]. Transcytosis is defined by endocytosis of HIV-1 into the BMVEC and its shuttling through this layer of cells, followed by releasing of the virions on the CNS side of BBB [14]. (**Fig. 2A-2**).

Direct infection of BMVEC (**Fig. 2A-3**) has also been proposed as a mechanism of HIV-1 entry into the CNS. This model of entry suggests that the impairment of tight junctions between BMVEC as a result of viral protein production and the ensuing induction of pro-inflammatory cytokines such as tumor necrosis factor-α (TNFα) and interleukin-1 β (IL-1β) leads to the disruption of BBB and dissemination of the free virions (**Fig. 2A-4**) into the CNS. Proteins of the virus such as Tat and gp120 are mainly responsible for the pro-inflammatory responses and activation of BMVEC [22], and the consequent apoptosis of BMVEC causes the impairment in tight junctions [23-25].

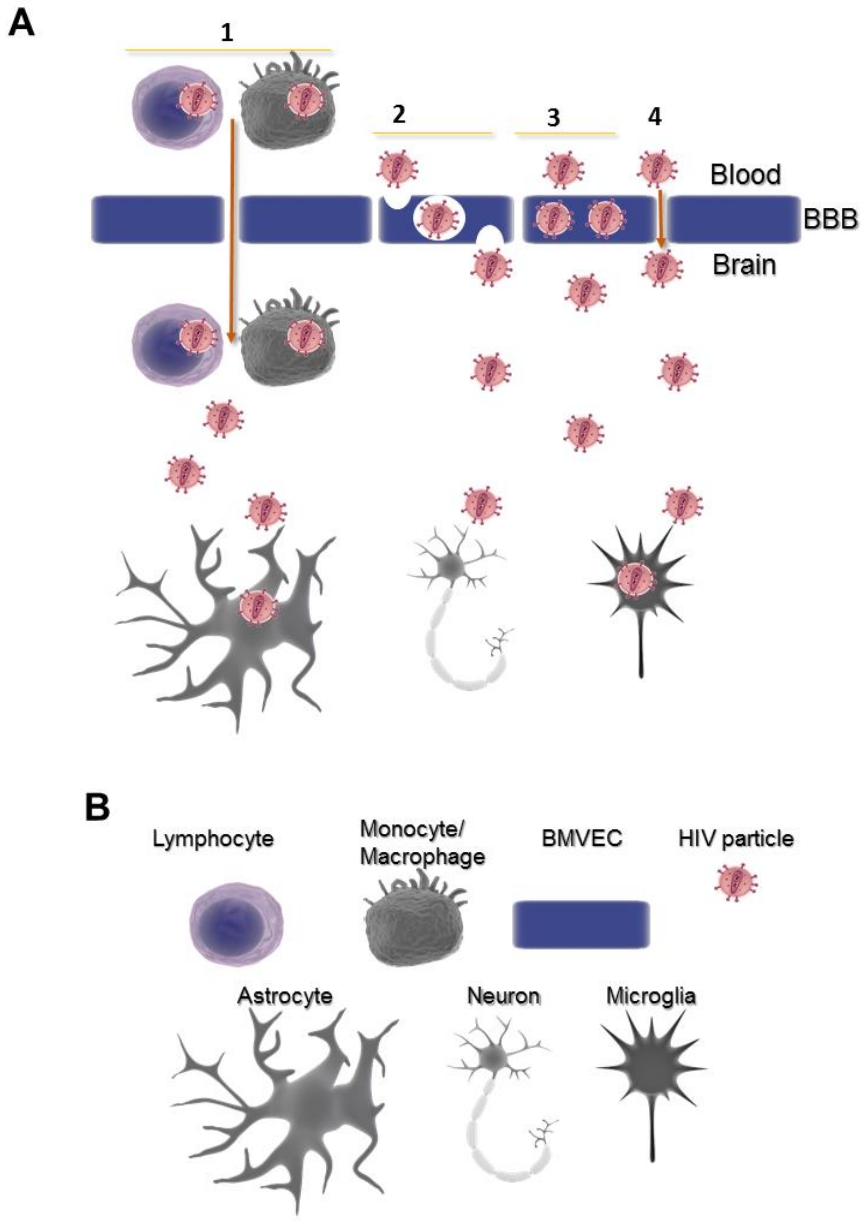
A
1
2
3
4
Blood
BBB
Brain
B
Lymphocyte
Monocyte/
Macrophage
BMVEC
HIV particle
Astrocyte
Neuron
Microglia

Figure 2. Proposed mechanisms of HIV-1 entry into the CNS. **A.** Depiction of common hypotheses of HIV-1 entry to the CNS. **1**. Trojan horse hypothesis: HIV-1 is crosses into the CNS by infiltrated HIV-infected lymphocytes, monocytes, and macrophages. **2**. Transcytosis: HIV-1 endocytosis and shuttling across endothelial cells. **3**. Direct infection of endothelial cells. **4**. Cell-free virus entry. **B.** Key

3.2 Infection of the CNS cells by HIV-1

Following CNS entry through a combination of the described mechanisms, HIV-1 infects microglia and astrocytes. Microglia are brain-resident macrophages which are differentiated from monocytes and migrate from bone marrow into the brain [26, 27]. Comprising about 15% of all cells in the brain, microglia serve as scavengers and antigen presenting cells with the potential to contribute to the pro-inflammatory response [28, 29]. Microglia are susceptible to HIV-1 infection because they express the CD4 receptor and one of the co-receptors, CCR5 or CXCR4 [30]. Susceptibility and permissiveness of microglia to HIV-1 has been demonstrated in vivo and in vitro, as Env and p24 are readily detected in microglia isolated from HIV-infected patients, and primary human microglia can be productively infected using M- and X-tropic strains of HIV-1 in culture [31]. Microglia play a crucial role in the HIV-1 invasion of the CNS since they are the main targets which productively support the viral replication, and activate neuroinflammatory cascades that substantially contribute to neuroAIDS pathology.

Astrocytes are the most abundant cell population in the CNS which are not only responsible for making up the BBB from their processes, but they also maintain homeostatic balance of other cell types. Although astrocytes do not support productive HIV-1 infection, components of the virus including proviral DNA, RNA and viral proteins such as Tat and Nef are readily detected in these cells [32]. In fact, about 19% of astrocytes have been reported to contain HIV-1 RNA in brain tissue from HIV-infected individuals [33]. Unlike microglia, astrocytes are susceptible but not permissive to HIV-1 infection. Their

susceptibility is mostly towards the T-tropic HIV-1 and is independent of chemokine receptors. Following infection, the production of viral structural gene products has been shown to be limited to a low or undetectable levels [34]. However, astrocytes express copious amounts of early, non-structural gene products such as Tat, Nef and Rev [34, 35]. Even in latently infected astrocytes, a low level of transcription of the provirus is evident since HIV-1 Tat protein is readily detected [36, 37].

The restrictive nature of infection in astrocytes has been explained in the context of viral entry blockage and post-entry restrictions at multiple steps in HIV life cycle. Astrocytes do not possess surface CD4 receptors and are therefore infected through the CD4-independent receptor-mediated endocytosis pathway characterized by binding of the virus to the human mannose receptors (hMR) [38, 39]. The efficiency of this cell-free virus infection of astrocytes has been proven extremely low. The expression of Nef has been described as one of the mechanisms of restricted astrocyte infection following entry. As the negative regulator of replication, Nef reduces LTR activity in astrocytes and contributes to the restricted virus production in astrocytes [40]. The Rev protein has been pointed out as another culprit since an abnormal accumulation of this protein has been documented in the cytoplasm of infected astrocytes which could lead to the blockage of viral mRNA export [41]. Previous studies from our laboratory indicate impairment of Rev function in astrocytes due to low constitutive expression of Sam68, an important cellular co-factor of Rev in these cells [42].The most convincing evidence on lack of new virion production in HIV-1 infected astrocytes however comes from epigenetic studies of astrocytes.

Accumulative evidence suggests that astrocytes serve as latent CNS reservoirs for HIV-1 and that reactivation of viral replication from latency is possible through stimulation of infected astrocytes with NF-κB, TNF-α and IL-1β [14]. This reactivation is also documented in co-culture experiments of actively infected monocytes and lymphocytes with latently infected astrocytes [34]. Evidence from blips in CNS-compartmentalized HIV replication also provide evidence that the source of the latent virus in the CNS is not from myeloid or lymphoid lineage [43]. Data from epigenetic investigation of HIV-1 latency in astrocytes has shown that class I histone deacetylases and lysine specific histone methyltransferases are responsible for the silencing of HIV-1 replication in astrocytes [44].

Other cell types in the CNS such as neurons, neuron progenitor cells, oligodendrocytes, and endothelial cells do not actively support HIV-1 infection. However, these cells are substantially affected by HIV-1 infection of microglia and astrocytes and this indirect negative impact of infection contributes significantly to the pathogenesis of neuroAIDS [14]. The source of this indirect damage is comprised of secreted viral proteins and cytokines produced by infected glial cells which dysregulates the functions of these uninfected cells or leads to injury and death [24, 45].

4. HIV/NeuroAIDS

4.1 Epidemiology of neuroAIDS

Following early HIV-1 invasion into the CNS [46], the direct and indirect consequences of viral infection lead to neurological symptoms that range from motor and cognitive dysfunctions and are collectively called neuroAIDS [47]. The specific neurological disorders associated with HIV/neuroAIDS are termed HIV-associated neurocognitive disorders (HAND), which are categorized into asymptomatic neurocognitive impairment (ANI), mild cognitive-motor disorders (MCMD), and the most sever but rare form, HIV-associated dementia (HAD) [48, 49]. In the pre-cART era, HAD was a common complication of AIDS which affected approximately 25% of the infected individuals [50]. The introduction of cART in 1996 suppressed systemic viral replication and improved the immune function. Interestingly the incidence of HAD also diminished substantially mainly due to the decreased burden of infected peripheral cells infiltrating the CNS. As a result, the life expectancy of infected individuals improved dramatically, to the extent that more than half of the HIV-infected population in the U.S is over 50 years of age [49]. Despite cART's success in shifting the consequence of HIV-1 infection from a death sentence to a chronic, manageable disease, HIV-associated neurological diseases, particularly MCMD not only did not subside, but became more prevalent [13]. Currently, greater than 50% of the individuals living with HIV-1 show some form of the HAND. Asymptomatic and mild cognitive impairment each comprise about 25% of cases and HAD has remained at about 2% of all cases [51, 52]. cART has not been able to completely prevent or reverse

neuroAIDS, and thus new approaches for the treatment of neuroAIDS and ultimately removal of the CNS reservoir are urgently needed [5].

4.2 CNS pathology in neuroAIDS

CNS infection by HIV-1 brings about clinical neurological symptoms that include impaired learning and memory, diminished focus, lethargy, slowing of locomotor activity, depression, personality disorder, and behavioral/mood problems [53]. In the initial phase of infection, pathology associated with the virus include gliosis, activation of microglia, and mild axonal damage [54, 55]. Concomitant with progress to the symptomatic stage of disease, the most significant pathologies include emergence of HIV encephalitis (HIVE), opportunistic infections, widespread reactive astrocytosis, cerebral atrophy, myelin pallor, microglial nodules, activated resident microglia, multinucleated giant cells, neuronal damage, and loss of BBB integrity [56, 57].

In the post-cART era, the most prominent hallmark of HIV-1 pathology in the CNS is synaptodendritic damage. Injury of the dendritic arbor strongly and positively correlates with worsening of cognitive status in neuroAIDS [58] and with HIV-1 burden in the CNS tissue [59]. In fact, synaptodendritic damage is considered the major source of impairment in cognitive status of HIV-affected individuals as opposed to neuronal loss [59-61]. Synaptic loss has been described in the context of neuroinflammation associated with HIV-1 invasion of the CNS [62, 63]. HIV-1 Tat protein alone is capable of reducing synaptic

protein levels [64-66] and dendritic arbor [1, 67, 68]. However, the exact molecular details of Tat's effect on dendritic degeneration have not been elucidated.

4.3 Mechanisms of neuroAIDS pathogenesis

Neurons are most severely affected in the CNS invasion of HIV-1, yet they are not directly infected by the virus. As discussed in previous sections, macrophages, microglia, and to a lesser extent, astrocytes are primary cell targets for HIV infection in the CNS [39, 69-72]. Therefore, indirect mechanisms of pathogenesis have been proposed for HIV/neuroAIDS. These mechanisms are mainly categorized into three groups: improper immune activation of macrophages and microglia, release of viral and host soluble factors from infected cells, and dysfunction of astrocytes. Although all three of the proposed mechanisms may potentially be involved in the pathogenesis of HIV/neuroAIDS, the driving force behind the progressing of neuroAIDS is considered to be the activation of macrophages and microglia, since it facilitates the migration of other immune cells form the periphery into the CNS [73]. Activation of microglia induces neuronal damage due to the release of potentially neurotoxic levels of oxidative radicals, nitric oxide and/or the cytokines, such as TNF-α and IL-1 [74-76]. On the other hand, soluble viral proteins, such as gp120 and Tat have been shown be able to directly damage the BBB, lead to inflammation, induce oxidative stress, impact intracellular Ca2+ homeostasis, and cause neurotoxicity [77-80].

Dysfunction of astrocytes due to reactive astrocytosis leads to the disruption of homeostasis in the CNS. Especially, astrocytosis leads to failure in uptake of toxic levels of glutamate, the major excitatory neurotransmitter [81, 82]. Astrocytosis also induces a pro-

inflammatory profile in astrocytes characterized by the expression of cytokines and chemokines such as MCP-1, IL-1β, IL-6, RANTES, and CXCL10 [83-86]. This inflammatory phenotype in turn leads to the recruitment of more monocytes, macrophages, and lymphocytes into the CNS. Astrocyte dysfunction also leads to the disruption of BBB and results in vulnerability of the CNS to opportunistic infections [87, 88].

5. HIV-1 Tat protein

The HIV-1 genome is about 9.7 kb in length and its proviral DNA consists of two regulatory regions called the long terminal repeat (LTR) flanking at both sides of the HIV-1 coding region [89-91]. The LTR contains the U3, R and U5 regions, which are essential for the binding of cellular transcription factors, transactivator of transcription (Tat)-mediated transactivation, and proviral DNA integration [92-94]. The RNA genome of HIV-1 consists of 9 open reading frames which give rise to 15 proteins. Six of these proteins are non-structural and are called accessory proteins [95, 96] (**Fig. 3**) HIV-1 Tat (Trans-Activator of Transcription) is one of the accessory proteins encoded by the tat gene, which consists of 2 exons: the first exon encodes 72 amino acids, and the second one encodes an additional 14 to 31 amino acids depending on the viral strain [97]. The primary function of HIV-1 Tat is to promote HIV-1 transcription via transactivation of the HIV-1 LTR. In HIV transcription, Tat first binds to cyclin T1 and recruits cyclin T1/CDK9 complex termed positive transcription elongation factor b (P-TEFb) to the HIV- 1 LTR promoter [98-100], a process that requires binding of Tat to the TAR RNA bulge and of cyclin T1 to

the TAR loop. The cyclin T1-associated CDK9 kinase then phosphorylates the C-terminal domain of RNA polymerase II (Pol II), leading to a critical transition of Pol II from a non-processive state to a processive state and hence transcription of HIV genome and synthesis of full-length HIV RNA transcripts. A number of cellular factors have been identified to interact with Tat and regulate HIV- 1 replication [101-106].

Examination of Tat primary amino acid sequence reveals five distinct domains (**Fig. 4**) [107-109]: N-terminal activation domain which is also known as acidic domain (aa 1-20), central cysteine-rich domain (aa 21-37) which contains seven cysteines that are highly conserved between different isolates of HIV-1. Mutations in six of the seven cysteines abolish Tat function completely [110, 111], core domain for Tat binding to TAR RNA (aa 38-48), basic domain contains a basic RKKRRQRRR motif and is essential for nuclear localization, TAR binding, and transactivation (aa 49-57). Mutations in the basic domain lead to abolishment of Tat induced LTR transactivation [112-114]. C-terminal domain of Tat contains a highly conserved tripeptide sequence Arg-Gly-Asp, known as an RDG sequence, which has been found important for Tat binding to cell surface via integrin-mediated cell adhesion [115, 116]. Tat, not only plays important roles in productive HIV-1 replication, but also acts as a major pathogenic factor in HIV-1 associated pathogenesis [117].

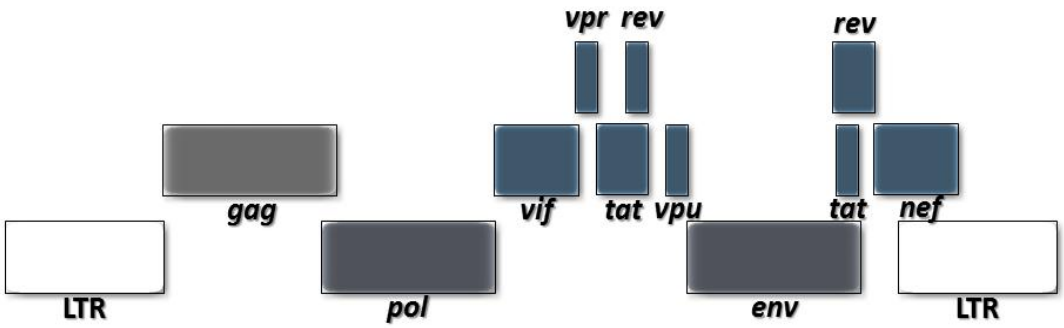
vpr
rev
rev
gag
vif
tat
vpu
tat
nef
LTR
pol
env
LTR

Figure 3. Genomic organization of HIV-1. HIV-1 provirus is composed of three structural genes including *gag*, *pol*, *env* flanked by two LTR promoters. HIV-1 contains 6 unique accessory genes that include *tat, rev, nef, vif, vpr, vpu*.

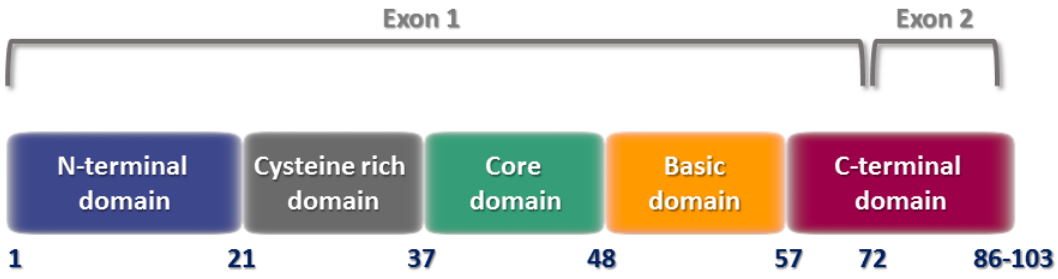
Exon 1
Exon 2
N-terminal domain
Cysteine rich domain
Core domain
Basic domain
C-terminal domain
1
21
37
48
57
72
86-103

Figure 4. Structural domains of HIV-1 Tat protein. Tat consists of five essential domains: N-terminal domain, cysteine-rich domain, core domain, basic domain and C-terminal domain. The ordered number of amino acids comprising each domain has been labeled at the bottom.

5.1 Tat protein secretion and uptake

In addition to being a transcriptional regulator of HIV-1 replication, intact and biologically active HIV-1 Tat secretes out of HIV-infected cells [118, 119] and Tat-expressing cells [120-127]. A substantial amount of Tat protein (0.1-10 ng/ml) is detected in the serum of HIV positive individuals [118]. Tat's exit from cells does not rely on cell apoptosis [118, 121]. However, Tat can be released from cells via cell death and turnover of the HIV-infected cells [128]. Antibodies that specifically bind Tat have been found to effectively inhibit viral replication in cultures, pointing to the functional integrity of secreted Tat protein [129]. Several studies including ours have demonstrated that Tat protein can be taken up by cells in culture and lead to transactivation of HIV LTR. [130-132]. Peptides of Tat have been utilized to successfully deliver protein cargo inside cell targets [133-136] and basic peptides have been found to enhance Tat protein internalization [131, 134, 135]. The fact that Tat is a basic protein and contains strongly basic domains could possibly explain non-discriminative Tat uptake into cells. It is shown that the basic domain of Tat is critical for Tat protein transportation. It not only allows Tat traffic though the plasma membrane, but also facilitates other proteins to be delivered into cells [133, 135]. This feature of the basic domain is explained through local invagination of the plasma membrane, caused by ionic interactions between the side chains of Tat basic domain and the negative charged phospholipid head of the membrane, leading to the reorganization of lipid bilayer and the penetration of the Tat basic domain into the membrane [135, 137]. We have previously demonstrated that Tat can enter neurons by specifically interacting with the lipoprotein receptor (LRP) on these cells and lead to the disruption of metabolic balance

of LRP ligands and suggests the adverse impact of Tat in HIV-associated neurodegenerative disease [132]. HIV-1 Tat secretion occurs through unconventional secretory pathways since the gene encoding Tat does not contain a signal sequence [121, 122, 138]. Such alternative secretory pathways have been documented for other growth factors, such as interleukin-1β and basic epidermal growth factor [122].

A number of functions have been proposed for extracellular Tat protein, resulting from transactivation of either LTR or cellular genes following direct Tat uptake, or as a consequence of intracellular signaling induced following the interaction of Tat with cell surface receptors. These include activated production and expression of growth factors [139] and cytokines [140-142] and of cytokine receptors [143-145], stimulation of cell proliferation and migration [146, 147] and protease production, chemoattractant activity of monocytes [148, 149], and angiogenic activity [150-154]. Extracellular Tat also transforms and immortalizes keratinocytes in cultures [155]. Extracellular Tat induces apoptosis in peripheral blood mononuclear cells [156] which indicates Tat's involvement in the depletion of CD4+ T cells and progression to AIDS. Extracellular Tat has also been implicated in the initial outburst of HIV-1 replication [157], and for increased HIV-1 gene expression in glial cells through induction of cell arrest at G1 phase [158]. Finally, extracellular Tat represses the transcription of the MHC class I gene and negatively affects the immune system [159, 160], human mannose receptor [161], and interleukin-12 [162]. Tat has been shown to activate expression of the murine cytomegalovirus promoter [163] and the JC virus [164-166], suggesting that Tat can alter the replication of other viruses,

probably through interaction with upstream enhancer elements. Thus these findings support the important role of extracellular Tat in the progression of HIV/AIDS, and different HIV-associated pathologies including HIV-associated neurocognitive diseases.

5.2 The role of Tat in HIV/neuroAIDS

Tat is readily detected in the CNS of patients with HIV-associated dementia [167] deriving from HIV-infected-microglia and astrocytes or HIV-infected monocytes, macrophages and infiltrated CD4+ T lymphocytes [79, 121, 168, 169]. There is a strongly positive correlation between CNS Tat levels and HIV-associated cognitive impairments [167, 170]. Tat induces direct toxicity to neurons [171-173]. Direct Tat exposure alters integrity, homeostasis, neuroexcitatory property, endoplasmic reticulum calcium load, and oxidative state in neurons [171-176]. Minute amounts of extracellular Tat, ranging from 1 μM to 0.1 mM is sufficient to cause acute loss of neuronal integrity and excitotoxicity [177-179]. Studies from the transgenic mouse model created in our laboratory have established that neuropathologies associated with induction of Tat expression in the brain are identical to those noted in the brain of AIDS patients [1]. It has also been reported that intracerebral injection of the basic domain of Tat leads to neuronal loss, inflammation, and reactive astrocytosis [180]. Aside from causing acute neurotoxicity, Tat is also considered to be the major pathogenic factor in neuroAIDS due to indirect interactions with other cells in the CNS such as astrocytes, microglia, and BMVEC which lead to their dysfunction or over-activation [181-183].

5.2.1 Tat effects on astrocytes

Astrocytes have crucial roles in the maintenance of CNS homeostasis and neuronal integrity and their dysregulation has been observed in the process of several neuropathological conditions. In the context of HIV-1 CNS invasion, astrocytes have been shown to be significant contributors to pathology by changing the CNS environment: astrocytosis leads to dysregulation in glutamate metabolism and uptake [184-187], production of pro-inflammatory cytokines and chemokines and subsequent attraction of immune cells into the CNS, and facilitation of virus spread to other CNS cells [188, 189].

Reactive astrocytosis is one of the hallmarks of neuroAIDS and defined as the increase in the number and size of astrocytes along with amplified expression of glial fibrillary acidic protein (GFAP) [184, 190]. GFAP is a cellular marker of astrocytes whose expression is developmentally and pathophysiologically regulated [191, 192]. GFAP forms extensive networks that maintain mechanical strength and shape of astrocytes and provide dynamic platforms for the organization of the cytoplasm at a structural and functional level [193, 194]. This important structural protein is involved in astrocyte volume regulation [195], glial scar formation [196], and anchoring glutamate transporters to the plasma membrane to facilitate neurotransmitter recycling [197]. Besides, GFAP has important roles in glia-neuron interactions and CNS morphogenesis [198, 199]. Recent findings suggest GFAP involvement in the long-term maintenance of brain architecture, proper functioning of the BBB, and modulation of neuronal functions [198, 200, 201]. Several studies including ours have demonstrated that HIV-1 Tat alone is sufficient to lead to astrocytosis and up-

regulation of GFAP, which result in astrocytes-mediated neurotoxicity [202-206]. We have shown that Tat-induced GFAP upregulation plays an essential role in astrocyte-mediated Tat neurotoxicity [206]. Our unpublished results have also shown that the accumulation and aggregation of GFAP by Tat leads to unfolded protein response (UPR) and endoplasmic reticulum stress (ERS), which in turn causes lysosomal exocytosis and comprised neuronal integrity and survival. This process is abolished when GFAP is completely knocked out. These findings support the notion that astrocytes play important roles in Tat-induced neurotoxicity and HIV/neuroAIDS.

5.2.2 Tat effects on microglia

Microglia are brain-resident macrophages with significant roles in the pathophysiology of HIV-1 infection. Macrophages and microglia both support viral replication and are capable of affecting other cells in the CNS. Following infection and activation, these cells secrete high levels of cytokines and bioactive metabolites, such as TNF-α, matrix metalloproteinase (MMP), platelet activating factor (PAF), and arachidonic acid [207-210]. TNF-α and PAF are elevated in the central nervous system of patients with HAD and have been shown to contribute to neuronal apoptosis in glutamate mediated excitotoxicity [211, 212]. MMP is detected in the CSF of HIV-infected individuals and its presence is associated with increased CSF white blood cell count and elevated CSF-to-serum albumin ratio, which is considered as the marker of BBB leakage [213, 214].

5.2.3 Tat effects on BMVEC

BMVEC, similar to astrocytes, are a major component of BBB and therefore important for the preservation of the BBB integrity. Treatment of BMVEC in culture with HIV-1 Tat leads to the release of nitric oxide (NO) which in turn induces signaling for apoptosis in thymocytes [24]. Tat protein also increases the permeability of BMVEC by decreasing the production of occludin via MMP [215]. Tight junctions are critical structural and functional elements that secure BMVEC layers in the BBB. Tat expression in BMVEC, both in vitro and in vivo, alters the expression of claudin-5, one of the most important components of tight junction, suggesting Tat's disturbance of the BBB integrity which contributes to increase in trafficking of immune cells and HIV into the brain [216]. In addition, Tat increases intracellular reactive oxygen species (ROS) levels, which in turn phosphorylates the VE-cadherin complex and increases the BMVECs permeability [217].

5.2.4 Tat effects on cytokine and chemokine expression

Tat promotes the secretion of cytokines and chemokines from astrocytes, microglia, and infiltrated immune cells in the CNS [218, 219]. These include: TNF-α, TGF-β, MCP-1, IL-1β, IL-6, RANTES, and CXCL10 [83-86]. Tat induction of TNF-α causes apoptosis in neuronal cells [220]. Another toxic effect of TNF-α is due in part to its ability to inhibit glutamate uptake by astrocytes, leading to excitotoxicity of neurons [221]. Induction of IL-6 by Tat increases GFAP transactivation, leading to astrocytosis [222, 223]. Tat leads to a dramatic expression of MCP-1 which is reflected by accumulation of this chemokine in the CSF and positively correlates with the severity of cognitive impairments in patients with

HIV encephalitis [83]. MCP-1 also increases the permeability of the BBB and facilitates the transmigration of monocytes across the BBB [224]. CXCL10 overexpression has been observed in several neurodegenerative diseases including multiple sclerosis (MS), Parkinson's disease (PD), Alzheimer's disease (AD), and HIV-associated dementia, and can lead to neuronal apoptosis by elevating intracellular calcium levels [225-227].

5.2.5 Tat and oxidative stress

Oxidative stress is defined as a shift in the REDOX system towards the production of damaging oxidative moieties which cannot be neutralized efficiently by anti-oxidant mechanisms. This imbalance is modulated by various kinds of ROS, which lead to the oxidation of proteins and DNA, and peroxidation of lipids [228]. Signs of oxidative stress can be detected in the brain and the CSF of HIV patients. For instance, peroxidation products are predominantly found in neurons, glia, and BMVEC in the brain of patients with HIV encephalitis and macaques with SIV encephalitis [229]. Proteins of HIV-1 including gp120 and Tat are implicated in the induction of oxidative stress during infection of the brain [230]. Tat direct interaction with neuronal receptors stimulates the production of ROS and triggers the oxidative stress-dependent apoptotic cascades [175]. Striatal injections of Tat have also shown to cause elevation in protein and lipid peroxidation [231]. In addition, Tat induction of free radical synthase and pro-oxidant production, such as nitric oxide (NO), is potentially toxic to other types in the CNS [232].

6. Exosomes and their role in HIV-1 infection

6.1 Extracellular vesicles

Extracellular vesicles (EVs) are organelles secreted by both prokaryotic and eukaryotic cells. They were first identified under the electron microscope (EM) in the biofluids and cell cultures, and initially considered to be experimental artifacts from damaged neighboring cells before their specific biogenesis mechanisms and distinct functions were discovered [233, 234]. EVs are classified into several different types according to their size and origin: 1) Exosomes: vesicles of 50-150 nm in diameter with endocytic-multivesicular body (MVB) origin. 2) Ectosomes: also called shedding micro-vesicles (SMV), 50-1000 nm in diameter and directly bud from plasma membrane. 3) Apoptotic bodies: 50-5000 nm in diameter, generated by dying cells during apoptosis [235]. Each of these vesicles has distinct cargo profiles and carries out different functions in a given biological process.

6.2 Biogenesis and function of exosomes

Exosomes are bi-layered extracellular vesicles with a size range of 50-150 nm and constitutively secreted by many cells and carry significant RNA and protein cargos and serve as intercellular messengers to regulate physiological and pathophysiological processes in target cells [236-238]. They are generated by inward budding of the MVB membrane, formation of intraluminal vesicles, fusion of the MVB membrane with the plasma membrane, and release of the intraluminal vesicles from MVB into the extracellular environment [239]. The intraluminal vesicles in the MVB could be formed by endosomal

sorting complex required for transport (ESCRT)-dependent pathway and ceramide-dependent pathway [240]. The ESCRT-dependent pathway involves the sorting of monoubiquitinated cargos on the MVB membrane and the packaging of cargos into the vesicles [241]. The ceramide-dependent pathway mostly relies on lipids such as ceramide to induce inward vesicle budding of the MVB membrane and lipid raft formation [242, 243] (**Fig. 5**). Thus, exosomes derived from those two pathways can by identified by specific markers: TSG101 for exosomes from ESCRT pathway [241, 244], GM1, CD63 and AchE for lipid raft-rich exosomes from ceramide pathway [243, 245-251].

Many proteins universally found in exosomes produced by various cell types are commonly used as exosome markers, including integrins and tetraspanins (CD9, CD63, CD81 and CD82), heat shock proteins (HSP70), proteins involved in MVB biogenesis (TSG101 and Alix) and proteins involved in membrane transportation and fusion (Rab GTPases, annexins, flotillins) [252-254]. Besides the universal markers listed above, exosomes are documented to associate with over 4400 different proteins and over 1500 mRNAs and 700 miRNAs [255]. This number is rapidly growing and these special features of exosomes have made them potent vehicles for intercellular substance exchange and signal transduction.

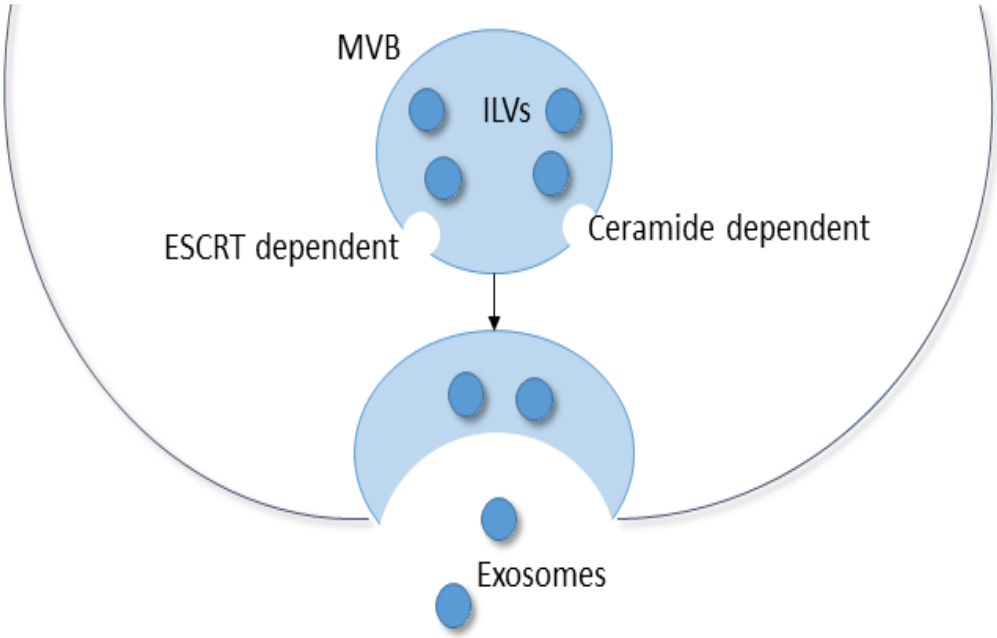
MVB
ILVs
ESCRT dependent
Ceramide dependent
Exosomes

Figure 5. Exosome biogenesis and release. Illustration of general exosome biogenesis and release process. Sorting of cargo and internal budding of MVB membrane occurs through two mechanisms: ESCRT-dependent and Ceramide-dependent. The MVB membrane invagination creates ILVs. Fusion of MVB membrane with plasma membrane will release ILV content which are now called exosomes

6.3 Exosomes in HIV-1 infection

Exosomes are involved in intercellular protein and RNA transportation. They share similarities in size and biogenesis with many enveloped viruses which make them perfect vehicles for virus and viral product transmission. Viral proteins and nucleic acids and intact viruses have been shown to be present in exosomes from infected cells. In fact, several pathogens are found to be capable of hijacking exosomes for spreading their own infectious agents including herpes simplex virus (HSV) and hepatitis C virus (HCV) [256-261]. In case of HIV, the intact virus, Gag protein, unspliced HIV-1 RNA, and HIV-derived microRNA have been detected in exosomes from HIV-infected cells [262-265]. Thus, exosomes from HIV-infected cells could contribute to transmission of the virus or work as a mechanism of defense against the virus. Although HIV-1 was detected in purified exosomes in many early studies, whether HIV-1 is incorporated into exosomes is still remaining controversial due to the technology limitations in exosome purification and exosome-virus separation [266]. Some recent studies have successfully separated HIV-1 from exosomes using new advanced methods, which remain to be further validated [267].

7. MicroRNA and HIV-1 infection

7.1 MicroRNA biogenesis

MicroRNA (miRNA) are small, non-coding RNA which function in silencing mRNA and are involved in virtually all physiological and pathological processes of life [268]. They are 18-22 nucleotides long and are transcribed by RNA polymerase II in the nucleus as

primary miRNA (Pri-miRNA). Following capping and poly-adenylation steps, they are processed and trimmed by the RNase III enzyme Drosha into pre-miRNAs. These structure are then transported to the cytoplasm by Exportin 5 and processed by another RNase III called Dicer to produce a double stranded miRNA duplex. The duplex becomes associated with Argonaut (AGO) proteins, unwinds, and one of the strands gets loaded into the RNA-induced silencing complex (RISC). Once in the RISC complex, the mature strand works as a guide RNA to recognize the mRNA target and bind its 3' UTR region via base-pairing [269]. Nucleotides 2-6 (seed region) of the majority of miRNA pair with the 3' UTR imperfectly and lead to the translational repression of target mRNA via a complex and incompletely understood mechanism. A perfect base-pairing between the seed region of miRNA and 3' UTR of mRNA will lead to degradation of the target mRNA which is the mechanism of siRNA silencing in plants and synthetic siRNA methodologies (**Fig. 6**)

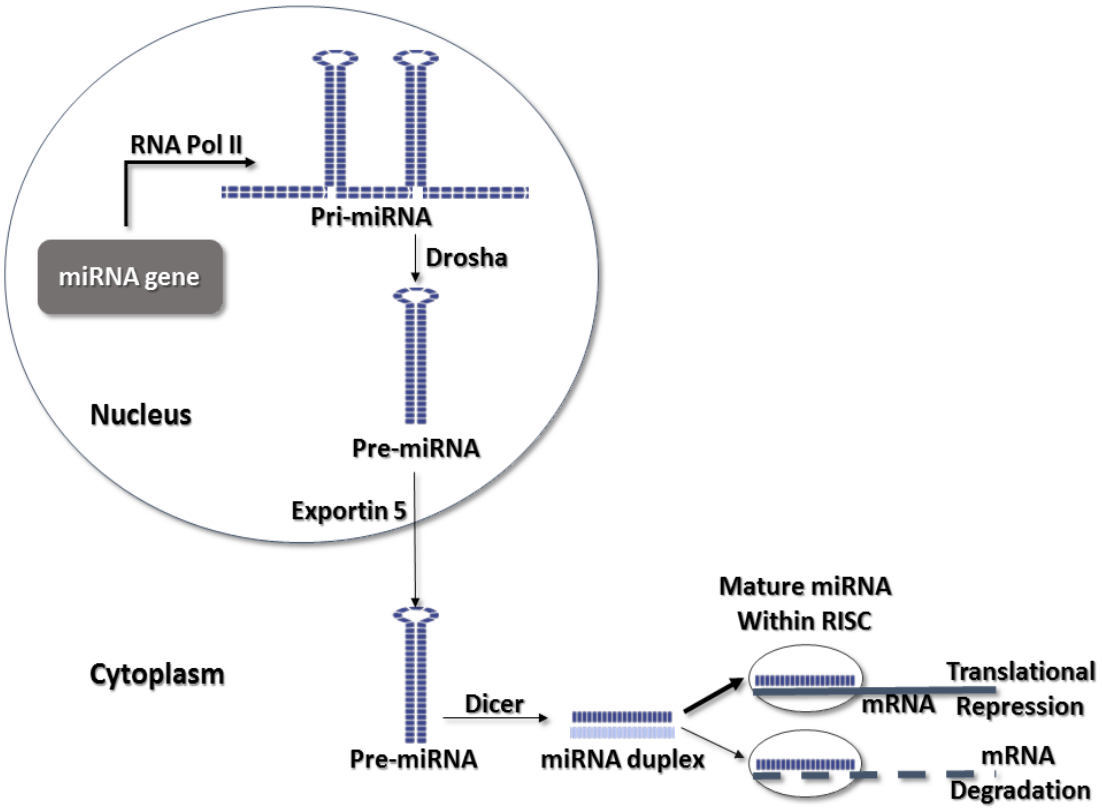
RNA Pol II
Pri-miRNA
miRNA gene
Drosha
Nucleus
Pre-miRNA
Exportin 5
Mature miRNA
Within RISC
Cytoplasm
Translational
Repression
mRNA
Dicer
Pre-miRNA
miRNA duplex
mRNA
Degradation

Figure 6. MicroRNA biogenesis pathway. RNA polymerase II transcribes primary miRNA (pri-miRNA) which are then processed by Drosha into precursor miRNA (pre-miRNA) hairpins. These are transported into the cytoplasm by Exportin 5 and further processed by Dicer into miRNA duplexes. Following strand separation, the mature miRNAs are loaded into RNA-induced silencing complexes (RISCs) to guide the repression of protein synthesis or mRNA degradation.

7.2 miRNA and disease

Dysregulation of miRNA in the context of disease has become increasingly evident. As rapid responders to change in cellular environment, miRNA expression alters accordingly and at times, these modifications in expression can fight against or contribute to pathology [270]. This nature of rapid response to change has made miRNA extremely attractive candidates of biomarker discovery. Extracellular miRNA can be detected in all biofluids in association with lipoproteins, proteins of the argonaute family, or exosomes, which adds to their value as resistant molecules capable of tolerating common problems of sample handling without degradation. Profiling of miRNA has been performed in the context of various CNS disorders including AD, Parkinson, Schizophrenia, ALS, and MS and have led to identification of specific miRNA expression patterns associated with each of the diseases [271]. In cancer, expression of miRNA has been shown to follow identifiable signatures during each step of cancer development, progression, and response to therapy [272].

7.3 Dysregulated miRNA in HIV-1 infection

miRNA are master regulators of protein expression in major physiological processes and are dysregulated in disease [273]. Viral infections in particular have been shown to disrupt cellular miRNA profiles mainly due to the fact that they tweak the host's replication or transcription machinery [274]. In HIV-1 infection, downregulation of host miRNA involved in anti-viral immunity [275] or replication [276, 277] has been observed. HIV-1 Tat itself has been shown to inhibit production of host anti-viral miRNA in peripheral blood

mononuclear cells (PBMC) [278]. In the context of HAND, Tat's disruption of neuronal function through alterations in miRNA profile of these cells has been reported [279, 280], adding another dimension to the toxicity of this protein to neurons. Investigating the global expression pattern of miRNA in response to HIV infection has revealed disease-specific miRNA signatures that could potentially be used as biomarkers of staging, progression, and therapeutic monitoring. The initial study compared miRNA expression in peripheral blood mononuclear cells (PBMC) between HIV patients and healthy controls [281]. Expression of 63 miRNA is altered in PBMC of HIV infected patients. Several mostly down-regulated miRNA are T-cell specific and have the anti-HIV property. In a follow-up study, HIV patients are divided into four groups: asymptomatic, cART naïve, cART treated, and cART resistant, significant correlation is found in miRNA expression between plasma and PBMC. In addition, two differentially expressed miRNA in both plasma and PBMC could potentially predict progression of disease and response to therapy [282, 283]. miRNA profile in PBMC of viremic subjects and elite controllers show the same pattern of down-regulation of anti-HIV miRNA in both groups, but also differentially expressed miRNA specific to patients with HIV viremia [283]. Down-regulation of the let-7 miRNA family has been noted in HIV-infected T cells and correlated with increase in IL-10 expression and inhibition of T cell responses against HIV infection [284]. Besides those studies, the other study also shows a general trend in down-regulation of anti-viral defenses in T cells and PBMC following infection with HIV [285]. Overall down-regulation in miRNA expression in HIV infection has also been associated with RNA silencing suppressor (RSS) activity of HIV Tat [286, 287] and Vpr [288]. To date, four

comprehensive miRNA profiling studies have been conducted to identify suitable biomarkers for HIV/neuroAIDS. Two of these studies have been performed on archived and post-mortem brain tissue, one on plasma, and one on CSF. Parallel analysis of mRNA and miRNA expression profiles in the frontal cortex of HIV patients with or without HAD have shown 68 differentially expressed miRNA in HAD, 49 of which are down-regulated and 19 are up-regulated [289]. Further gene ontology and clustering analysis reveals involvement of significantly altered miRNA in axon guidance and down-stream signaling. Five miRNA are identified as potential biomarkers of neurodegeneration based on the fact that they are all enriched in neurons and have previously been shown to be involved in processes related to pathology in AD, Huntington, MS, and Schizophrenia. miRNA expression profiling in the brains of four HIV patients with encephalitis shows that the majority of up-regulated miRNA are involved in the transcriptional control of gene products important in immune response and inflammation, nucleotide metabolism, and cell cycle control [290]. These findings are consistent with infiltration and proliferation of immune cells in the CNS. Down-regulated miRNA are shown to be involved in cell death and resting state of glial cells [290]. Paired miRNA profiling of the plasma in HIV patients with or without cognitive impairment shows that 30 pairs of miRNA are differentially expressed but only 10 of them can be used to distinguish cognitively impaired HIV patients from unimpaired [291]. Interestingly, three of these identified miRNA targeted brain-derived neurotrophic factor [291]. The first and only CSF miRNA profiling study compared frontal cortex tissue and CSF of HIV patients with or without neurocognitive impairment to healthy controls [292]. The study found 66 differentially expressed miRNA

in CSF samples and 35 of those miRNA were also detected in frontal cortex. There were 4 miRNA with identical expression patterns between both sample sources and one miRNA with more than 20 fold higher expression in CSF compared to brain tissue. Computer-assisted target prediction of significantly altered miRNA indicated involvement in cytoskeletal remodeling, cell adhesion, chemokine expression, neurogenesis, axonal guidance, notch signaling, synaptogenesis, and nerve impulses.

7.4 Involvement of miRNA in the regulation of neurite outgrowth

Several miRNA have been shown to be involved in processes specific to the nervous system owing to their expression patterns and control of CNS-specific targets [293]. Amongst discovered miRNA regulated processes, roles in brain development [294] neuronal differentiation [295], fate determination of neuronal cells [296] regulation of spine development [297], and neurite morphogenesis [298] have been very well established.

Dendritic pruning and shrinkage of neurite outgrowth remains the pathological hallmark of HAND in the post-cART era [61]. Tat protein itself has been implicated in causing aberrant morphology of dendrites and loss of synapse [299]. Studies on miRNA profiling of brain tissue in cognitively impaired HIV patients have revealed differential expression signatures of miRNA that are involved in the regulation of dendrite formation and branching [289, 292, 300, 301]. Interestingly, a brain-enriched microRNA, miR-132, which regulates several proteins involved in controlling dendritic plasticity [302], was found to be upregulated substantially in brain tissue from HIV patients with neurocognitive

impairment [292]. This microRNA is required for the proper development, maturation, and function of neurons by regulating neuronal outgrowth [302]; and its downregulation has been observed in several neurological disorders such as Alzheimer's and Taupathies [303]. Outside of CNS environment, miR-132 has been shown to be highly upregulated in HIV infected CD4+ T cells [304]. A major target of miR-132, methyl CpG binding protein 2 (MecP2) with significant roles in neurogenesis [305], neuronal differentiation [306], and proper development of dendritic arbor [307] has also been found to be dysregulated in HIV/neuroAIDS cases [308]. Brain derived neurotrophic factor (BDNF), another important regulator of dendritic growth [309-311] and synaptic function [312, 313] which shows notable reduction in the brain and serum of HIV infected subjects [314, 315], is directly and positively regulated by MecP2 [316]. In fact, an axis of regulation exists in the brain involving BDNF, miR-132, and MecP2 [317], in which BDNF induces miR-132 through phosphorylation of cAMP response element binding protein (CREB), the transcription controller locus of miR-132 [318, 319]. As a target of miR-132, MecP2 is ultimately repressed, leading to the repression of BDNF due to the negative regulatory feedback nature of this axis. Improper timing or duration of miR-132 expression has been shown to be neurotoxic, indicating the delicate balance in the regulation of this axis [320]. Another target of miR-132, Rho GTPase-activating protein 32 (p250GAP/RICS) regulates dendritic spine morphology of neurons in a negative manner [321].

HIV-1 Tat can potentially induce miR-132 because of its capability in phosphorylating CREB through several pathways [322-325] and promoting the binding of p-CREB to CBP

which leads to the transactivation of loci containing CREB-responsive elements (CRE) [326]. On the other hand, Tat directly binds CBP, recruiting this histone acetyltransferase to the CRE [327]. Both CREB phosphorylation and CBP binding activities of Tat have been shown to be dependent on the basic domain integrity of this protein [328, 329]. Continued expression of Tat in CNS despite cART, along with pathological evidence of reduced neurite outgrowth warrant the investigation of Tat involvement in molecular pathways associated with miRNA-dependent control of neurite morphogenesis.

8. Doxycycline-inducible astrocyte-specific Tat-transgenic mouse model (iTat)

Rodent models of lentiviral infection and HIV disease were created soon after the discovery of the virus [330]. These models can reflect HIV-1 pathology and are useful in therapeutic testing and vaccine development [331]. The major advantage of these models compared to larger animals required for lentiviral infection models is that they are easy to handle and their genomes can be manipulated to produce specific proteins of HIV-1 that cause significant pathology. Early models of HIV disease in rodents included transgenic rat or mouse models that contained the provirus and were capable of expressing relevant HIV-1 proteins. Our laboratory created a mouse model that specifically expresses Tat in astrocytes following treatment with doxycycline [1]. Inducible Tat transgenic mouse colonies (iTat) were created by generation of two separate transgenic lines: Teton-GFAP mice, and TRE-Tat86 mice, and then cross-breeding of these two lines of transgenic mice (See **Figure 7**). Our group has conducted extensive studies on the physical and behavioral effects of Tat expression in this model. We have also uncovered significant molecular pathways of Tat-

induced neurotoxicity by studying the brain tissue as well as primary cultures established from our iTat model. Our group's initial studies of iTat mice show that following Tat expression, these mice show behavioral and neuropathological characteristics similar to cognitively impaired HIV patients. Physical characteristics following DOX treatment in these mice include: failure to thrive, hunched gesture, tremor, ataxia, slow cognitive and motor functions, seizure, and premature death. Histological examination of brain tissue from DOX-treated iTat mice reveal complete collapse of the cerebellum, progressive loss of the cortex, and significant vacuolation. Widespread reactive astrocytosis and infiltration of monocytes/ macrophages was also observed identical to the brain of HIV patients. Our data prove that our iTat mouse model reflects accurately the neuropathologies associated with neuroAIDS [1].

Further studies by our group using this model led to the discovery of molecular pathways in Tat-induced astrocytosis. We first showed that GFAP activation was directly involved in neurotoxicity induced by Tat [332]. Next, we found that p300 is involved in GFAP expression in astrocytes and that Tat positively regulates p300, leading to GFAP upregulation [204]. These findings helped us determine the signaling pathway involved in Tat-induced GFAP upregulation and present a model for this important effect of Tat on astrocytes. We showed that STAT3 expression and phosphorylation by Tat happens upstream of Egr-1 and p300 activation, leading to GFAP transactivation [205, 333]. Investigating the effects of Tat expression on growth inhibition of DOX-induced iTat primary astrocytes, we found anti-proliferative properties of Tat due to this protein's

interactions with several cell cycle regulators [334]. Lastly, observing a significant increase in the infiltration of T lymphocytes in iTat mouse brains following Tat expression, we showed that chemokine induction by Tat is responsible for this event. In addition to inducing CCL2, CCL3, CCL4, CCL5, CXCL2, and CXCL10, we found that Tat also upregulates XCL1 which has significant roles in tissue-specific recruitment of T lymphocytes [335].

Other groups have also taken advantage of our iTat mouse model and have reported similar findings on astrogliosis, neuronal dendrite degeneration, and infiltration of immune cells [331]. Some of these studies have made novel discoveries regarding the involvement of Tat in neurodegenerative mechanisms. A study on the involvement of Alzheimer's disease-like pathology in HIV infection has found significant neuronal damage and accumulation of phosphorylated tau in our mouse model, concluding that Tat promotes AD pathology [336]. Investigation of neuronal autophagy functions using our mouse model has shown that Tat induces abnormal fusion of autophagosomes and lysosomes, leading to dysregulated clearance of neuronal components [337]. A study on disruption of neuronal microRNA by Tat has shown that specific target genes of Tat-induced miRNA show decreased levels in histological preparations of our iTat mouse brains, confirming Tat-specific alterations in neuronal miRNA [279].

Behavioral studies of our iTat mice have also been performed by several groups. One study has revealed disruption of synaptic protein distribution and near total suppression of long

term potentiation (LTP) in the cortex and CA1 regions of the iTat mouse brain [67]. This loss in LTP coincides with the disruption of spatial memory and learning in these mice which shows Tat expression in the brain results in deficits in memory consolidation or retrieval. Assessment of multiple behavioral tasks using the iTat mice has also shown that Tat expression is followed by significant induction of anxiety-like behavior in all of the tasks performed [338] and that female iTat mice were significantly protected from Tat-induced anxiety-like response by progesterone [339]. Tat expression has also been found to potentiate cocaine-mediated psychostimulation and reward in male iTat mice, indicating the potential role of Tat in psychostimulant abuse among the HIV-infected population [340]. Collectively, these results from our own group and others reinforce the relevance of our iTat mice as an excellent model of neurocognitive impairment associated with HIV infection.

9. Summary of the background and our hypotheses

Although the implementation and expansion of access to cART has dramatically reduced new infections and HIV-related deaths over the past few two decades, the prevalence of HIV/AIDS remains high and the number of individuals living with the virus has increased [341, 342]. Suppression of systemic viral replication and prolonged life expectancy of the infected population under HAART come with the cost of preserving latent viral reservoirs in both periphery and the CNS [343, 344]. In addition, our yet to achieve ability in eradicating the integrated provirus is potentiating the development of drug resistant mutations [341, 342, 344, 345]. Despite the dramatic response of the neurodegenerative

process associated with HIV-1 to anti-retroviral therapy, over 50% of the infected population demonstrate neurological disease of significant detriment to daily function with a dangerous potential to affect attachment to therapeutic intervention.

There is substantial evidence to support Tat protein as a major culprit in the ongoing inflammation and synaptodendritic pathology associated with HIV-1 infection of the CNS [171-173]. Tat is produced and released from both actively infected cells and non-permissive cells within the CNS, and applying concentrations of this protein relevant to amounts reported in the brain and CSF to in vitro cultures demonstrates identical signs of pruning in dendrites and retraction of neurites [177-179]. More importantly, the dendritic injury induced by Tat is reversible [346]. These findings indicate that by completely blocking Tat production or inhibiting its associated mechanism(s) involved in the affliction of synaptodendritic injury, we might be able to protect neurons while other approaches in excising the provirus are investigated. Hence, a better understanding of Tat's unconventional secretion mechanisms in the CNS and Tat's effects on regulators of synaptodendritic plasticity is warranted.

In the first part of our studies, we investigated the possibility of Tat exosomal release from astrocytes. As the most abundant cells in the CNS with crucial roles in maintaining the BBB, ensuring homeostatic balance, and providing nutrition for neurons, astrocytes employ exosomal delivery of trophins and danger associated molecular patterns to neurons [347]. Astrocytes are known to secrete Tat protein as it can be detected in the culture

supernatants of these cells once they are infected with the virus or transfected with Tat expression plasmids [1]. Exosomes provide a long range of molecular delivery of protein and nucleic acid cargo without a compromise in the stability of carried material which makes them excellent vehicles of nano delivery. Considering the established biological activity of extracellular Tat protein, combined with its ability to interact with biological membranes, we hypothesized that Tat could also access endosomal membranes, traffic to the MVB, and be released in exosomal form. In order to test the possibility of Tat incorporation into exosomes, we examined the specificity and efficiency of its secretion into different subpopulation of exosomes using traditional ultracentrifugation, advanced OptiPrep gradient fractionation, and HIV-1 LTR-driven luciferase reporter-based cell system.

In the second part of our work, we characterized the mechanism for Tat shortening effect on neurites. Tat is known to reduce the dendritic arbor in a reversible manner [346]. The molecular details of this effect however are not clear. Several regulators of synaptodendritic plasticity are rapidly and post-transcriptionally controlled by specific, brain-enriched microRNA. One of these miRNA, miR-132, has been found to have significant upregulation following HIV-1 infection in T-cells [304] and in the post-mortem brain tissue from cognitively impaired HIV patients [292] An important target of this miRNA in the brain, MecP2, is a positive regulator of dendrite and neurite outgrowth [307]. Interestingly, the expression of this microRNA is under the control of CREB, a molecule which Tat is known to activate via several kinase pathways [324]. We hypothesized that

continuous Tat expression in the CNS is leading to phosphorylation of CREB and induction of miR-132 which in turn leads to MecP2 repression and loss of dendritic arbor. Using astrocyte cell lines and primary astrocytes, we studied the expression levels of this microRNA following Tat expression and HIV-1 infection. In order to investigate the specificity of Tat in upregulating this miRNA, we constructed a mutant Tat expression plasmid that lacked CREB phosphorylation capacities. Finally, by incorporating synthetic antagonizers of miR-132 expression, we determined the effect of Tat induced miR-132 overexpression on viability and neuritogenesis of primary cortical neurons.

MATERIALS AND METHODS

MATERIALS

Media and supplements

Dulbecco's Modified Eagle's Medium (DMEM), Ham's F12 Medium (F12) and Kaighn's modification of Ham's F-12 medium (F12k) were purchased from Lonza (Walkersville, MD). Neurobasal-A Medium and Penicillin-streptomycin-glutamine and trypsin were purchased from Gibco (Grand Island, NY). Fetal bovine serum was purchased from Hyclone (Logan, UT). Ampicillin sodium salt and Kanamycin sulfate were purchased from United States Biological (Swampscott, MD). The bacterial culture media were prepared as follows: Luria broth (LB) media were made of 10 g/L Bacto tryptone and 5 g/L Bacto yeast extract (BD Biosciences, San Jose, CA) plus 5 g/L NaCl. Solid LB culture plates were prepared from complete LB medium with the addition of 15 g/L Bacto agar (BD

Biosciences). Super optimal broth with catabolite repression (SOC) was purchased from Life technologies (Grand Island, NY). Working concentrations of antibiotics were 100 μg/ml ampicillin and 50 μg/ml kanamycin. Exosome-free media were obtained by ultracentrifugation of the complete media (serum with antibiotic) at 100,000 g for 16 hr and removal of the exosomes and used in all studies involving exosomes.

Antibodies

Rabbit anti-Myc (sc-789) (WB 1:1000), mouse anti-MAP2 (sc-13561) (IF 1:200), mouse anti-Cytochrome c (Cyto c) (sc-13561) (WB 1:250), mouse anti-CREB, goat anti-P-CREB (Ser^{133}), rabbit anti-BDNF, goat anti-RICS, rabbit anti-MecP2, mouse anti-SYP, mouse anti-PSD-95, and rabbit anti-CBP were purchased from Santa Cruz Biotechnology (Santa Cruz, CA).

Phycoerythrin (PE)-conjugated mouse-anti-p24 (KC57) was purchased from Beckman Counter (Brea, CA). Mouse anti-His was purchased from Applied Biological materials ABM (Richmond, BC). Rabbit anti-green fluorescence protein (GFP) (632592) (WB 1:1000) was purchased from Clontech (Mountain View, CA). Mouse anti-GFAP (WB 1:1000, IF 1:200), mouse anti-β-actin (WB 1:2000), rabbit anti-TSG101 (T5701) (WB 1:1000), normal mouse, rabbit IgG, and mouse anti-β-actin (WB 1:2000) were purchased from Sigma-Aldrich (Sigma-Aldrich, St. Louis, MO). Mouse anti-CD63 (WB 1:1000) was purchased from System Biosciences (Mountain View, CA). Rabbit anti-GFAP (Dako) (IF 1:500) , Sheep anti-mouse IgG-horseradish peroxidase (HRP) and donkey anti-rabbit IgG-HRP (WB 1:3000) were purchased from GE Healthcare (Little Chalfont, Buckinghamshire,

UK). Mouse anti-p24 derived from p24 hybridoma cells (#1513) was obtained from NIH AIDS Reagent Program, and donated by Dr. Bruce Chesebro of National Institute of Allergy and Infectious Diseases, Hamilton, Montana [348]. Donkey-anti-Rat Alexa-Fluor-555, donkey-anti-goat Alexa-Fluor-555, goat-anti-mouse Alexa-flour-555, g goat-anti-mouse Alexa-flour-488, and goat-anti-rabbit Alexa-Fluor 488 (IF 1: 1000) were purchased from Molecular Probes (Eugene, Oregon, USA).

Reagents

Enhanced chemiluminesence (ECL) reagents for Western blotting detection were made in house. Protease inhibitor cocktail set V were purchased from Roche (Indianapolis, IN). T4 DNA polymerase, T4 DNA ligase, calf intestinal phosphatase (CIP), and all restriction endonucleases were from New England Biolabs (Beverly, MA). Poly-L-lysine, Yeast mannan, dextran sulfate, and 4',6'-diamidino-2-phenylindol (DAPI) were purchased from Sigma. All other chemicals were from Fisher (LaGrange, KY).

Biotechnology systems

The expand high fidelity PCR system, Gel and PCR clean-up kit and firefly luciferase assay system were purchased from Promega (Madison, WI). The Bio-Rad DC protein assay kit was from Biorad Laboratories (Hercules, CA).

METHODS

Cells and cell cultures

Cell lines

The human embryonic kidney cell line 293T, human astrocytoma U373.MG and neuroblastoma cell line SH-SY5Y were purchased from American Tissue Culture Collection (ATCC) (Manassas, VA). Human T cell leukemia cell line MT4 was obtained from NIH AIDS Reagent Program, and donated by Dr. Douglas Richman of University of California, San Diego [349]. TZM-bl cells were obtained from NIH AIDS Reagent Program (contributed by Dr. John C. Kappes, Dr. Xiaoyun Wu and Tranzyme Inc.) [350] and maintained in DMEM.

Primary cells

Mouse primary astrocytes were isolated from 18.5-day-old embryonic brain tissue of the Tat-inducible transgenic mice described previously [1, 203, 335]. Human primary fetal astrocytes were isolated, similarly to mouse primary astrocytes, from aborted 16-week fetal tissues (Advanced Biosciences Resources, Alameda, CA). Primary mouse cortex neurons, isolated and cryopreserved from C57BL/6 embryonic day-17 mice were purchased from GIBCO (OK).

Competent cells for cloning

GC5TM chemically competent E. coli was purchased from GeneChoice (Frederick, MD). XL-10 Gold Ultracompetent cells were purchased from Agilent Technologies (Santa Clara, CA).

Cell cultures

293T and U373.MG were maintained in DMEM. SH-SY5Y were maintained in F12 and DMEM (1:1 mix). MT4 cells were maintained in RPMI-1640. Mouse and human primary astrocytes were maintained in F12K. All culture media were supplemented with 10% fetal bovine serum (FBS) and 100 μg/ml Penicillin-streptomycin and 2 mM glutamine. Mouse primary cortex neurons were maintained in Neurobasal-A supplemented with 1% B27, 20 ng/ml EGF, 20 ng/ml bFGF, 50 U/ml penicillin, and 50 μg/ml streptomycin. All cells were cultured at 37℃ with 5% CO2.

Animals and tissue

Mouse strains

Wild type C57BL/6J mice were purchased from The Jackson Laboratory (Bar Harhor, Maine, USA). Doxycycline (Dox)-inducible brain-specific HIV-1 Tat transgenic mouse model (iTat) mouse model was described previously [351].

Plasmids

cDNA3 and EGFP-N3 plasmids were purchased from Clontech (Mountain View, CA). Tat.Myc, Tat.His and Tat.GFP plasmids were previously described [132]. ΔBD Tat mutant was constructed using a QuikChange II XL siite-directed mutagenesis kit (Stratagene, La Jolla, CA) with Tat.His as the template and primers 5`- GGC ATC TCC TAT GGC CCT CCT CAA GGA TCC-3` and 5`- GGA TCC TTG AGG AGG GCC ATA GGA GAT GCC-3`. The mutant deleted of the basic domain region (aa 49-57) was verified by sequencing.

Bacterial transformation

Plasmids were transformed into GC5TM or XL-10 Gold competent cells according to the manufacturer's directions. Briefly, cells (25 µl) were mixed with 0.5-2 µl (50-200 ng) DNA ligation product and incubated on ice for 30 min. The cells were then heat-shocked at 42°C for 45-60 sec, followed by incubation on ice for another 2 min, and addition of 250 µl of SOC medium. The cells were then incubated at 37°C for less than 1 hr with shaking at 225 RPM, and plated on LB plates containing the appropriate antibiotics. For large-scale cultures, transformed cells were grown in LB medium at 37°C for 16 hr with shaking at 225 RPM.

Cell transfections

Transfections were carried out using the standard calcium phosphate precipitation or lipofection method. Media were replaced 6 hr post-transfection. Transfection efficiency as

monitored by GFP expression was 80%-90% for 293T, and 20%-40% for U373.MG, primary mouse astrocytes, and primary human astrocytes.

miR-132 mimic and inhibitor transfection

Synthetic miR-132 mimic (Mission microRNA hsa-miR-132, Cat. HMI0190, mature sequence ACCGUGGCUUUCGAUUGUUACU) and miR-132 inhibitor (Mission microRNA, hsa-miR-132, Cat. HSTUD0191, mature sequence UAACAGUCUACAGCCAUGGUCG) duplexes along with negative control miRNA (Mission microRNA Negative Control 1, Cat.HMC003, mature sequence CGGUACGAUCGCGGCGGGAUAUC) were purchased from Sigma (Sigma-Aldrich,Mo). For 24-well seeded neurons or astrocytes, 5 nM miR-132 mimic and 50 nM miR-132 inhibitor was transfected into each well according to Lipofectamine 2000 (Invitrogen, Carlsbad, CA, USA) siRNA transfection or siRNA/DNA co-transfection protocol. Cells were assessed for target repression through Western blotting analysis 48 hours after transfection. For flow cytometric tracing of miR-132 mimic, covalent labeling by Cy^3 was carried out using Mirus LablelIT miRNA Cy^3 Kit as instructed by the manufacturer. Following the transfection of labeled miR-132 mimic, cells were analyzed for orange-red CY^3 signal detected through FL-2 red laser of a BD Accuri C6 flow cytometer.

Western blotting

Cells were harvested and lysed in RIPA buffer [1 mM EDTA, 0.5 mM EGTA, 1% Triton X-100, 1% sodium deoxycholate, 140 mM NaCl, 0.1% sodium deoxycholate, 10 mM Tris HCl, pH 8.0] with protease inhibitor and PMSF (phenylmethylsulfonyl fluoride) (Sigma) for 20 min on ice. Lysates were sonicated on ice and cleared of cell debris by 16000 g, 15 min centrifugation and the protein concentration was determined using a Bio-Rad DC protein assay kit with a BIO-RAD microplate reader. Equal amounts of protein were pre-incubated with 1x SDS loading buffer at 100°C for 10 min. Each sample was loaded onto and separated by 10% sodium dodecyl sulfate-polyacrylamide gel electrophoresis (SDS-PAGE). Proteins were transferred onto nitrocellulose membrane and probed with desired primary antibodies and then with appropriate HRP or fluorescence-conjugated secondary antibodies. Chemiluminesence visualization was performed using a homemade ECL system. Florescence visualization was performed using a BIO-RAD Chemi Doc imaging system (BD imager).

RNA isolation and semi-quantitative RT-PCR

Total RNA was isolated using a TRizol Reagent kit (Invitrogen, Carlsbad, CA) according to the manufacturer's instructions. Reverse transcription-PCR (RT-PCR) was performed using a Titan One Tube RT-PCR kit (Boehringer Mannheim, Indianapolis, IN) on a PE Thermocycler 9700 (PE Applied Biosystem, Foster City, CA). The primers for Tat were 5'-GTC GGG ATC CTA ATG GAG CCA GTA GAT CCT-3' and 5'-TGC TTT GAT AGA GAA ACT TGA TGA GTC-3'; the primers for the internal control glyceraldehyde-

3-phosphate dehydrogenase (GAPDH) were 5'-CTC AGT GTA GCC CAG GAT GC-3' and 5'-ACC ACC ATG GAG AAG GCT GG-3'. The expected sizes for Tat and GAPDH amplification product were 216 and 500 bp, respectively.

Quantitative RT-PCR

For the analysis of miR-132 levels, small RNA was isolated from cells in culture or exosomal pellets using miRvana miRNA Isolation kit (Ambion, Austin, TX) according to the manufacturer's protocol. A total of 1 μg RNA was used in the TaqMan MicroRNA Reverse Transcription Kit (Applied Biosystems, Foster City, CA, USA). miR-132 fold expression change was calculated based on 2-ddCT method normalized to snRNA U-6 and plotted in log values. For measurement of miR-132 levels in exosomes, let-7b was chosen as normalizing control based on consistent expression patterns of this miRNA in astrocytes and their exosomes [352]. Real time PCR primers were designed for BDNF, MecP2, IL-6, MCP-1, and TNF-α with the following sequences. BDNF-3' CCT GGT GGA ACT TCT TTG CGG, BDNF-5' GAA AGC GAG CCC CAG TTT GG, MecP2-3' GGA GCC TGA CCC TTC TGA TG, MecP2-5' GGA TGT TAG GGC TCA GGG AAG, MCP1-3' CTT CTT TGG GAC ACT TGC TGC, MCP1-5' CTC AGC CAG ATG CAA TCA ATG. All real time PCR assays were run on a BioRad CFX system. All CT values were normalized to CT of β-actin.

3-(4, 5-dimethylthiazol-2-yl)-2,5-diphenyl tetrazolium bromide (MTT) assay

The neurotoxicity of astrocyte culture supernatants was determined by the MTT assay using mouse primary neurons, or SH-SY5Y. The cells were plated in a 48-well plate at a density of 1 x 105 cells/well and cultured for two days. Then, the cells were exposed to culture supernatants (2:1 ratio) collected from astrocytes that were either transfected with plasmids or induced with Dox and continued to culture for 3 days. MTT (5 mg/ml) was added directly to the culture medium to the final concentration of 1 mg/ml, the cultures were incubated at 37℃ for 4 hr. The medium was then removed, and the purple crystal precipitates were dissolved in 200 µl acid-isopropanol (44 ml isopropanol plus 6 ml 0.2 N HCl). Aliquots of the acid-isopropanol solvent were transferred into a 96-well plate, and the optical density was taken using a microplate reader at a test wavelength of 490 nm and a reference wavelength of 650 nm and used to represent the relative cell viability.

Lactate dehydrogenase (LDH) cytotoxicity assay

A Takara LDH Cytotoxicity Detection Kit (Takara Bio INC.) was used for this assay. Briefly, astrocytes and neurons were seeded in a 96-well plate and transfected with Tat, miR-132 mimic or Inhibitor. After 72 hr, Triton x-100 was added to one well as a high positive control. The plate was centrifuged and 150 µl of each culture supernatant was transferred to a new 96-well plate. Substrate reagent (100 µl) was then added to each well and incubated at 37°C for 30 minutes. The plate was immediately placed in a reader and absorbance at 490 nm was measured. Percentage of cytotoxicity was calculated based on

the absorbance of each sample at 490 nm compared with the low and high controls. The high positive control was confirmed to have 100% cell lysis microscopically.

Preparation of pseudotyped HIV-GFP virus and infection of human primary fetal astrocytes

For preparation of HIV-infected T cells, 1 million MT4 were exposed to HIV-1 virus equivalent to 10,000 cpm in 1 ml RPMI complete medium at 37°C with 5% CO2 for 4 hr and washed with PBS twice then continued for cultured in fresh medium with cell density of 0.3-1.0 million per ml at 37°C with 5% CO2. Percentages of infected cells were monitored every other day by immunostaining of p24 followed by flow cytometry. For cell-free virus infection of astrocytes, U373.MG or human primary astrocytes were seeded at 50-70% confluency one day before infection. HIV-1 viruses (NL4-3, HIV.GFP) equivalent to 15,000 cpm were added to astrocyte cultures and incubated for 4-16 hr at 37°C with 5% CO2. For VSV-G pseudotyped virus infection of primary astrocytes, viruses equivalent to 30,000 cpm were added to cells in a 6 well plates in 3 ml fresh medium and spun at 600 g in room temperature (RT) for 2 hr. Cells were washed and cultured in fresh medium.

Reverse transcriptase (RT) assay

Viruses were pelleted and suspended in 10 µl of the dissociation buffer (50 mM Tris–HCl, pH 7.5, 0.25% Triton X-100, 20% glycerol, 1 mM DTT, and 0.25 M KCl) followed by three rounds of freeze–thawing. Thirty five microliters of the RT assay buffer (50 mM Tris–HCl, pH 7.5, 1 mM DTT, 10 mM MgCl2, and 0.25% Triton X-100), 5 µl of 1 mg/ml

poly (A).(dT)15 (Roche, Indianapolis, IN) and 1 μl of [3H]-thymidine 5′-triphosphate tetrasodiun salt (ICN, Irvine, CA) was added to each sample then incubated at 37°C for 1 h. The reactions were spotted onto the DE81 ion exchange chromatographic disk (Whatman, Clifton, NJ) and then wash with 2× SSC (0.3 M NaCl and 30 mM Na citrate, pH 7.0) three times, 5 min each, and dehydration with 100% ethanol. The disks were air dried and counted for H3-incorporation using a scintillation counter after air dry. Reverse transcriptase activity was expressed as cpm.

Exosome preparation

Exosome-free medium was prepared by overnight (16 hr) centrifugation of complete medium at 100,000 g. Transfected 293T, U373.G, primary astrocytes, or HIV-infected MT4 were cultured in the exosome-free medium for 3 days. The culture medium was then collected and processed as follows: The first step was to remove cells and cell debris by performing three sequential centrifugations: 300 g for 10 min, 2,000 g for 10 min (alternatively, filtration through 0.22 μm filter), and 10,000 g for 30 min. Between each centrifugation step, the supernatant was carefully recovered and used for the next centrifugation. The next step was to obtain crude exosomes by subjecting the cleared supernatant from the first step to ultracentrifugation at 100,000 g for 70 min (SW28 rotor, Beckman, Indianapolis, IN). Following the ultracentrifugation, the supernatant was carefully removed and discarded, while the pellet was saved and either lysed in the RIPA buffer for Western blotting, or suspended in PBS for the next step of OptiPrep gradient fractionation, or exosome-free medium for exosome uptake analysis.

OptiPrep gradient fractionation

The crude exosomes in PBS (about 500 µl) from above were loaded on the top of a 5 ml 6-18% OptiPrep gradient that was prepared using a gradient maker Hoefer SG15 (Hoefer, Inc., Hilliston, MA), followed by ultracentrifugation at 250,000 g for 1.5 hr (SW55Ti rotor, Beckman). OptiPrep was diluted in 235 mM KCl, 12 mM MgCl2, 25 mM CaCl2, 30 mM EGTA, 150 mM Hepes-NaOH, pH 7.0. A total of 12 fractions from top to bottom, 450 µl each were collected. Trichloroacetic acid (TCA) precipitation was used to recover the proteins from each fraction. Briefly, TCA was added to each fraction to a final concentration of 20%, the mixture was incubated on ice for 15 min and then spun to obtain the precipitates. The precipitates were washed with cold acetone twice, dried, and dissolved in 1X SDS loading buffer for Western blotting. Alternatively, the fractions were diluted with 4 ml PBS and spun at 100,000 g for 70 min to obtain crude exosomes. The pellets were lysed in the RIPA buffer for Western blotting.

TZM-bl assay

TZM-bl assay was performed as previously described [353]. Briefly, TZM-bl cells were plated in a 24-well plate at a density of 50,000 cells/well and cultured for 24 hr. Supernatants, exosomes, exosome fractions (200 µl each unless otherwise stated) were added to each well and continued to culture at 370C for 24 hr. The cells were washed with PBS and lysed in 1X firefly luciferase lysis buffer (Promega, Madison, WI). Lysates were briefly centrifuged, mixed with firefly luciferase substrate (Promega), and the luciferase (Luc) activity was measured by an Opticomp Luminometer (MGM Instruments, Hamden,

CT). The units of Luc measurement are recorded as relative light units (RLUs). RLU readings of exosomal fractions were normalized to background reading of a preparation of reagents identical to Optiprep but lacking exosomes.

Acetylcholinesterase (AChE) activity assay

Factions obtained from the OptiPrep gradient centrifugation (15 µl) were mixed with 85 µl 1.25 mM acetylthiocholine and 100 µl 0.1 mM 5,5'-dithiobis-(2-nitrobenzoic acid) in a 96-well plate. The mixture was incubated at room temperature until a yellowish color was developed. Then, the optical density (OD) at a wavelength of 450 nm was determined using a 96-well plate reader (BioRad, Hercules, CA).

Slot Blotting for ganglioside GM1 detection

Exosome fractions (150 µl each) from OptiPrep gradient fractionation were directly blotted onto nitrocellulose membrane using a slot blotting manifold (Schliecher and Schuell, Keene, NH). Ganglioside GM1 in each fraction was probed with HRP-conjugated Cholera toxin subunit B (Sigma) [354]. The GM1 level in each fraction was determined using the ImageJ (NIH) software and calculated as a percentage of the total GM1 in all fractions.

Exosome immunodepletion

Protein-A agarose beads (Millipore, Billerica, MA) were used to capture AchE+ exosomes as described previously [355]. Briefly, protein-A agarose beads (25 µl) were coated with

1.6 µg anti-AchE antibody (Sigma, St. Louis, MO) or isotype control IgG by shaking 1 hr at room temperature. After washing with 1X PBS, the antibody-coated beads were incubated at room temperature for 1 hr with 200 µl exosomes produced from culture supernatants of iTat and WT primary mouse astrocytes with or without doxycycline treatment, U373.MG transfected with pcDNA3 or pTat.MYC, and mock or NL43 infected MT4. Following this step, the bead-exosome complexes were pelleted down by centrifugation and the exosome-depleted supernatants were tested for Luc activity using the TZM-bl assay as described above.

Immunofluorescence staining

To detect MAP-2, SYP, and PSD-95 in neurons or GFAP in astrocytes, cells were washed with ice-cold PBS at room temperature for 10 min and fixed with 4% paraformldehyde for 30 min, and followed by permeabilizing with 1% Triton-X 100 in PBS for 30 min and blocking with PBS-BB (5% BSA, 1% non-fat milk and 0.3% Triton-X 100 in PBS) for 1 hr. Cells were then incubated in appropriate primary antibodies with dilution of 1:200 in PBS-BB at 4°C for overnight. Secondary antibodies with the dilution of 1:500 in PBS-BB was applied to cells at room temperature for 1 hr. Nuclei were counterstained with 0.1 µg/ml 4', 6-diamidino-2-phenylindole (DAPI). Extensive washes with PBS were performed after each step. Omission of the primary antibody in parallel staining was included as a control to ensure no non-specific staining.

Data acquisition and statistical analysis

All experiment data were analyzed by one-way ANOVA and 2-tailed student's t test as indicated. A $p < 0.05$ was considered to be statistically significant and marked as "*", a $p < 0.01$ was considered to be statistically highly significant and marked as "**", and a $p < 0.001$ was considered was considered to be statistically highly significant and marked as "***".

RESULTS

PART I. Exosome-associated release, uptake and neurotoxicity of HIV-1 Tat protein

1.1 Detection of Tat in exosomes derived from Tat expressing cells

1.1.1 Primary mouse astrocytes

Our previous studies have shown secretion of Tat protein in culture supernatants of DOX-induced primary mouse astrocytes [334, 335]. To determine whether HIV-1 Tat is secreted in the exosomes, we first took advantage of the doxycycline-inducible astrocyte-specific Tat-transgenic mice (iTat), which was created in our laboratory [1, 203] (**Fig. 7A**). Mouse primary astrocytes were isolated from iTat and WT mice and cultured in the absence or presence of doxycycline (Dox) for 48 hr to induce Tat expression (**Fig. 7B & 7C**). In order to detect extracellular Tat, we used the HIV-1 LTR promoter-driven luciferase (Luc) reporter gene-based TZM-bl assay (**Fig. 8**). Culture supernatants were collected from astrocytes and added to TZM-bl cells for 24 hr. The cells were then lysed and FLuc was measured in the lysates (**Fig. 9A**). Culture supernatants from treated astrocytes were further processed for exosome isolation using the gold standard ultracentrifugation method (Fig. 10). These exosome preparations were then added to TZM-bl cells as preciously described and measured for FLuc. Exosomes derived from the very same Tat-expressing primary astrocytes showed transactivation of the Luc reporter gene expression in the same assay (**Fig. 9B**).

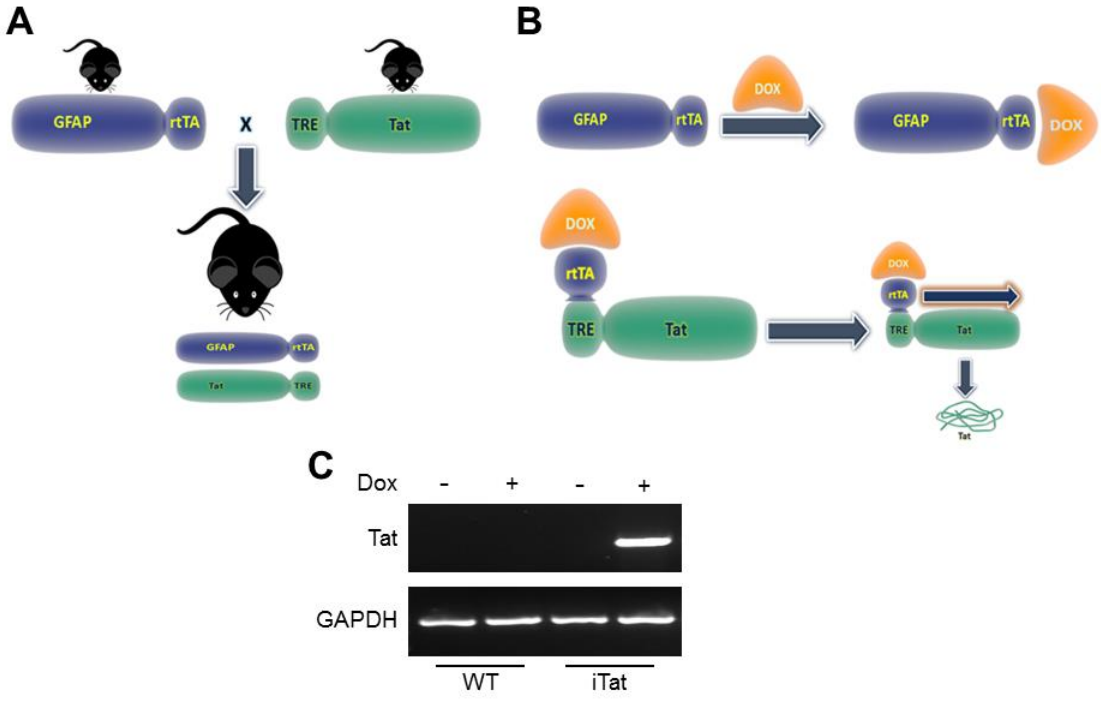
A
GFAP
rtTA
X
TRE
Tat
B
DOX
C
Dox - + - +
Tat
GAPDH
WT
iTat

Figure 7. Doxycycline (Dox)-inducible brain-specific HIV-1 Tat transgenic mouse model. In our bigenic mouse model, Dox regulatory element rtTA is under control of GFAP promotor (**A**). In the presence of Dox, Tat is expressed under the control of GFAP promotor (**B**). RT-PCR results showing Tat expression following DOX treatment of isolated astrocytes (**C**) [1].

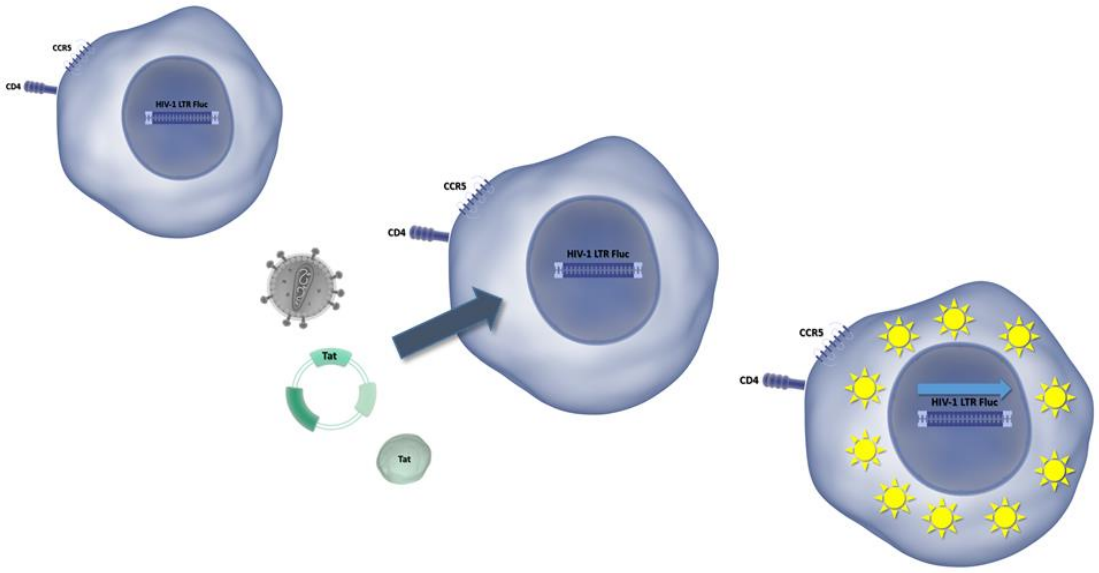
CCR5
CD4
HIV-1 LTR Fluc
CCR5
CD4
HIV-1 LTR Fluc
Tat
Tat
CCR5
CD4
HIV-1 LTR Fluc

Figure 8. Schematic of TZM-bl assay used for detection of Tat driven HIV-1 LTR expression. TZM-bl cells are genetically engineered Hela cells that express all receptors and co-receptors that make them susceptible to HIV-1 infection. They also contain integrated HIV-1 LTR promoter fused with firefly luciferase (FLuc) reporter genes. Following infection, Tat expression, or Tat treatment, FLuc will be expressed and is detectable in lysates from TZM-bl cells.

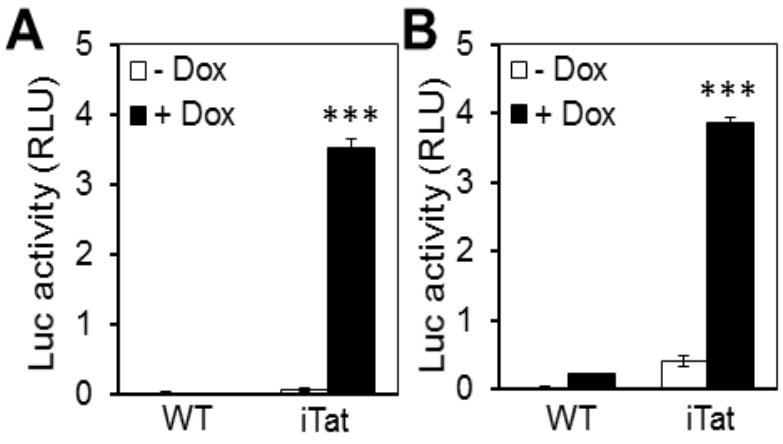
A
B
Luc activity (RLU)
- Dox
+ Dox
***
WT
iTat
0
1
2
3
4
5

Figure 9. Transactivation of HIV-1 LTR promoter by exosomes derived from Tat-expressing primary mouse astrocytes. Primary astrocytes were prepared from wild type (WT) or Tat transgenic mice (iTat) and cultured in the absence of doxycycline (-Dox) or presence of Dox (+ Dox) for 48 hr. The culture media were collected, cleared of cell debris, and saved as supernatants, or further processed to isolate exosomes. TMZ-bl were plated in a 24-well plate at a density of 50,000 cells/well, cultured for 24 hr, added 200 μl supernatants (A) or exosomes (B) prepared from primary astrocytes above, cultured for additional 24 hr, and harvested for the luciferase reporter gene assay. The data were mean ± SD of triplicates and representative of three independent experiments. Statistical analysis was performed using one-way ANOVA.

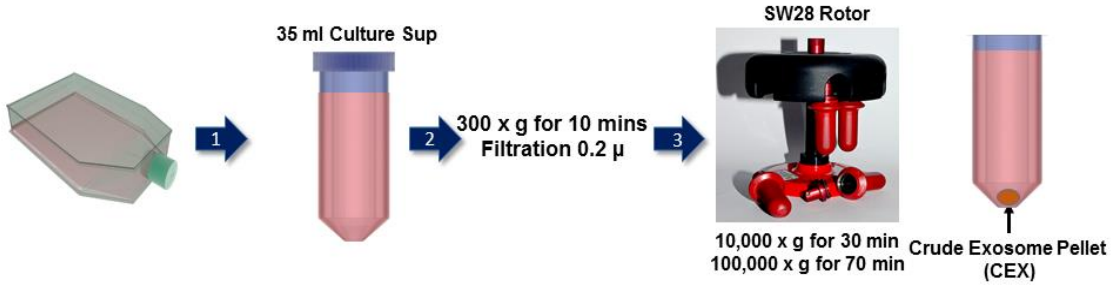
35 ml Culture Sup
SW28 Rotor
1
2
300 x g for 10 mins
Filtration 0.2 µ
3
10,000 x g for 30 min
100,000 x g for 70 min
Crude Exosome Pellet
(CEX)

Figure 10. Schematic presentation of ultracentrifugation method for exosome isolation. Culture supernatants are first cleared of cell debris and then centrifuged at 100,000 x g. The crude exosome pellet (CEX) is collected from the bottom of the tube, washed with PBS, and either used immediately for experiments or frozen at -80°C.

To ascertain Tat presence in the exosomes, crude exosomes were further fractionated through a 6-18% OptiPrep density gradient (**Fig. 11**). By using this method, exosome populations can first be distinguished based on density. Equal volume fractions will then be removed from the gradient in order to analyze each fraction for exosomal markers which further identifies the composition and source of exosomes in each fraction. The fractions will then be tested for Tat presence using the TZM-bl assay. Only a background level of Luc activity was detected in all fractions of exosomes from Dox-treated WT primary astrocytes (**Fig. 12A**). Exosome marker analysis confirmed that OptiPrep gradient successfully separated the exosomes into AchE+CD63+ and TSG101+ subpopulations (**Fig. 12B**). In comparison, the highest Luc activity was detected in the first fraction of exosomes from Dox-treated iTat astrocytes, and all other fractions also showed a higher Luc activity (**Fig. 12D**). There were also AchE+CD63+ and TSG101+ subpopulations of exosomes detected in those fractions (**Fig. 12E**). These results together suggest that HIV-1 Tat is associated with exosomes, particularly enriched in the AchE+CD63+ exosomes.

AchE and CD63 are often associated with lipid microdomains [356]. Thus, biogenesis of AchE+CD63+ exosomes is likely ceramide-dependent. To further investigate Tat association with AchE+CD63 exosomes, Dox-treated iTat astrocytes were treated with GW4869, an inhibitor of neutral sphingomyelinase, which converts sphingomyelin to ceramide, exosomes were then prepared and fractionated through the same OptiPrep gradient. GW4869 treatment led to significantly lower Luc activity in the first fraction but higher Luc activity in all other fractions (**Fig. 12G**).

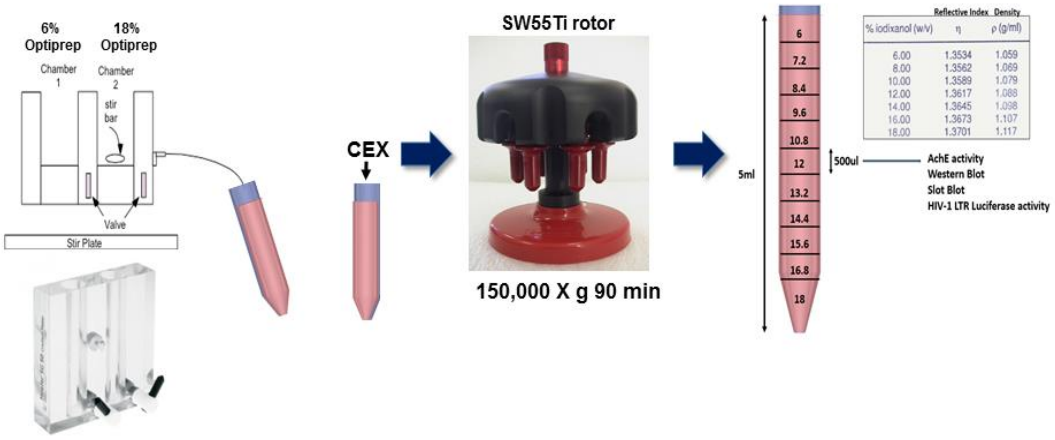
6%
Optiprep
18%
Optiprep
Chamber
1
Chamber
2
stir
bar
Valve
Stir Plate
CEX
SW55Ti rotor
150,000 X g 90 min
5ml
6
7.2
8.4
9.6
10.8
12
13.2
14.4
15.6
16.8
18
500ul
AchE activity
Western Blot
Slot Blot
HIV-1 LTR Luciferase activity
Reflective Index
Density
% iodixanol (w/v)
η
ρ (g/ml)
6.00 1.3534 1.059
8.00 1.3562 1.069
10.00 1.3589 1.079
12.00 1.3617 1.088
14.00 1.3645 1.098
16.00 1.3673 1.107
18.00 1.3701 1.117

Figure 11. Schematic presentation of Optiprep gradient purification method for exosome isolation. Crude exosome pellets produced by ultracentrifugation are loaded on a 6-18% Iodixanol gradient and centrifuged at 150,000 g for 90 min. Then, 11 fractions each 500 µl are pipetted off the gradient from top to bottom. These fractions can then be further tested for exosomal marker analysis and presence of Tat protein.

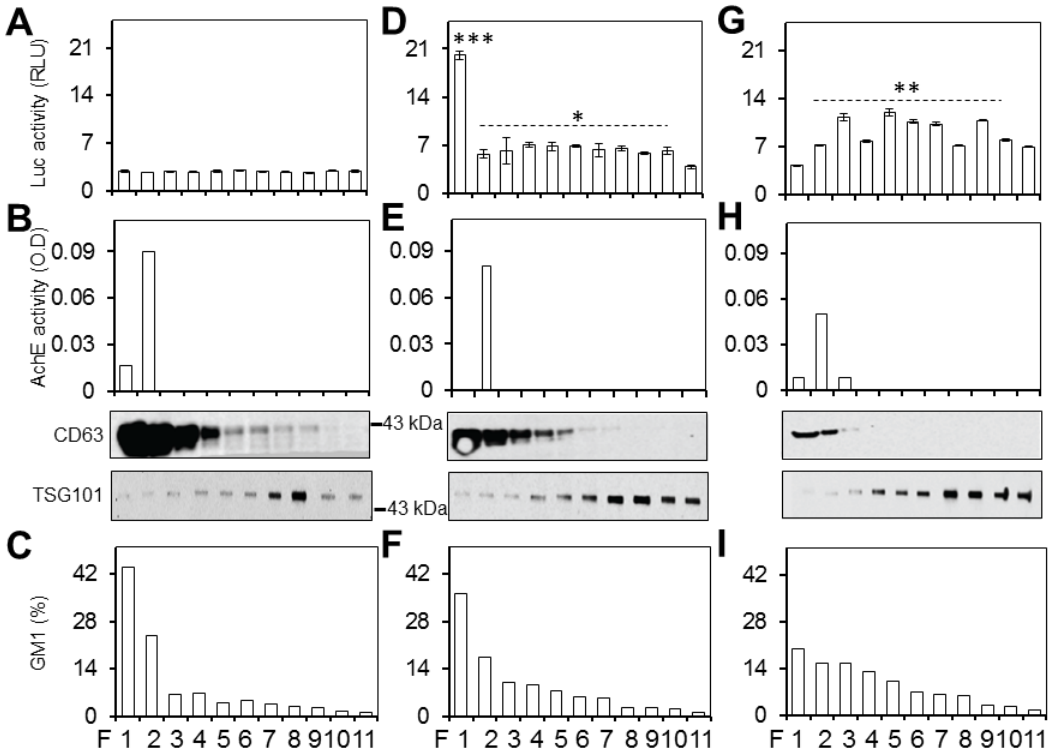
A
D
G
B
E
H
C
F
I
Luc activity (RLU)
AchE activity (O.D)
GM1 (%)
CD63
TSG101
43 kDa
43 kDa
***
*
**
F 1 2 3 4 5 6 7 8 9 10 11

Figure 12. Transactivation of HIV-1 LTR promoter by exosomes derived from Tat-expressing primary mouse astrocytes followed by OptiPrep fractionation. Exosomes derived from WT + Dox primary astrocytes (A-C) and iTat + Dox astrocytes (D-F) in Fig.9 were further fractionated in 6-18% OptiPrep. G-I. Exosomes were derived from iTat primary astrocytes that were treated with 10 μM GW4869 for 24 hr between Dox treatment and collection of culture medium. All fractions were analyzed for their transactivation activity on the LTR promoter activity as in Fig. 9 (A, D, G), for exosome markers AchE activity (top panels in B, E, H), CD63 expression (middle panels in B, E, H) and TSG101 expression (bottom panels in B, E, H) by Western blotting, or for GM1 expression by slot blotting, followed by densitometry (C, F, I). GM1 expression in each fraction was expressed as a percentage of the total GM1 in all fractions. The data were mean ± SD of triplicates and/or representative of three independent experiments. Statistical analysis was performed using 2-talied student's t test and one-way ANOVA.

In parallel, there were decreases in AchE+CD63+ exosomes (**Fig. 12H**). Decreases of ganglioside GM1, a glycosphingolipid abundant in lipid microdomains in AchE+CD63+ exosome fractions supported the notion that those exosomes were rich in lipid microdomains (**Fig. 12C, F & I**). These results not only further confirm Tat presence in the exosomes with more in AchE+CD63+ exosomes, but also suggest that AchE+CD63+ exosomes are generated in a ceramide-dependent manner.

1.1.2 Astrocyte and non-astrocyte cell lines

In order to further investigate the possibility of Tat's access to MVB and incorporation into exosomes, we tested exosomes from Tat expressing U373.MG astrocytoma cell line and 293T embryonic kidney cell line. Following Tat transfection, the culture supernatant of these cells was processed as described in previous data to produce exosomes. These exosome were then tested for Tat presence by TZM-bl assay. Similar to our findings in primary mouse astrocytes, Tat was also detected in the exosomes from Tat-transfected U373.MG (**Fig. 13B**) and in the exosomes from Tat-transfected 293T (**Fig. 13D**). In addition to the Luc activity assay, Tat were detected in the exosomes from both Tat-transfected U373.MG (**Fig. 13A**) and 293T (**Fig. 13C**) by Western blotting, in which the exosome purity was verified by lack of cytochrome c in the exosomes. Crude exosomes produced from previous step were further fractionated on 6-18% Optiprep gradients and assayed for FLuc expression and exosomal markers. In U373.MG cells, compared to primary astrocytes (**Fig. 12D**), higher Luc activity was detected in the first three fractions

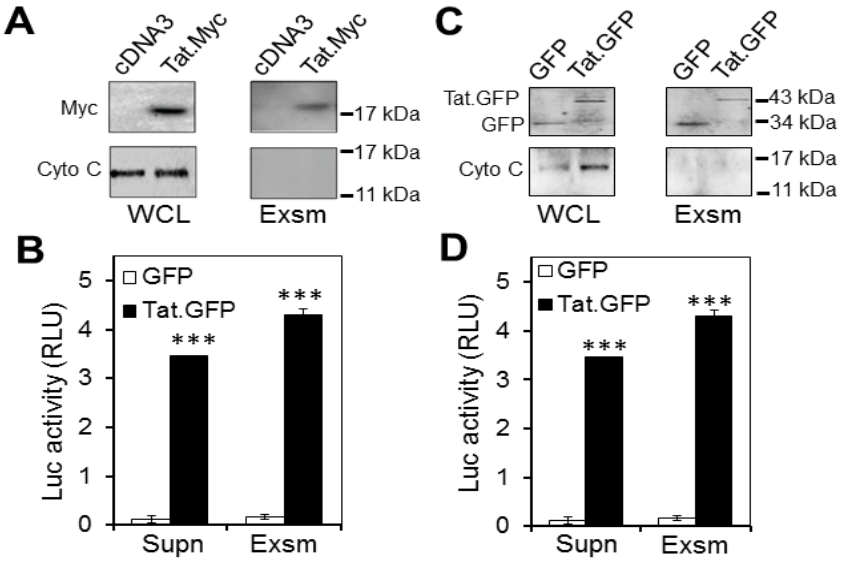
A
cDNA3
Tat.Myc
cDNA3
Tat.Myc
Myc
Cyto C
17 kDa
17 kDa
11 kDa
WCL
Exsm
C
GFP
Tat.GFP
GFP
Tat.GFP
Tat.GFP
GFP
Cyto C
43 kDa
34 kDa
17 kDa
11 kDa
WCL
Exsm
B
GFP
Tat.GFP
Luc activity (RLU)
***
***
Supn
Exsm
D
GFP
Tat.GFP
Luc activity (RLU)
***
***
Supn
Exsm

Figure 13. Detection of Tat in exosomes derived from Tat-transfected U373.MG and 293T cells. U373.MG were transfected with Tat.Myc expression plasmid and 293T were transfected with Tat.GFP plasmid and cultured for 48 hr. cDNA3 and GFP plasmids, the cloning backbones were included as controls. Supernatants (Supn) and exosomes (Exsm) were prepared as above. Cells were harvested for whole cell lysates (WCL). Tat expression in WCL and Exsm was detected by Western blotting against anti-Myc and anti-GFP antibody (A & C). Cytochrome c (Cyto c) was included in Western blotting to ensure the exosome purity. The transactivation activity of Supn and Exsm was determined as above (B & D). The data were mean ± SD of triplicates and/or representative of three independent experiments. Statistical analysis was performed using 2-tailed student's t test.

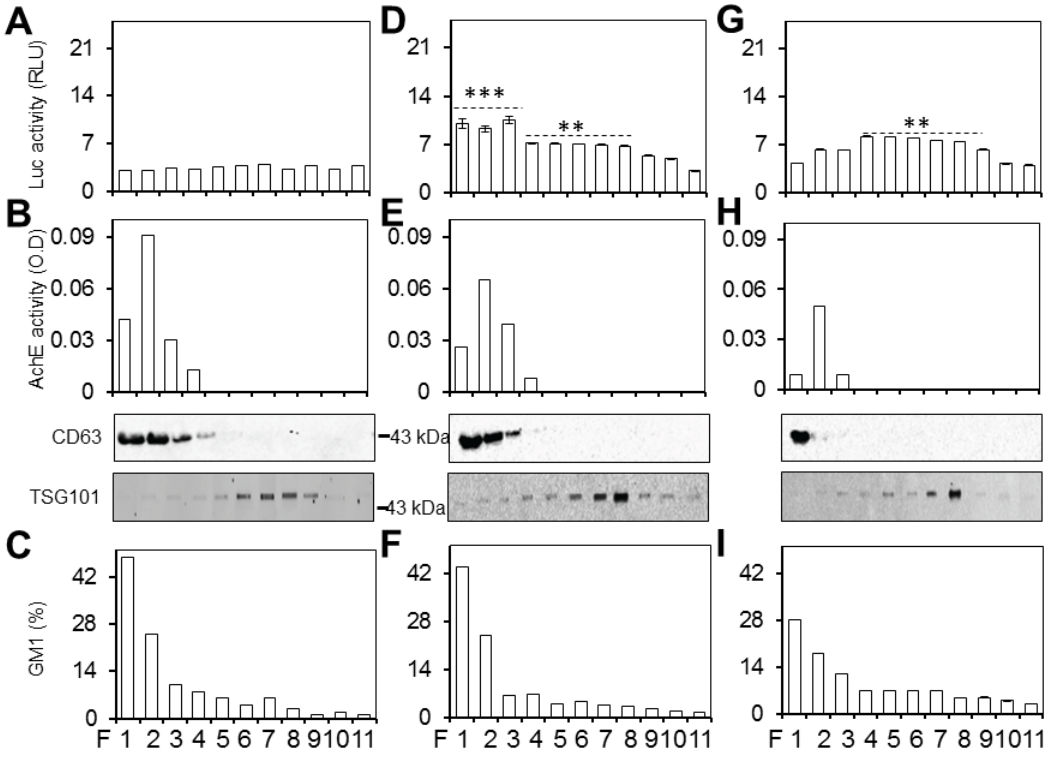
A
D
G
B
E
H
C
F
I
Luc activity (RLU)
AchE activity (O.D)
GM1 (%)
CD63
TSG101
43 kDa
43 kDa
***
**
**
F 1 2 3 4 5 6 7 8 9 10 11

Figure 14. OptiPrep fractionation of exosomes derived from Tat-transfected U373.MG. Exosomes derived from cDNA3-transfected U373.MG (A-C) or Tat.Myc-transfected U373.MG (D-F) in Fig. 13 were further fractionated in 6-18% OptiPrep. G-I. Exosomes were derived from Tat.Myc-transfected U373.MG that were treated with 10 μM GW4869 for 24 hr between Dox treatment and collection of culture medium. All fractions were analyzed for their transactivation activity on the LTR promoter activity (A, D, G), for exosome markers AchE activity (top panels in B, E, H), CD63 expression (middle panels in B, E, H) and TSG101 expression (bottom panels in B, E, H) by Western blotting, or for GM1 expression by slot blotting, followed by densitometry (C, F, I). GM1 expression in each fraction was expressed as a percentage of the total GM1 in all fractions. The data were mean ± SD of triplicates and/or representative of three independent experiments. Statistical analysis was performed using 2-talied student's t test and one-way ANOVA.

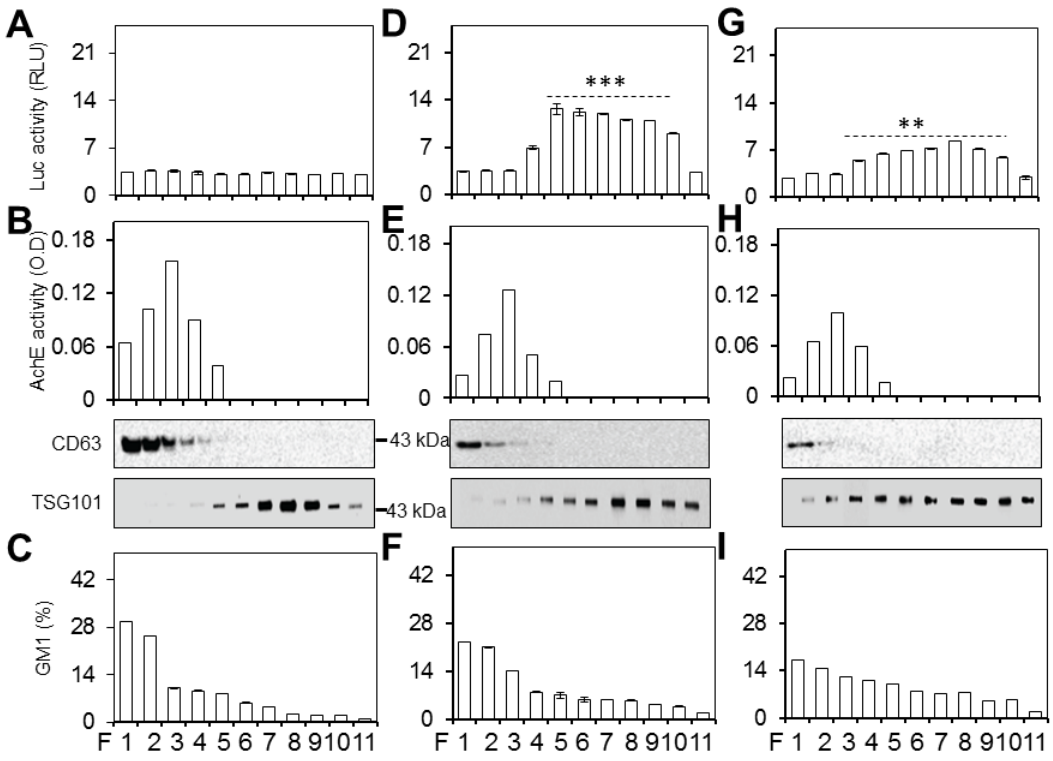
A
D
G
Luc activity (RLU)
21
14
7
0
***
**
B
E
H
AchE activity (O.D)
0.18
0.12
0.06
0
CD63
43 kDa
TSG101
43 kDa
C
F
I
GM1 (%)
42
28
14
0
F 1 2 3 4 5 6 7 8 9 10 11

Figure 15. OptiPrep fractionation of exosomes derived from Tat-transfected 293T. Exosomes derived from GFP-transfected 293T (A-C) or Tat.GFP-transfected 293T (D-F) in Fig. 13 were further fractionated in 6-18% OptiPrep. G-I. Exosomes were derived from Tat.GFP-transfected 293T that were treated with 10 μM GW4869 for 24 hr between Dox treatment and collection of culture medium. All fractions were analyzed for their transactivation activity on the LTR promoter activity (A, D, G), for exosome markers AchE activity (top panels in B, E, H), CD63 expression (middle panels in B, E, H) and TSG101 expression (bottom panels in B, E, H) by Western blotting, or for GM1 expression by slot blotting, followed by densitometry (C, F, I). GM1 expression in each fraction was expressed as a percentage of the total GM1 in all fractions. The data were mean ± SD of triplicates and/or representative of three independent experiments. Statistical analysis was performed using 2-talied student's t test and one-way ANOVA.

(**Fig. 14D**), while little Luc activity above the background was detected in the first three fractions in 293T (**Fig. 15D**). This difference is likely due to the different levels of AchE and CD63 expression among those cells.

1.2 Detection of Tat in HIV-1 infected CD4+ T cells

Next, we determined whether Tat is present in the exosomes in the context of HIV infection. For this purpose, MT4 cells which are human T cell leukemia cell lines were infected with the NL4-3 strain of HIV-1. Culture media were collected 6 days following infection, and exosomes were prepared. RT activity assay of the supernatants confirmed successful HIV infection in those cells (**Fig. 16A**). A significant Luc activity was detected in exosomes from NL4-3-infected cells as well (**Fig. 16B**). HIV-1 and exosomes are similar in size and density, and exosome preparations have been shown to contain HIV [267]. Thus, the significant Luc activity of exosomes derived from NL4-3-infceted cells could likely be due to both transactivation of Tat in the exosomes on the HIV LTR promoter and HIV infection of TZM-bl. To distinguish these two contributing factors, exosomes from Mock- and NL4-3-infected cells were further fractionated through the same OptiPrep gradient. Compared to the mock infection (**Fig. 17A**), significant Luc activity was detected in all fractions of exosomes from NL4-3-infected MT4 (**Fig. 17D**). As reported previously [357], there were no HIV, measured by Western blotting for p24 in the fractions of exosomes from mock infection (**Fig. 17B**), while there were HIV detected around single fraction #9 (**Fig. 17E**). Exosome markers AchE, CD63, and TSG101 showed similar fractionation patterns as before, regardless of HIV infection (**Fig. 17C & F**).

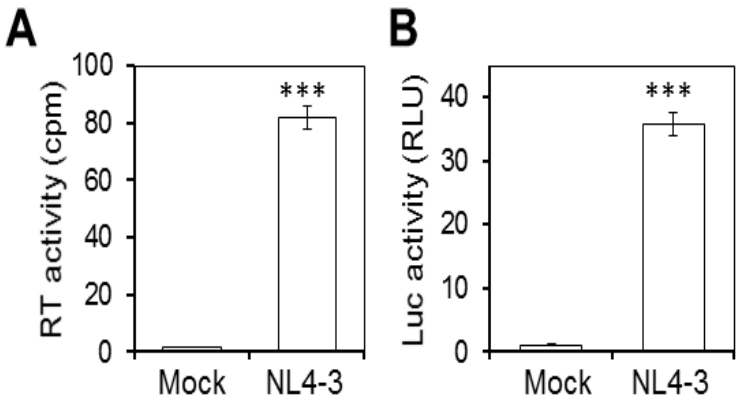
A
RT activity (cpm)
100
80
60
40
20
0
***
Mock
NL4-3
B
Luc activity (RLU)
40
30
20
10
0
***
Mock
NL4-3

Figure 16. Transactivation of HIV-1 LTR promoter by exosomes derived from HIV-infected MT4. MT4 cells were inoculated with NL4-3 at 37° C for 2 hr. A mock infection (Mock) was included as a control. After removing the input virus, the cells were cultured for 6 days. The culture medium was collected and used to prepare supernatants and exosomes as above. The supernatants were determined for virus replication using the RT activity assay (A); the exosomes were assayed for the transactivation activity of HIV-1 LTR promoter as above (B). The data were mean ± SD of triplicates and representative of three independent experiments. Statistical analysis was performed using 2-tailed student's t test.

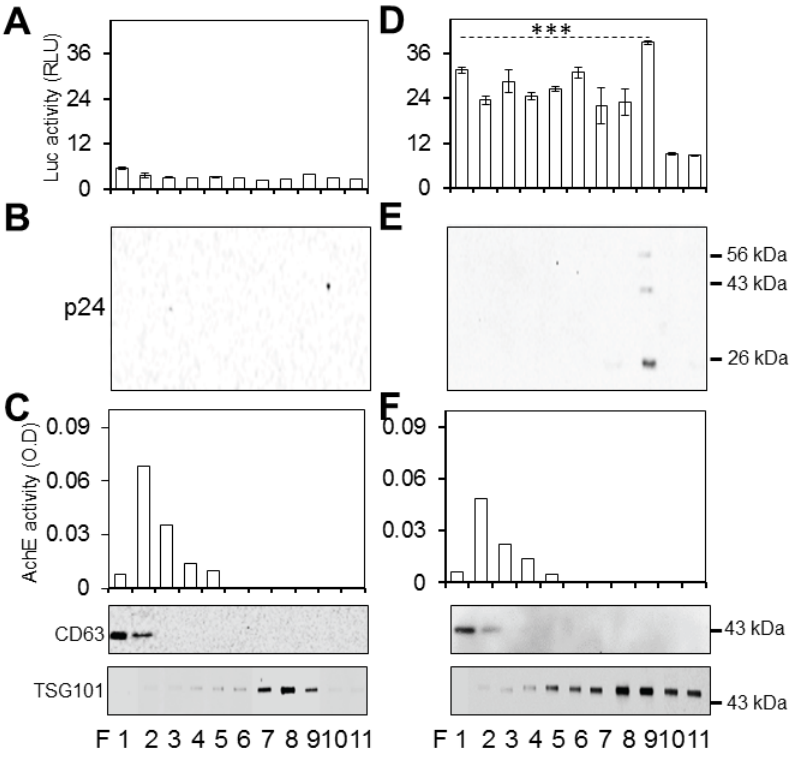
A
Luc activity (RLU)
36
24
12
0
D
***
36
24
12
0
B
p24
E
56 kDa
43 kDa
26 kDa
C
AchE activity (O.D)
0.09
0.06
0.03
0
F
0.09
0.06
0.03
0
CD63
43 kDa
TSG101
43 kDa
F 1 2 3 4 5 6 7 8 9 10 11
F 1 2 3 4 5 6 7 8 9 10 11

Figure 17. Transactivation of HIV-1 LTR promoter by exosomes derived from HIV-infected MT4 followed by OptiPrep fractionation. Exosomes derived from mock-infected MT4 (A-C) or NL4-3-infected MT4 (D-F) in Fig. 7 were further fractionated in 6-18% OptiPrep. All fractions were analyzed for their transactivation activity on the LTR promoter activity (A, D), for p24 level by Western blotting (B, E), or for exosome markers AchE activity (top panels in C, E), CD63 expression (middle panels in C, E) and TSG101 expression (bottom panels in C, E) by Western blotting. The data were mean ± SD of triplicates and/or representative of three independent experiments.

Clear separation of HIV from exosomes by the OptiPrep gradient [357] and a significant Luc activity detected in fractions without HIV indicates that Tat was also present in exosomes derived HIV-1 infected CD4+ T cells.

1.3 Significant levels of Tat in AchE+CD63+ exosomes

AchE is a GPI-anchored protein located at the surface of exosomes [248], and anti-AchE antibodies have successfully been used to immunodeplete AchE+ exosome population [355]. Thus, to determine the relative contribution of AchE+CD63+ exosomes to Tat association with exosomes, we immunodepleted AchE+CD63+ exosomes using anti-AchE-coated agarose beads and performed the Luc activity assay. Exosomes from Tat-expressing primary astrocytes, Tat-transfected U73.MG, and HIV-infected MT4 were used. Compared to IgG control, anti-AchE antibody depletion decreased the Luc activity of exosomes from Tat-expressing astrocytes by 43% (**Fig. 18A**), exosomes from Tat-transfected U373.MG by 40% (**Fig. 18B**), and exosomes from HIV-infected MT4 by 70% (**Fig. 18C**). These results provide additional evidence to support Tat presence in exosomes, particularly in AchE+CD63+ exosomes from astrocytes and CD4+ T cells.

1.4 Shortened neurites and decreased neuron survival by Tat-containing exosomes from Tat-expressing astrocytes

HIV-1 Tat expression in astrocytes causes neurite shortening and neuron death [1, 36, 132, 332, 334, 358]. To further characterize the biological activity of exosome-associated Tat, we cultured differentiated SHSY-5Y in the presence of exosomes from Tat-expressing primary

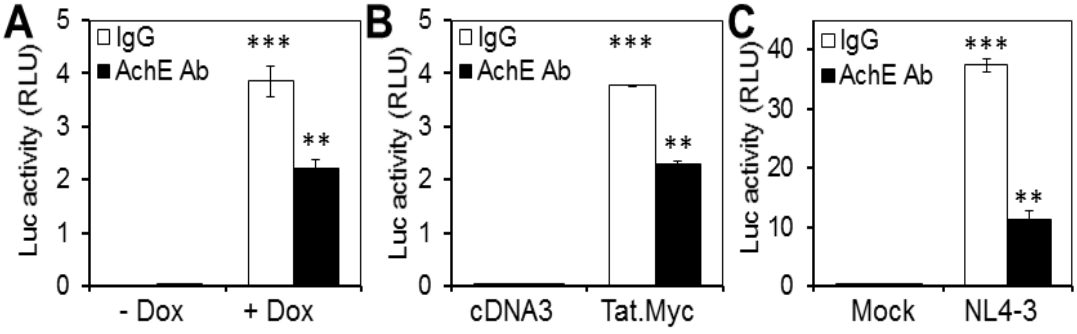
A
B
C
IgG
AchE Ab
Luc activity (RLU)
***
**
- Dox
+ Dox
cDNA3
Tat.Myc
Mock
NL4-3

Figure 18. Tat level in the AchE+ exosomes. Exosomes derived from iTat-Dox and iTat+Dox primary mouse astrocytes (A), cDNA3- and Tat.Myc-transfected U373.MG (B), or Mock- and NL4-3-infected MT4 (C) were incubated with anti-AchE antibody-coated protein A agarose beads (AchE Ab), or a matched IgG-coated protein A agarose beads. After removing the beads, the remaining exosomes were determined for the transactivation activity of HIV-1 LTR promoter as above. The data were mean ± SD of triplicates and representative of three independent experiments. Statistical analysis was performed using one-way ANOVA.

astrocytes and determined the effects of exosomes on neurites and neuron survival. Exosomes were first tested for their transactivation activity on HIV-1 LTR promoter as before. Compared to mock and exosomes from primary astrocytes without Tat expression, more exosomes from Tat-expressing astrocytes gave rise to a higher Luc activity (**Fig. 19A**), meanwhile more neurons with shorter or no visible neurites (**Fig. 19B**) and more neuron death (**Fig. 19C**). Next, we used anti-AchE antibody-coated agarose beads to immunodeplete AchE+ exosomes from supernatants, and determined effects of AchE+ exosome depletion on neurites and neuron survival. As shown before (**Fig. 19B & C**), only supernatants and exosomes from Tat-expressing primary astrocytes showed shortened neurites (**Fig. 20A**) and neuron death (**Fig. 20B**). Depletion of AchE+ exosomes from supernatants from Tat-expressing primary astrocytes significantly improved neurite morphology (**Fig. 20A**) and neuron survival (**Fig. 20B**) and as expected, resulted in lower Luc activity (**Fig. 20C**). These results together provide further evidence to support that exosome-associated Tat is biologically active.

1.5 Role of Tat basic domain in Tat trafficking into exosomes

Tat basic domain has been shown to be responsible for binding to the endolysosomal membranes [359], which likely provides Tat access to the multivesicular bodies in exosome biogenesis. To address this possibility and to understand the molecular mechanisms of Tat association with exosomes, we constructed a Tat mutant ΔBD deleted of the basic domain (aa 48-57). U373.MG were transfected with Tat or ΔBD. Supernatants and exosomes from Tat- and ΔBD transfected cells were prepared and tested for LTR transactivation.

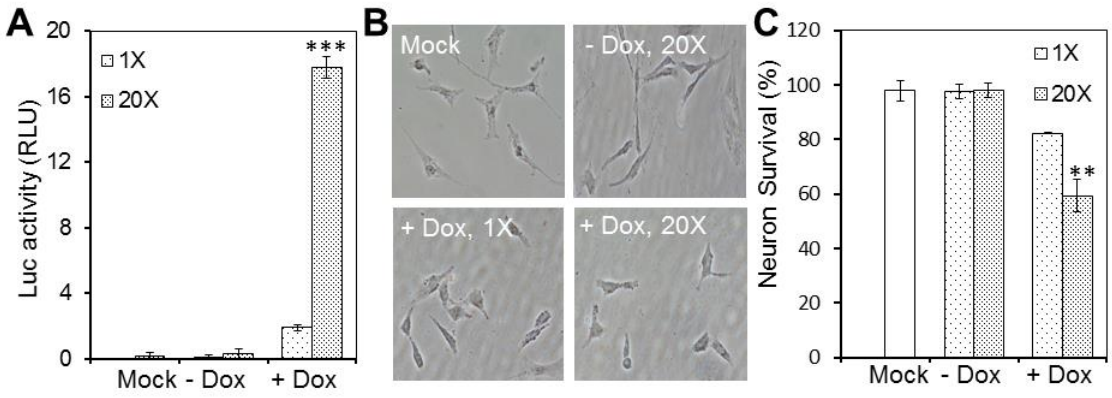
A
Luc activity (RLU)
20
16
12
8
4
0
1X
20X
***
Mock - Dox
+ Dox
B
Mock
- Dox, 20X
+ Dox, 1X
+ Dox, 20X
C
Neuron Survival (%)
120
100
80
60
40
20
0
1X
20X
**
Mock - Dox
+ Dox

Figure 19. Effects of Tat-containing exosomes on neurite growth and neuron survival. Exosomes (1X: 10 μl; 20X: 200 μl) from iTat-Dox and iTat+Dox primary mouse astrocytes in Fig. 1 were determined for the transactivation activity of HIV-1 LTR promoter as above (A), or added into differentiated SHSY-5Y, cultured for 24 hr, and imaged for neurite growth (B), or cultured for 48 hr, and determined for neuron survival using MTT assay (C). A regular medium was included as a mock control (Mock). Neuron survival was calculated using Mock as a reference, which was set at 100%. The data were mean ± SD of triplicates and representative of three independent experiments. Statistical analysis was performed using one-way ANOVA.

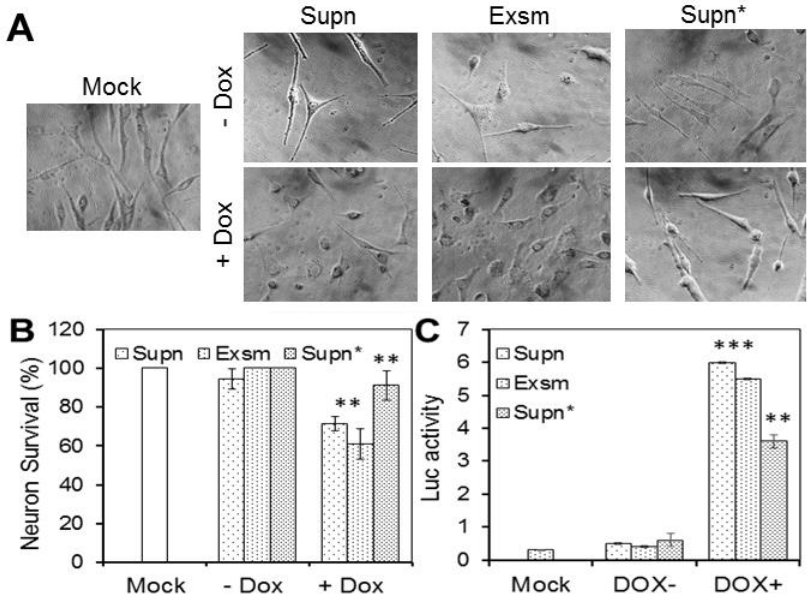
A
Supn
Exsm
Supn*
Mock
- Dox
+ Dox
B
Neuron Survival (%)
120
100
80
60
40
20
0
Supn
Exsm
Supn*
**
**
Mock
- Dox
+ Dox
C
Luc activity
7
6
5
4
3
2
1
0
Supn
Exsm
Supn*
***
**
Mock
DOX-
DOX+

Figure 20. Effects of AchE+ exosomes on neurite growth and neuron survival. Supernatants (Supn) and exosomes (Exsm) from iTat-Dox and iTat+Dox primary mouse astrocytes in Fig. 9 and AchE+Ab-depleted exosomes (Supn*) were added into differentiated SHSY-5Y, cultured for 24 hr, and imaged for neurite growth (A), or cultured for 48 hr, and determined for neuron survival using MTT assay (B), or determined for the transactivation activity of HIV-1 LTR promoter as above (C). A regular medium was included as a mock control (Mock). Neuron survival was calculated using Mock as a reference, which was set at 100%. The data were mean ± SD of triplicates and representative of three independent experiments. Statistical analysis was performed using one-way ANOVA.

As expected [360], both supernatants and exosomes from ΔBD-transfected cells showed little Luc activity (**Fig. 21A**). However, ΔBD and Tat were detected in the exosomes at a comparable level (**Fig. 21B**). ΔBD functions as a dominant negative for Tat in the LTR transactivation [361-363]. Consistent with these findings, co-transfection of Tat and ΔBD into TZM-bl showed significantly lower Luc activity than Tat transfection alone, by 70% (**Fig. 21C**). Interestingly, exosomes from Tat and ΔBD co-transfected cells showed a lower Luc activity than those of Tat transfection alone, but to a much lesser extent, only by 16% (**Fig. 21D**). These results do not support any significant roles of the basic domain in Tat trafficking to exosomes and cannot completely rule out roles of the basic domain in regulation of Tat release from exosomes. Based on the presented data, a schematic model of Tat incorporation into exosomes is provided (**Fig. 22**). Tat's access to endolysosomal membranes and MVB, leads to the incorporation of Tat into ILVs of both ceramide and ESCRT origin and its consequent release inside exosomes to the extracellular environment. Exosomal Tat, similar to non-exosomal soluble Tat, is biologically active and more stable due to protection inside exosomal membranes. Following uptake in neurons, Tat induces neurotoxicity and shortening of neurites.

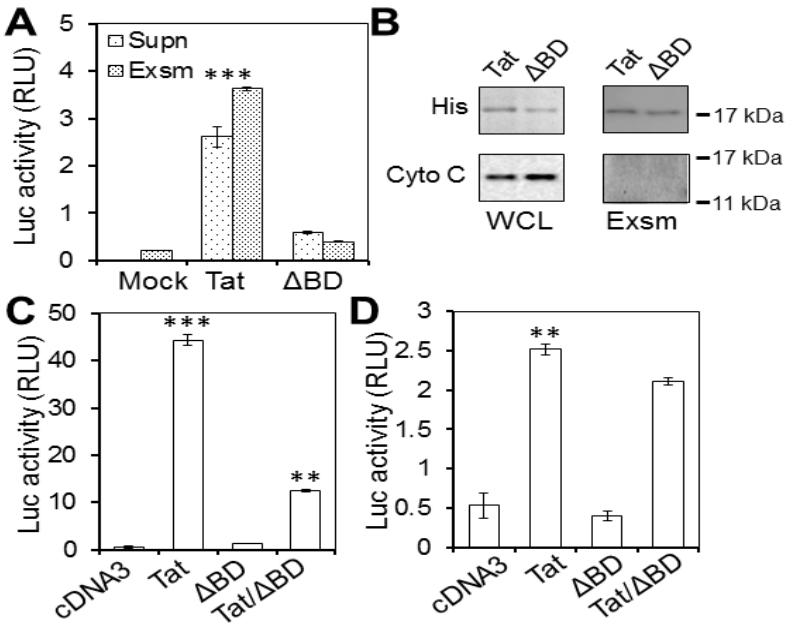
A
Luc activity (RLU)
Supn
Exsm
***
Mock
Tat
ΔBD
B
Tat
ΔBD
Tat
ΔBD
His
Cyto C
17 kDa
17 kDa
11 kDa
WCL
Exsm
C
Luc activity (RLU)
***
**
cDNA3
Tat
ΔBD
Tat/ΔBD
D
Luc activity (RLU)
**
cDNA3
Tat
ΔBD
Tat/ΔBD

Figure 21. Role of Tat basic domain in Tat sorting into exosomes. A & B. U373.MG were transfected with Tat.His (Tat) or its basic domain deletion (ΔBD). Supernatants (Supn), exosomes (Exsm), and whole cell lysates (WCL) were prepared as above and determined for transactivation activity of HIV-1 LTR promoter (A), Tat expression by Western blotting against anti-His antibody (B). C. TZM-bl were transfected with Tat, ΔBD, or Tat/ΔBD and assayed for the Luc activity. D. 293T were transfected with Tat, ΔBD, or Tat/ΔBD. Exosomes were assayed for transactivation activity of HIV-1 LTR promoter. The data were mean ± SD of triplicates and representative of three independent experiments. Statistical analysis was performed using one-way ANOVA.

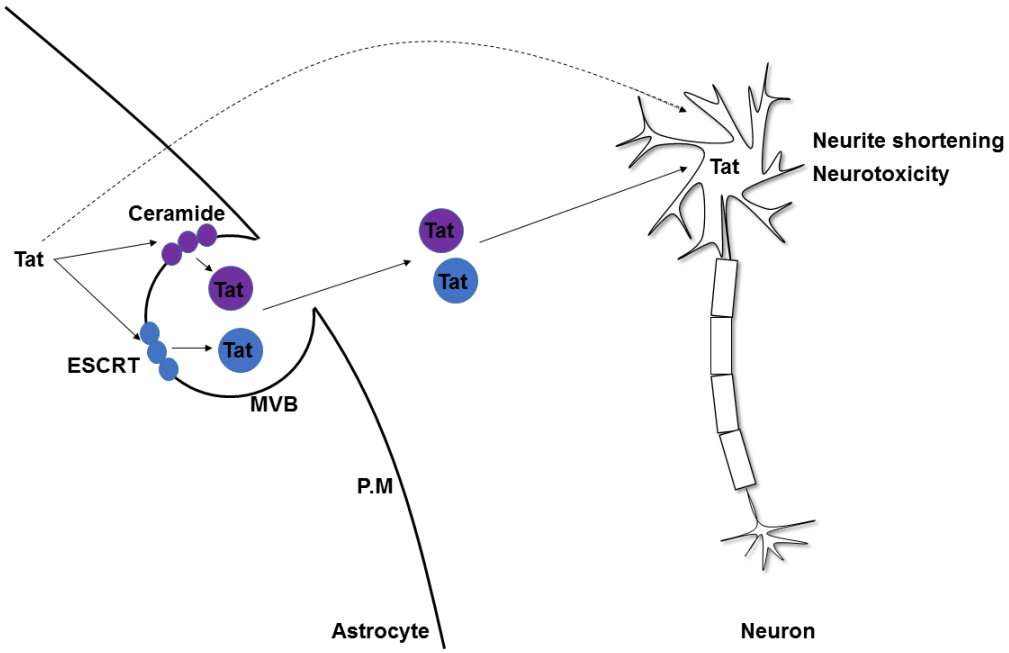
Tat
Ceramide
Tat
Tat
ESCRT
MVB
P.M
Astrocyte
Tat
Tat
Tat
Neurite shortening
Neurotoxicity
Neuron

Figure 22. Schematic model of Tat exosomal secretion. Tat binds MVB membrane, leading to its incorporation into ILVs of both ceramide and ESCRT origin. Fusion of MVB membrane with plasma membrane then releases Tat in exosomes which are biologically active and can induce shortening of neurites and toxicity following uptake in neurons.

Part II. HIV-1 Tat induces miR-132 leading to neurite shortening and neurotoxicity

2.1 Levels of miR-132 in Tat-transfected astrocytoma and neuroblastoma cell lines

Dendritic pruning and shrinkage of neurite outgrowth are prominent pathological hallmarks of HIV-1 associated neurocognitive disorders in the post-cART era [61]. As shown in our data from Part I along with other groups, Tat protein causes neurite shortening [299]. Although chronic neuroinflammation associated with neuroAIDS is blamed for the aberrant morphology of neurons, the direct role of Tat in this process is evident despite lack of detailed molecular explanation of events. Regulation of dendritic morphology has been shown to be controlled heavily by microRNA, and small RNA array data from brain tissue of HIV patients is indicative of dysregulation in miRNA with potential involvement in this process [335]. A brain-enriched microRNA, miR-132, which regulates several proteins involved in controlling dendritic plasticity [302] has been found to be upregulated substantially in brain tissue from HIV patients with neurocognitive impairment [292]. Outside of CNS environment, miR-132 has also been shown to be highly upregulated in HIV infected CD4+ T cells [304]. Considering CREB-dependent expression of this miRNA [364] and the fact that Tat activates CREB via several pathways [324], we decided to investigate whether Tat can induce this microRNA and lead to the morphological abnormalities observed in HIV CNS and in vitro with Tat treatment of neurons. To determine the effects of Tat on miR-132 expression, we first expressed Tat in human astrocytoma cells U373.MG and human neuroblastoma SYH-SY5Y and determined miR-132 expression in those cells. Tat expression significantly induced miR-132 level in U373

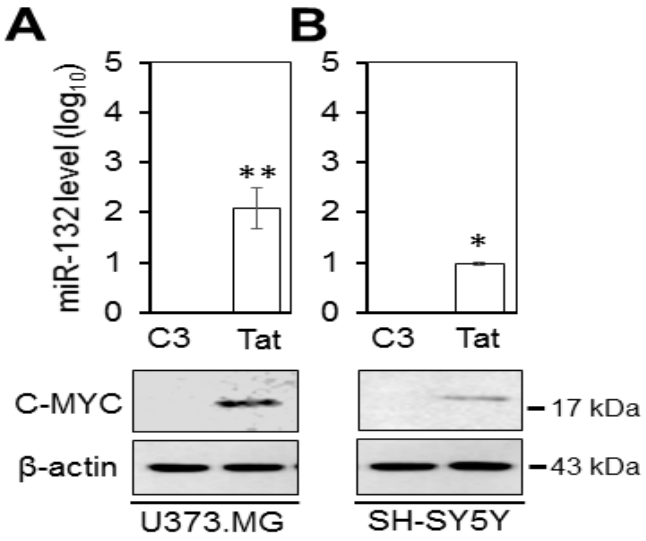
A
B
miR-132 level (log10)
5
4
3
2
1
0
**
*
C3
Tat
C-MYC
β-actin
17 kDa
43 kDa
U373.MG
SH-SY5Y

Figure 23. miR-132 induction following Tat expression. U373.MG (A) and SH-SY5Y (B) were transfected with Tat.Myc plasmid (Tat) or the cloning vehicle pcDNA3 (C3), and cultured for 48 hr, and harvested for RNA extraction, followed by qRT-PCR for miR-132 level (upper panels), or cell lysates, followed by Western blotting for Tat expression using an anti-C-MYC antibody (lower panels). β-actin was including as a loading control for Western blotting. Statistical analysis was performed using 2-tailed student's t test.

(**Fig. 23A**) and SH-SY5Y (**Fig. 23B**).

2.2 miR-132 levels in iTat primary mouse astrocytes following DOX induction

To ascertain Tat-induced miR-132 expression, we took advantage of the doxycycline (Dox)-inducible astrocyte-specific Tat-transgenic mice (iTat) [1, 203], in which Tat expression level and resulting neuropathologies following doxycycline treatment are comparable to those in the brain of HIV-infected subjects. Primary mouse astrocytes from wild-type (WT) and iTat mice were isolated and cultured to induce Tat expression by Dox. miR-132 was significantly induced in Dox-treated astrocytes derived from iTat mice but not in other astrocytes (**Fig. 24**). Tat expression was confirmed by semi-quantitative RT-PCR.

2.3 miR-132 levels in HIV-infected astrocytes

Next, we determined whether miR-132 was induced in astrocytes in the context of HIV infection. U373.MG were infected with VSV-G-pseudotyped HIV. Compared to the mock infection control (HIV containing no envelope), miR-132 was significantly induced in cells infected with VSV-G pseudotyped HIV (**Fig. 25A**). Similar results were obtained in human primary astrocytes (PHA) infected with VSV-G pseudotyped HIV-1 (**Fig. 25B**). HIV infection was confirmed by Western blotting for p24. These results show that miR-132 was significantly induced in Tat-expressing astrocytes and neurons and HIV-infected astrocytes.

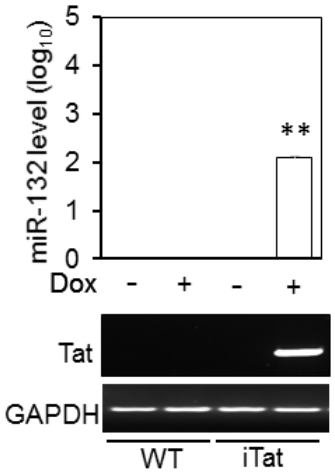
miR-132 level (log10)
5
4
3
2
1
0
**
Dox
-
+
-
+
Tat
GAPDH
WT
iTat

Figure 24. miR-132 induction following Tat induction in primary mouse astrocytes. Primary astrocytes were isolated from wild type (WT) mice and doxycycline (Dox)-inducible and astrocyte-specific HIV Tat transgenic mice (iTat), cultured in the presence of 5 mg/ml Dox (+), or in the absence of Dox (-) for 48 hr, and harvested for RNA isolation, followed by qRT-PCR for miR-132 level (upper panel), or semi-quantitative RT-PCR for Tat (lower panel). GAPDH was included as a loading control for Tat RT-PCR. Statistical analysis was performed using one-way ANOVA.

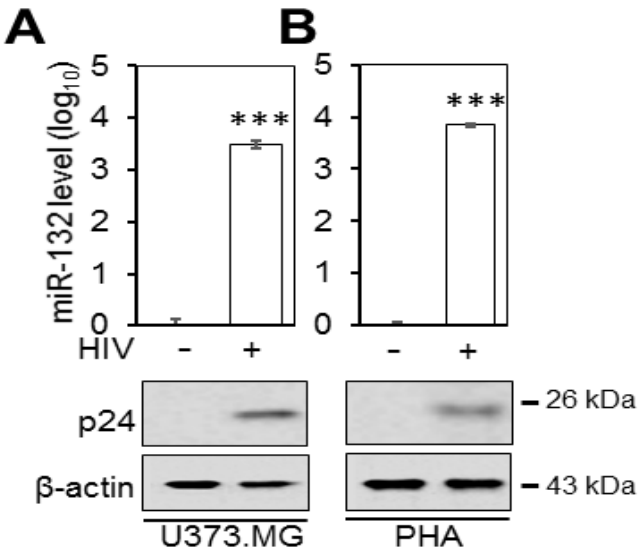
A
B
miR-132 level (log10)
5
4
3
2
1
0
***
***
HIV
-
+
-
+
p24
β-actin
26 kDa
43 kDa
U373.MG
PHA

Figure 25. miR-132 induction following HIV-1 infection of astrocytes. U373.MG (A) and primary human astrocytes (PHA) (B) were infected with VSV-G pseudotyped HIV (+), cultured for 3 days, and harvested for RNA extraction, followed by qRT-PCR for miR-132 level, or cell lysates, followed by Western blotting for p24 expression using an anti-p24 antibody. Pseudotyped HIV containing no envelope (-) was included as an infection control (Mock). snRNA U6 level was also determined by qRT-PCR. miR-132 level was normalized to snRNA U6 level and expressed as fold changes compared to the control. The data were mean ± SD of triplicates and/or representative of three independent experiments. Statistical analysis was performed using one-tailed student's T test between control and Tat transfected cells.

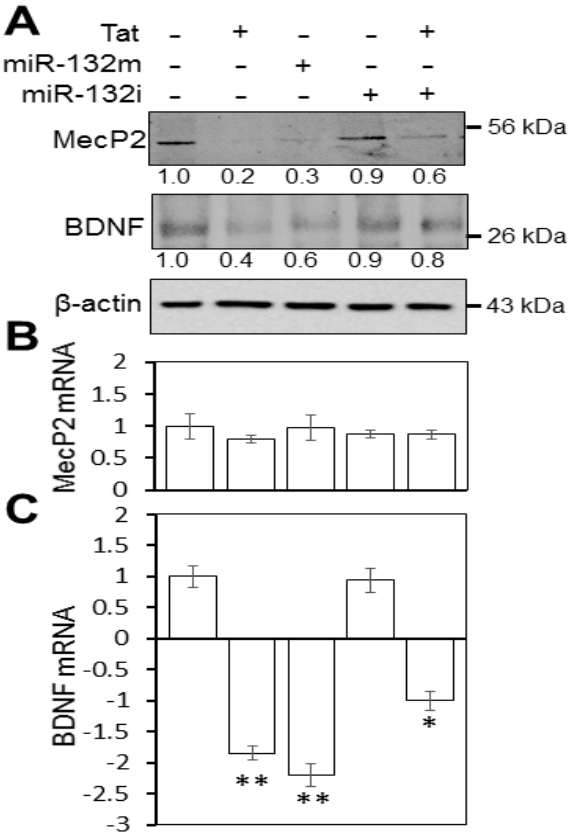
A
Tat - + - - +
miR-132m - - + - -
miR-132i - - - + +
MecP2
56 kDa
1.0 0.2 0.3 0.9 0.6
BDNF
26 kDa
1.0 0.4 0.6 0.9 0.8
β-actin
43 kDa
B
MecP2 mRNA
2
1.5
1
0.5
0
C
BDNF mRNA
2
1.5
1
0.5
0
-0.5
-1
-1.5
-2
-2.5
-3
**
**
*

Figure 26. Effects of Tat expression on miR-132 targets in primary human astrocytes. Primary human astrocytes were transfected with Tat.Myc, miR-132 mimic (miR-132m), and/or miR-132 inhibitor (miR-132i), cultured for 48 hr, and harvested for cell lysates, followed by Western blotting (A), or RNA isolation, followed by qRT-PCR for MecP2 (B) and BDNF (C). Statistical analysis was performed using one-way ANOVA.

2.4 Tat expression down-modulated expression of miR-132 target genes

2.4.1 miR-132 target repression in Tat-transfected primary human astrocytes

The mRNA targets of miR-132 within the CNS include MecP2 and p250GAP. BDNF transcription is directly controlled by MecP2 and therefore BDNF is an indirect target of miR-132. Thus, we determined whether Tat expression altered expression of those miR-132 target genes. Human primary astrocytes were first used. miR-132 mimic (miR-132m) was included as a control. Both Tat and miR-132 expression led to a lower level of MecP2 and BDNF protein expression in human primary astrocytes (**Fig. 26A**). To further determine whether Tat-induced down-modulation of MecP2 and BDNF was mediated through miR-132, we included miR-132 inhibitor (miR-132i) in the experiments. miR-132i expression alone did not significantly affect constitutive MecP2 and BDNF expression but considerably abrogated the down-modulation of MecP2 and BDNF expression by Tat. In addition, MecP2 and BDNF mRNA levels were determined. There were no changes of MecP2 mRNA by Tat, miR-132m, and/or miR-132i (**Fig. 26B**), while BDNF mRNA exhibited a pattern of changes similar to its protein (**Fig. 26C**).

2.4.2 miR-132 target repression in DOX-induced primary mouse astrocytes

Next, we determined the relationship between Tat expression and miR-132 target gene expression in mouse primary astrocytes from WT or iTat mice. Compared to WT primary astrocytes (**Fig. 27A-C**), Dox treatment of iTat primary astrocytes led to a lower level of

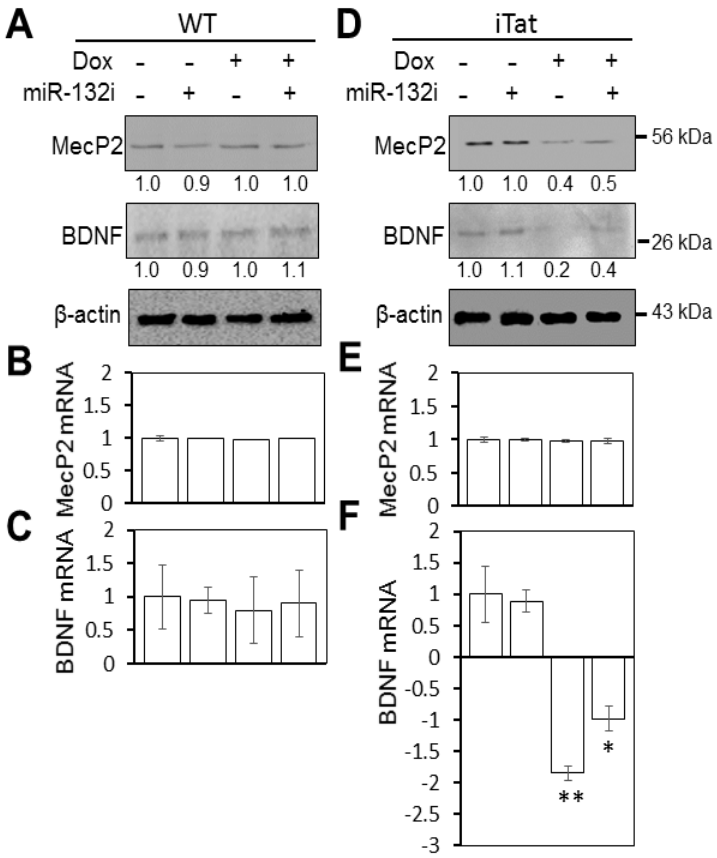
A
WT
Dox - - + +
miR-132i - + - +
MecP2
1.0 0.9 1.0 1.0
BDNF
1.0 0.9 1.0 1.1
β-actin
D
iTat
Dox - - + +
miR-132i - + - +
MecP2
56 kDa
1.0 1.0 0.4 0.5
BDNF
26 kDa
1.0 1.1 0.2 0.4
β-actin
43 kDa
B
MecP2 mRNA
2
1.5
1
0.5
0
E
MecP2 mRNA
2
1.5
1
0.5
0
C
BDNF mRNA
2
1.5
1
0.5
0
F
BDNF mRNA
2
1.5
1
0.5
0
-0.5
-1
-1.5
-2
-2.5
-3
*
**

Figure 27. Effects of Tat expression on miR-132 targets in primary mouse astrocytes. Primary astrocytes were isolated from WT (A-C) and iTat mice (D-F), cultured in the presence (+) or absence (-) of 5 mg/ml Dox for 48 hr, transfected with miR-132i, cultured for additional 24 hr, harvested for cell lysates, followed by Western blotting (A & D), or RNA isolation, followed by qRT-PCR for MecP2 (B & E) and BDNF (C & F). A control miRNA and pcDNA3 were included to equalize the input DNA or miRNA. The qPCR data were mean ± SD of triplicates and representative of three independent experiments. Western blots were quantitated using Image J software and were representative of three independent experiments. Statistical analysis was performed using one-way ANOVA between control, Tat, miR-132m, miR-132i, and combined Tat+miR-132i transfected samples.

MecP2 and BDNF protein expression, no changes in MecP2 mRNA, and a low level of BDNF mRNA, and miR-132i decreased the down-modulation of MecP2 and BDNF protein and BDNF mRNA (**Fig. 27D-F**).

2.4.3 miR-132 target repression in Tat-transfected neurons

We also assessed the protein levels of miR-132 targets in relation to Tat, miR-132m, and miR-132i expression in SH-SY5Y. In addition to MecP2 and BDNF, the protein level of p250GAP, a neuron specific target of miR-132, was analyzed. Similar to the findings in astrocytes, there were considerably lower levels of MecP2 and BDNF protein and slightly lower levels of p250GAP protein in Tat- and miR-132m-transfected cells (**Fig. 28**). miR-132i rescued MecP2 protein expression from Tat-induced down-modulation, but had no apparent effects on BDNF and p250GAP expression. Taken together, these results indicate that Tat expression resulted in down-modulation of miR-132 target genes through miR-132 induction.

2.5 Involvement of CREB phosphorylation and Tat basic domain in Tat-induced miR-132 expression

HIV-1 Tat has been shown to regulate transcription of a number of host genes and miRNA through a number of transcriptional factors including CREB [101, 204, 205, 322, 327, 333, 365-367]. miRNA expression is mainly regulated at the transcriptional level (see review

[368]). The primary sequence, the seed region, and the gene structure of miR-132 are well conserved between human and mouse [369]. A total of five transcriptional binding sites have been characterized within the miR-132 promoter [364, 370, 371]: four sites for CREB, one site for repressor element 1 silencing transcription factor/neuron-restrictive factor (REST/NRSF). Thus, we determined the possibility of the involvement of CREB phosphorylation in Tat-induced miR-132 expression. U373.MG were first used. Tat expression led to phosphorylation of CREB (**Fig. 29A**) and miR-132 induction (**Fig. 29B**). Deletion of Tat basic domain (ΔBD) completely abrogated Tat-induced CREB phosphorylation and miR-132 expression. Then, human primary astrocytes and SH-SY5Y

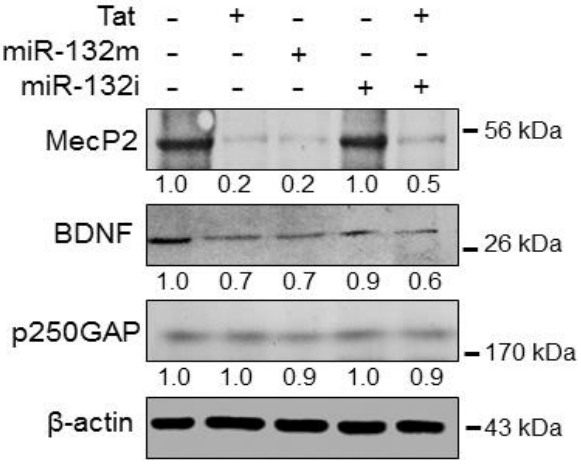
Tat - + - - +
miR-132m - - + - -
miR-132i - - - + +
MecP2
56 kDa
1.0 0.2 0.2 1.0 0.5
BDNF
26 kDa
1.0 0.7 0.7 0.9 0.6
p250GAP
170 kDa
1.0 1.0 0.9 1.0 0.9
β-actin
43 kDa

Figure 28. Effects of Tat expression on miR-132 targets in neurons. SH-SY5Y were transfected with Tat.Myc, miR-132 mimic (miR-132m), and/or miR-132 inhibitor (miR-132i), cultured for 48 hr, and harvested for cell lysates, followed by Western blotting. A control miRNA and pcDNA3 were included to equalize the input DNA or miRNA. Western blots were quantitated using Image J software and were representative of three independent experiments.

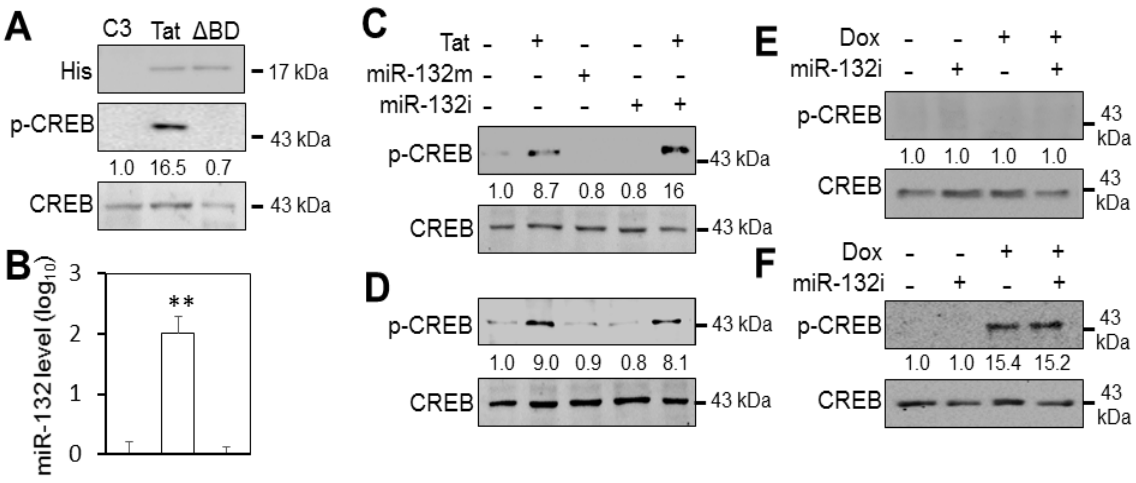
A
C3
Tat
ΔBD
His
17 kDa
p-CREB
43 kDa
1.0 16.5 0.7
CREB
43 kDa
B
miR-132 level (log10)
3
2
1
0
**
C
Tat - + - - +
miR-132m - - + - -
miR-132i - - - + +
p-CREB
43 kDa
1.0 8.7 0.8 0.8 16
CREB
43 kDa
D
p-CREB
43 kDa
1.0 9.0 0.9 0.8 8.1
CREB
43 kDa
E
Dox - - + +
miR-132i - + - +
p-CREB
43 kDa
1.0 1.0 1.0 1.0
CREB
43 kDa
F
Dox - - + +
miR-132i - + - +
p-CREB
43 kDa
1.0 1.0 15.4 15.2
CREB
43 kDa

Figure 29. CREB phosphorylation by Tat and its requirement for Tat basic domain. A & B. U373.MG were transfected with Tat.His or basic domain-deleted Tat (ΔBD.His) plasmid, cultured for 48 hr, and harvested for cell lysates, followed by Western blotting (A), or RNA isolation, followed by qRT-PCR for miR-132 level (B). C3 was used as the control, snRNA U6 was used to normalize miR-132 level. C & D. Primary human astrocytes (C) and SH-SY5Y (D) were transfected with Tat, miR-132m, and/or miR-132i, cultured for 48 hr, and harvested for cell lysates, followed by Western blotting. A control miRNA and pcDNA3 were included to equalize the input DNA or miRNA. E & F. Primary astrocytes were isolated from WT and iTat mice, cultured in the presence (+) or absence (-) of 5 mg/ml Dox for 48 hr, transfected with miR-132i, cultured for additional 24 hr, harvested for cell lysates, followed by Western blotting. A control miRNA was included to equalize the input miRNA. The qPCR data were mean ± SD of triplicates and representative of three independent experiments. Western blots were quantitated using Image J software and were representative of three independent experiments. Statistical analysis for B was performed using one-way ANOVA between c3, Tat, and ΔBD transfected samples.

were used along with miR-132m and miR-132i. In human primary astrocytes, Tat expression induced CREB phosphorylation (**Fig. 29C**). Although miR-132m and miR-132i expression did not lead to significant changes in constitutive CREB phosphorylation, co-expression of Tat and miR-132i resulted in a much higher level of CREB phosphorylation. In SH-SY5Y, Tat expression induced CREB phosphorylation (**Fig. 29D**) although both miR-132m and miR-132i showed no effects on the constitutive level of CREB phosphorylation. Furthermore, primary astrocytes from WT and iTat mice were also used to assess the relationship between Tat expression and CREB phosphorylation. Compared to the WT astrocytes (**Fig. 29E**), iTat astrocytes treated with Dox led to CREB phosphorylation (**Fig. 29F**), which was not affected by miR-132i expression. These results suggest that CREB phosphorylation and Tat basic domain are likely involved in Tat-induced miR-132 expression.

2.6 miR-132 induction did not contribute to Tat-induced astrocyte activation

Tat expression in astrocytes induces a highly inflammatory profile and leads to the dysregulation of astrocyte functions, termed astrocyte activation, or astrocytosis [205, 206], characterized by increased GFAP expression [206, 372] and expression of pro-Inflammatory cytokines such as IL-6 and TNF-α, and chemokines such as CCL2 [373-375]. Next, we determined whether miR-132 induction was involved in Tat-induced GFAP, CCL-2, IL-6, and TNF-α expression. As shown previously [203] Tat expression induced GFAP expression in human primary astrocytes when compared to the C3 control (**Fig. 30A**

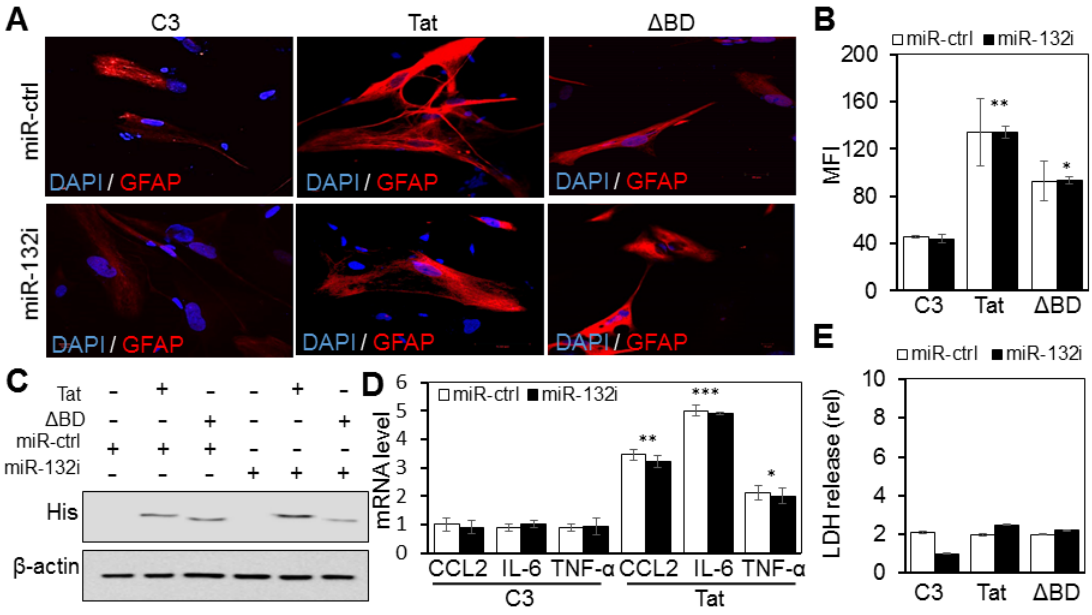
A
C3
Tat
ΔBD
miR-ctrl
miR-132i
DAPI / GFAP
B
miR-ctrl
miR-132i
MFI
200
160
120
80
40
0
**
*
C3
Tat
ΔBD
C
Tat
ΔBD
miR-ctrl
miR-132i
His
β-actin
D
miR-ctrl
miR-132i
mRNA level
6
5
4
3
2
1
0
**
***
*
CCL2
IL-6
TNF-α
CCL2
IL-6
TNF-α
C3
Tat
E
miR-ctrl
miR-132i
LDH release (rel)
10
8
6
4
2
0
C3
Tat
ΔBD

Figure 30. Effects of miR-132 induction on GFAP expression, cytokine/chemokine expression, and astrocyte survival. Primary human astrocytes were transfected with Tat.His (Tat), ΔBDTat.His (ΔBD), and miR-132i (miR-132i), cultured for 48 hr, and harvested for immunofluorescence staining for GFAP (A), Western blotting (B), or qRT-PCR (D). The mean fluorescence intensity (MFI) of GFAP expression was determined using ImageJ software (C). Meanwhile, the cell culture supernatants were collected and assayed for the LDH release (E). The data were mean ± SD of triplicates and representative of three independent experiments. Statistical analysis for B, D, and E was performed using one-way ANOVA.

& B). ΔBD Tat mutant also induced GFAP expression albeit to a lesser extent; and miR-132i did not show any effect on GFAP expression induced by Tat or ΔBD. Tat and ΔBD expression was confirmed by Western blotting (**Fig. 30C**). Similarly, Tat induced CCL-2, IL-6, and TNF-α expression when compared to the C3 control (**Fig. 30D**). But miR-132i had little effects on constitutive and Tat-induced expression of those molecules. In addition, we also determined effects of Tat on the LDH release, an indicator of cell viability. Compared to the C3 control, Tat or ΔBD expression showed little effects on the LDH release. Taken together, these results suggest that miR-132 induction is unlikely involved in Tat-induced astrocyte activation and that Tat expression itself does not affect astrocyte survival.

2.7 Tat-induced miR-132 expression contributed to Tat direct neurotoxicity

To determine whether Tat-induced miR-132 contributed to Tat direct neurotoxicity, SH-SY5Y were transfected with Tat and miR-132i and assayed for the LDH release from those cells. Compared to the C3 control, Tat expression increased the LDH release from those cells (**Fig. 31**). Meanwhile, miR-132i expression significantly diminished Tat-induced LDH release from those cells. These results confirm that Tat has direct neurotoxic activity and suggest that miR-132 induction could contribute to Tat neurotoxicity.

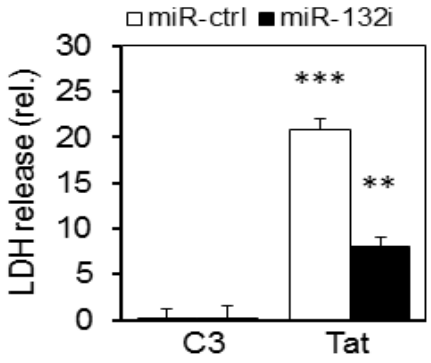
miR-ctrl
miR-132i
LDH release (rel.)
30
25
20
15
10
5
0
***
**
C3
Tat

Figure 31. Role of miR-132 induction in Tat neurotoxicity. SH-SY5Y were transfected with Tat.Myc (Tat), miR-132i, or both and cultured for 48 hr. The cell culture supernatants were collected and assayed for the LDH release. C3 and a control miRNA (miR-ctrl) were used to equalize the input amount of DNA and miRNA. The data were mean ± SD of triplicates and representative of three independent experiments. Statistical analysis was performed using one-way ANOVA.

2.8 Tat expression led to increased miR-132 in astrocyte-derived exosomes

Virtually all eukaryotic cells including astrocytes produce exosomes, which serve as a major extracellular vehicle to transport miRNA and proteins among cells [273, 352]. Thus, we first determined whether Tat-induced miR-132 expression would lead to increased miR-132 in astrocyte-derived exosomes. Compared to the C3 control, increased miR-132 was detected in exosomes derived from Tat-expressing cells (**Fig. 32A**). miR-132i expression significantly decreased Tat-induced miR-132 packaging into the exosomes from astrocytes, further supporting the notion that miR-132 is sorted into the exosomes. The exosome purity was confirmed by lack of cytochrome C and presence of TSG-101 in the exosomes using Western blotting (**Fig. 32B**). Consistent with our previous studies [376], Tat was also detected in the exosomes. In addition, we labeled miR-132m with Cy3 and transfected it into U373.MG, and further confirmed Cy3-labled miR-132m transfection by flow cytometry (**Fig. 32C**). Furthermore, we obtained exosomes from Cy3-labled miR-132m-transfected astrocytes and exposed them to SH-SY5Y and determined whether those cells would take up the labeled miRNA by flow cytometry. Cy3-labled miR-132m were detected in those cells (**Fig. 32D**). These results show that Tat-induced miR-132 is packaged into astrocyte-derived exosomes, which can be taken up by neurons.

2.9 Astrocyte-derived miR-132 shortened neurites

We next sought to determine whether transfer of exosome-associated miR-132 from astrocytes to neurons could affect the morphology of neuron dendrites and formation of synapse. To this end, WT and iTat primary astrocytes were prepared, cultured in the

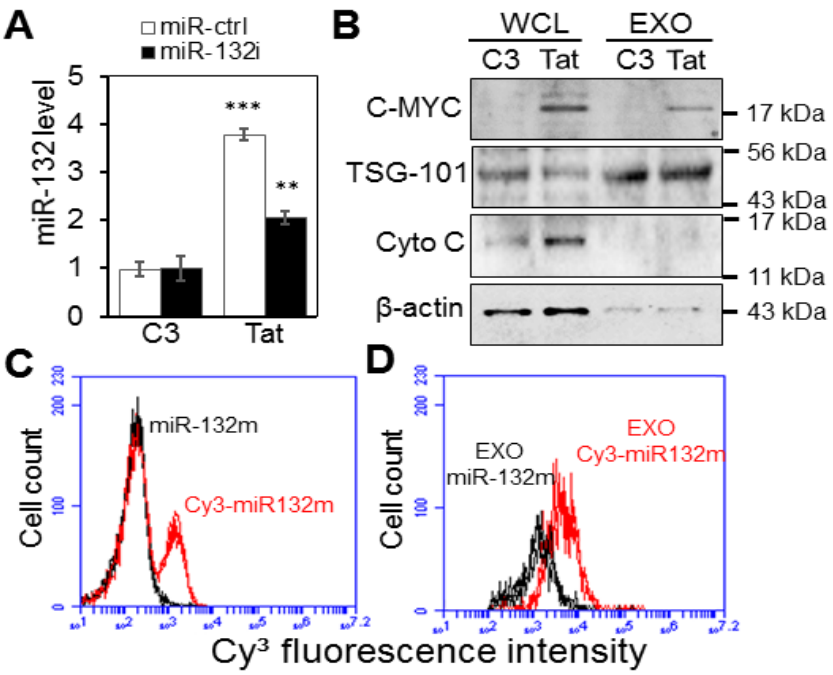
A
miR-ctrl
miR-132i
miR-132 level
5
4
3
2
1
0
***
**
C3
Tat
B
WCL
EXO
C3 Tat
C3 Tat
C-MYC
17 kDa
TSG-101
56 kDa
43 kDa
Cyto C
17 kDa
11 kDa
β-actin
43 kDa
C
Cell count
miR-132m
Cy3-miR132m
D
Cell count
EXO
miR-132m
EXO
Cy3-miR132m
Cy³ fluorescence intensity

Figure 32. Exosomal miR-132 and its transfer to neurons. A & B. U373.MG were transfected with Tat, miR-132i, or both, and cultured for 48 hr. The cell culture supernatants were collected and used to isolate exosomes. RNA was isolated from exosomes and analyzed for qRT-PCR for miRNA-132 level (A). Exosomal miR-132 was normalized to let-7b. Lysates were prepared from the cells (WCL) and exosomes (EXO) and analyzed by Western blotting (B). C & D. U373.MG were transfected with Cy^3 dye miR-132m (Cy^3-miR-132m) or unlabeled miR-132m as a control, cultured for 12 hr, and harvested for Cy^3 signal using flow cytometry (C). The cell culture supernatants were collected and used to isolate exosomes. SH-SY5Y were cultured in the presence of the exosomes for 6 hr and assayed for Cy^3 signal using flow cytometry (D). The qRT-PCR data were mean ± SD of triplicates and representative of three independent experiments. The Western blots and the flow cytometry histograms were representative of three independent experiments. Statistical analysis for A was performed using one-way ANOVA.

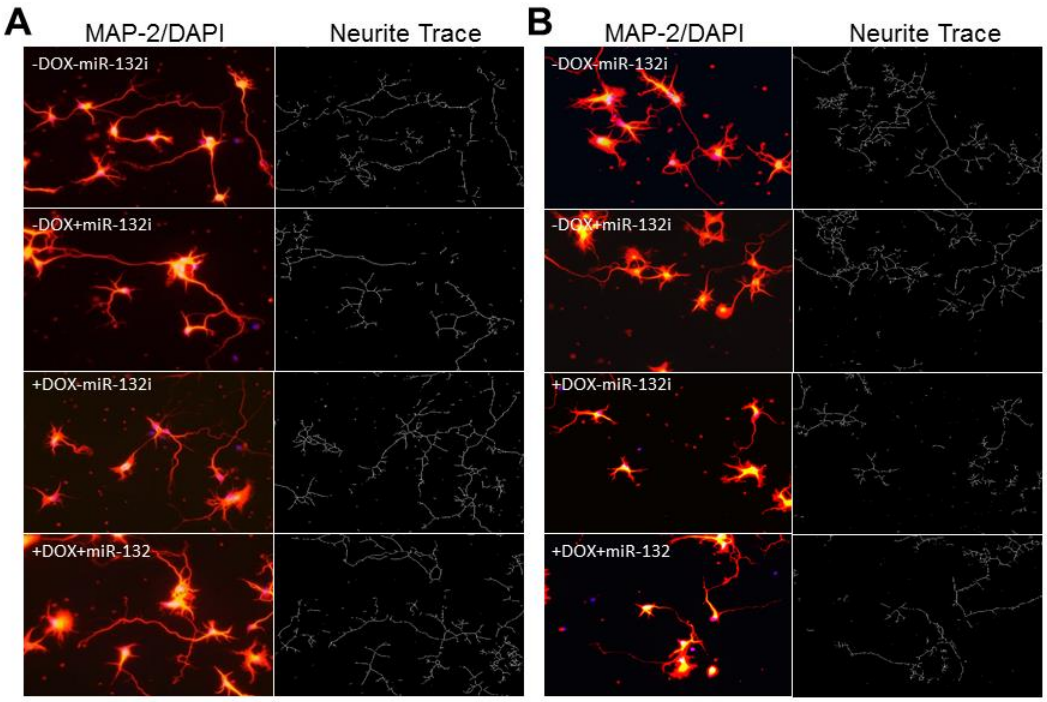
A
MAP-2/DAPI
Neurite Trace
-DOX-miR-132i
-DOX+miR-132i
+DOX-miR-132i
+DOX+miR-132
B
MAP-2/DAPI
Neurite Trace
-DOX-miR-132i
-DOX+miR-132i
+DOX-miR-132i
+DOX+miR-132

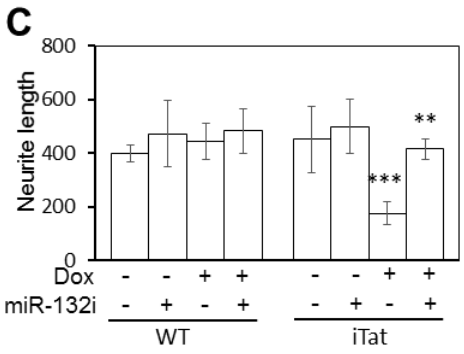
C
Neurite length
800
600
400
200
0
***
**
Dox - - + + - - + +
miR-132i - + - + - + - +
WT
iTat

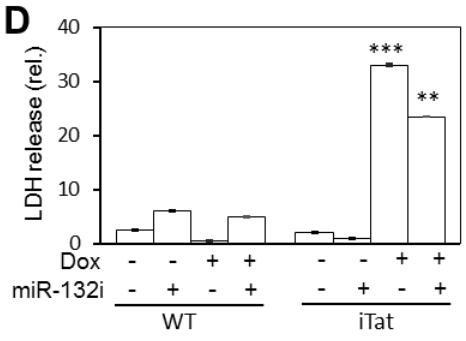
D
LDH release (rel.)
40
30
20
10
0
***
**
Dox - - + + - - + +
miR-132i - + - + - + - +
WT
iTat

Figure 33. Effects of Tat expression and exosomal miR-132 induction on neurite morphogenesis. Primary mouse astrocytes were isolated from WT (A) and iTat (B), cultured in the presence (+Dox) or absence of (-Dox) of 5 mg/ml for 48 hr, transfected with miR-132i (+miR-132i) or a control miRNA (-miR-132i) and continued to culture for 48 hr. The cell culture supernatants were collected and used to isolate exosomes. Primary mouse cortical neurons were plated and cultured on poly-lysine coated coverslips in a 24-well plate at the density of 85,000 cells/well for and continued to culture in the presence of the exosomes isolated above for 48 hr. Then, the cells were harvested for immunofluorescence staining for MAP-2 and counterstained with DAPI (A & B). The average length of neurites was determined using ImageJ Neurite Tracer and calculated based on the occupied pixel areas and three randomly selected images of each treatment group (C). The cell culture supernatants were collected and assayed for LDH release (D). The images and data were representative of three independent experiments. Statistical analysis was performed using one-way ANOVA.

presence or absence of Dox, and transfected with miR-132i, exosomes were prepared from those samples and exposed to primary mouse cortical neurons. The primary cortical neurons were stained for MAP-2, and the neurite length of the primary cortical neurons that were exposed to exosomes from WT astrocytes (**Fig. 33A**) and exosomes from iTat astrocytes (**Fig. 33B**) was quantitated using the neurite trace analysis. Compared to the WT controls, exosomes from Dox-treated iTat astrocytes showed significantly shorter neurites (**Fig. 33C**), which was significantly reversed by miR-132i expression. In parallel, exosomes from Dox-treated iTat astrocytes increased the LDH release from the neurons, which was significantly diminished by miR-132i expression (**Fig. 33D**).

2.10 Tat induced miR-132 did not affect synaptic formation

The exosome-treated primary cortical neurons were also stained for synaptophysin (SYP), a pre-synaptic marker, or post-synaptic density protein (PSD-95), a post-synaptic marker. The density of SYP and PSD-95 of the primary cortical neurons that were exposed to exosomes from WT astrocytes (**Fig. 34A**) and exosomes from iTat astrocytes (**Fig. 34B**) was similarly quantitated. Compared to the WT controls, exosomes from Dox-treated iTat astrocytes significantly decreased the density of both SYP and PSD-95 in those cells (**Fig. 34C**), which was not rescued by miR-132i expression. Similar results were obtained by Western blotting (**Fig. 34D**). These results showed that Tat-induced miR-132 in astrocytes adversely affects neurite morphogenesis and contributes to astrocyte-mediated Tat neurotoxicity.

2.11 Schematic model for Tat induced miR-132 expression in astrocytes and its effects on neurons

In summary, the findings from the current study support a new model of Tat-impaired neurite outgrowth and neuron survival (**Fig. 35**). Tat-impaired neurite outgrowth could be direct and astrocyte-mediated. Tat uptake into neurons induces miR-132 expression through CREB phosphorylation, down-regulates MecP2 and BDNF expression in neurons, and impairs neurite outgrowth and neuron survival; Alternatively, Tat expression in astrocytes resulting from HIV-1 infection or Tat uptake into astrocytes induces miR-132 expression through CREB phosphorylation and down-regulates BDNF expression. miR-132 induction in astrocytes leads to increased miR-132 release into exosomes from astrocytes, uptake of exosome-associated miR-132 into neurons, down-regulation of MecP2 and BDNF expression in neurons, and impairs neurite outgrowth and neuron survival. In addition, BDNF down-regulation in astrocytes results in less BDNF available for neurons and adversely affects neurite outgrowth and neuron survival.

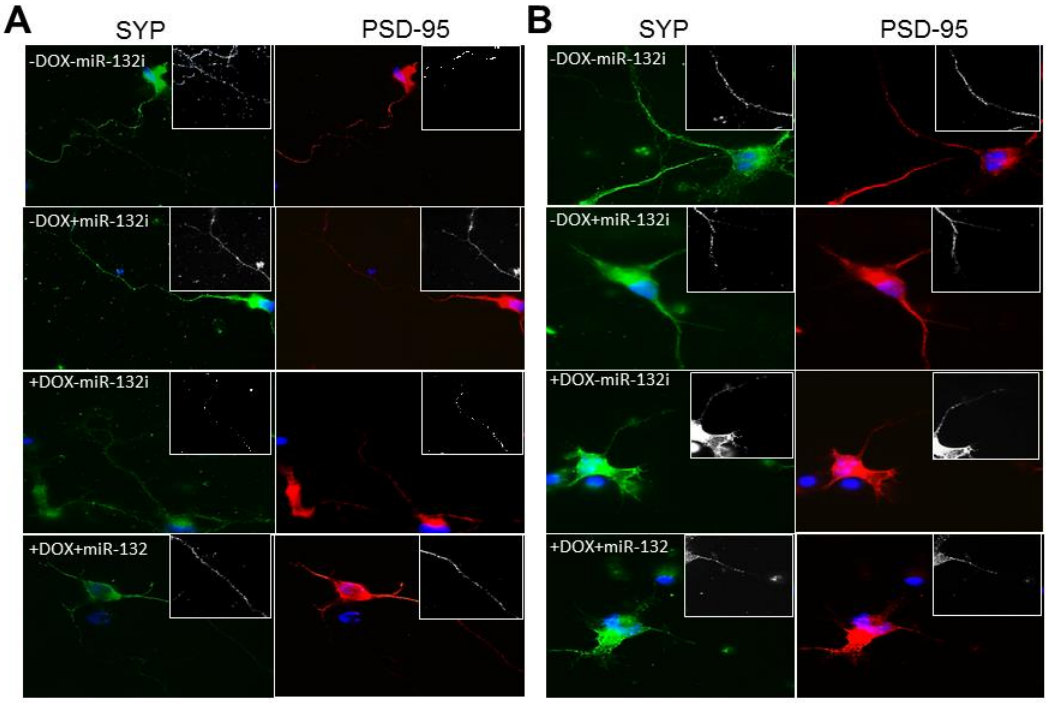
A
SYP
PSD-95
-DOX-miR-132i
-DOX+miR-132i
+DOX-miR-132i
+DOX+miR-132
B
SYP
PSD-95
-DOX-miR-132i
-DOX+miR-132i
+DOX-miR-132i
+DOX+miR-132

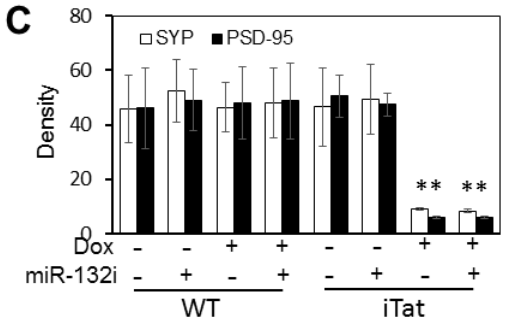
C
SYP
PSD-95
Density
80
60
40
20
0
**
**
Dox
miR-132i
WT
iTat

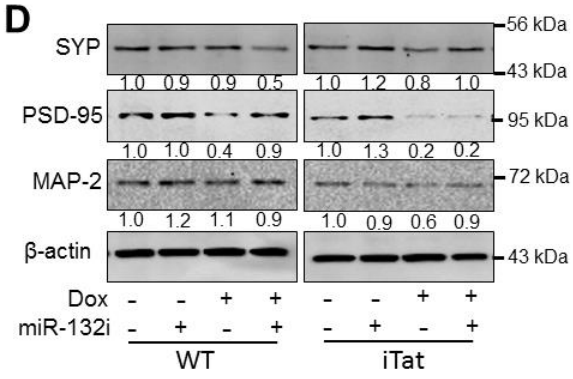
D
SYP
PSD-95
MAP-2
β-actin
56 kDa
43 kDa
95 kDa
72 kDa
43 kDa
1.0 0.9 0.9 0.5
1.0 1.2 0.8 1.0
1.0 1.0 0.4 0.9
1.0 1.3 0.2 0.2
1.0 1.2 1.1 0.9
1.0 0.9 0.6 0.9
Dox
miR-132i
WT
iTat

Figure 34. Effects of Tat expression and exosomal miR-132 induction on synaptic formation. Primary mouse astrocytes were isolated from WT (A) and iTat (B), cultured in the presence (+Dox) or absence of (-Dox) of 5 mg/ml for 48 hr, transfected with miR-132i (+miR-132i) or a control miRNA (-miR-132i) and continued to culture for 48 hr. The cell culture supernatants were collected and used to isolate exosomes. Primary mouse cortical neurons were plated and cultured on poly-lysine coated coverslips in a 24-well plate at the density of 85,000 cells/well for and continued to culture in the presence of the exosomes isolated above for 48 hr. Then, the cells were harvested for immunofluorescence staining for synaptophysin (SYP) for presynapse formation and for PSD-95 for postsynapse formation and counterstained with DAPI (A & B). SYP and PSD-95 immunostaining along with skeleton conversion of fluorescent images was performed, the density of synaptic protein staining was determined using ImageJ software and based on the occupied pixel areas and three randomly selected images of each treatment group (C). The cells were harvested for cell lysates, followed by Western blotting (D). The images and data were representative of three independent experiments.

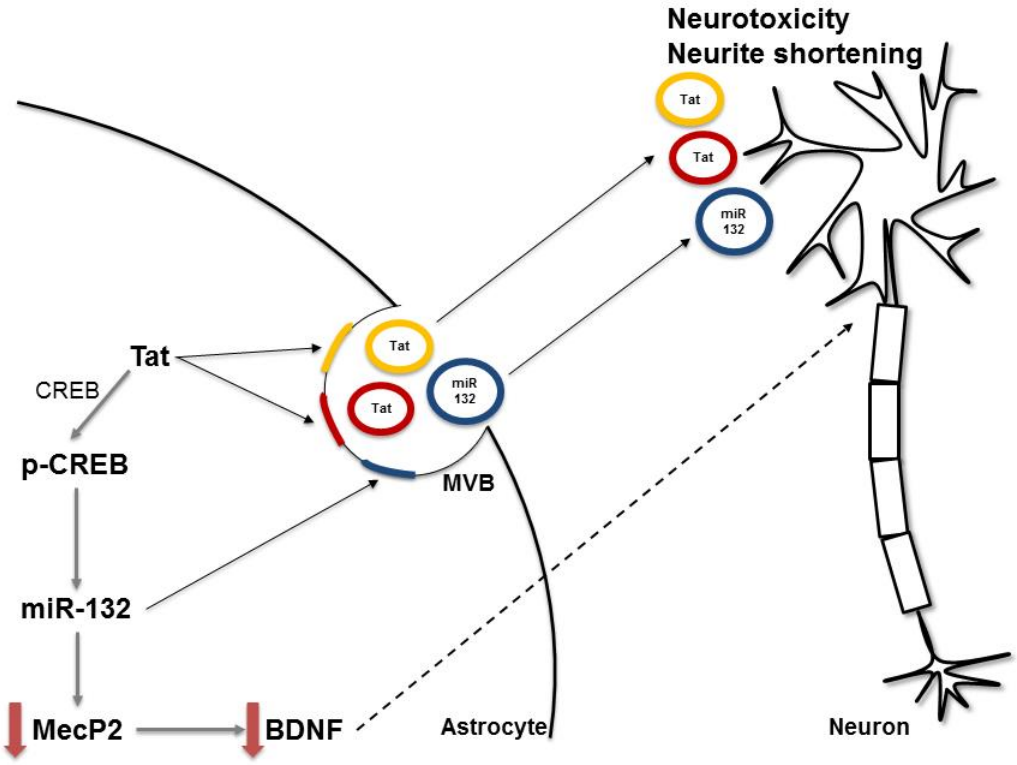
Neurotoxicity
Neurite shortening
Tat
Tat
miR
132
Tat
CREB
p-CREB
Tat
miR
132
MVB
miR-132
MecP2
BDNF
Astrocyte
Neuron

Figure 35. A new model for Tat-impaired neurite outgrowth. Tat impairs neurite outgrowth through its uptake into neurons, CREB phosphorylation, miR-132 induction and MecP2 and BDNF down-regulation; Alternatively, Tat-impaired neurite outgrowth results from HIV-1 infection and Tat expression in astrocytes, CREB phosphorylation, miR-132 induction, and BDNF down-regulation. miR-132 induction in astrocytes increases exosome-associated miR-132 release from astrocytes, uptake of exosome-associated miR-132 into neurons, MecP2 and BDNF down-regulation of MecP2 in neurons. In addition, BDNF down-regulation in astrocytes deprives neurons of BDNF, which impairs neurite outgrowth and neuron survival.

DISCUSSION

Summary of the results

In the first part of the study, we demonstrated Tat association with exosomes derived from Tat-expressing primary mouse astrocytes (**Fig. 9**), Tat-transfected U373.MG (**Fig. 13A, 13B**), Tat-transfected 293T (**Fig. 13C, 13D**), and HIV-infected MT4 (**Fig. 16**). Tat association with exosomes, particularly AchE+CD63+ exosomes was further confirmed by OptiPrep gradient fractionation (**Fig. 12, 14, 15 & 17**) and AchE antibody-based immunodepletion of exosomes (**Fig. 18**). In addition to the HIV-1 LTR promoter-based cell assay, Tat in the form of exosomes was shown to be biologically active, demonstrated by exosome-associated Tat-induced neurotoxicity such as shortened neurites and decreased neuron survival (**Fig. 19 & 20**). Lastly, we showed that deletion of the basic domain from Tat exhibited no apparent effects on Tat trafficking into exosomes, despite its dominant negative function remained (**Fig. 21**). Taken together, these results provide strong evidence to support exosome-associated Tat release and uptake, a previously unrecognized pathway for Tat.

In the second part, we first determined the potential of Tat in the induction of miR-132, a brain-enriched microRNA with substantial roles in the regulation of synaptodendritic plasticity. We found that Tat expression significantly induces this miRNA in astrocytoma (**Fig. 23A**), and neuroblastoma cell lines (**Fig. 23B**), and primary mouse astrocytes (**Fig. 24**). HIV infection of astrocytoma cells (**Fig. 25A**) and primary human astrocytes (**Fig. 25B**) also led to significant miR-132 upregulation. Next, we showed repression of miR-

132 targets following Tat expression in primary human astrocytes (**Fig. 26**), primary mouse astrocytes (**Fig. 27**) and in neurons (**Fig. 28**). We then demonstrated the mechanism of Tat induction of miR-132 through the phosphorylation of CREB by Tat (**Fig. 29**) and ruled out the possibility of miR-132 involvement in Tat's activation of astrocytes (**Fig. 30**). Using miR-132 antagomir, we showed that miR-132 overexpression leads to neurotoxicity (**Fig. 31**). Considering the significance of exosomal glia-neuron communications [377] and the direct link between the miRNA processing pathway and exosomal biogenesis [378], we determined the miR-132 content of Tat-expressing astrocyte exosomes. We found significant levels of miR-132 in exosomes from these astrocytes which were taken up by neurons (**Fig. 32**), and resulted in neurite shortening (**Fig. 33**). We did not find miR-132 involvement in reduction of synaptic protein levels by Tat (**Fig. 34**). These data provide new mechanistic insights of Tat's injury to dendritic arbor and identify novel pathways that potentially contribute to Tat neurotoxicity.

Presence of Tat in both ESCRT and Ceramide generated exosomes

Exosomes are bi-layered extracellular vesicles with a size range of 50-150 nm and constitutively secreted by many cells and carry significant RNA and protein cargos and serve as intercellular messengers to regulate physiological and pathophysiological processes in target cells [236-238]. They are generated by inward budding of the multivesicular body (MVB) membrane, formation of intraluminal vesicles, fusion of the MVB membrane with the plasma membrane, and release of the intraluminal vesicles from

MVB into the extracellular environment [239]. The intraluminal vesicles in the MVB could be formed by endosomal sorting complex required for transport (ESCRT)-dependent pathway and ceramide-dependent pathway [240]. The ESCRT-dependent pathway involves the sorting of monoubiquitinated cargos on the MVB membrane and the packaging of cargos into the vesicles [241]. The ceramide-dependent pathway mostly relies on lipids such as ceramide to induce inward vesicle budding of the MVB membrane and lipid raft formation [242, 243]. Thus, exosomes derived from those two pathways can by identified by specific markers: TSG101 for exosomes from ESCRT pathway [241, 244], GM1, CD63 and AchE for lipid raft-rich exosomes from ceramide pathway [243, 245-251]. Our results demonstrated the presence of Tat in exosomes derived from both ESCRT and ceramide pathways. More Tat was detected in exosomes from ceramide pathway than those from ESCRT pathway in astrocytes and HIV-infected CD4 T cells, while Tat was exclusively detected in ESCRT exosomes in 293T. These results are in agreement with the significant demand of astrocytes for major lipid raft components such as ceramide in their metabolism [379] and production of ceramide-rich exosomes in astrocytes [380]. Subsequent studies showed that disruption of ceramide synthesis by GW4869 abrogated Tat activity in ceramide-derived exosomes in astrocytes but did not have any effects on ESCRT-derived exosomes in 293T and that anti-AchE antibody depletion of AchE+/CD63+ exosomes significantly decreased Tat activity and astrocyte-mediated Tat neurotoxicity. These results further support Tat presence in both ceramide- and ESCRT-derived exosomes.

Involvement of the basic domain of Tat in membrane binding and trafficking

Unconventional secretion of Tat protein outside the cell has been attributed to Tat interaction with phosphatidylinositoal 4, 5-bisphosphate head groups in the phospholipid membranes and with negatively charged lipid groups in the membranes such as dioleoylphosphocholine head groups and lipid raft domains through its positively charged basic domain [381-385]. Tat has recently been shown to bind endolysosomal membranes resulting in enlarged and dysfunctional lysosomes [359]. Thus, it is conceivable that following exit from the nucleus or being taken up into the cell, Tat binds lipid raft domains on endocytic membranes that mature into late endosomes and MVB, leading to sorting of Tat into intraluminal vesicles and finally its release through exosomes. To directly determine if the basic domain of Tat is necessary for binding to endocytic membranes and gaining access to the exosome biogenesis machinery, we created a basic domain-deleted Tat mutant and studied its exosomal secretion. Although the basic domain deletion of Tat maintained dominant negative effects over Tat in Tat-mediated LTR transactivation, this mutant was detected in the exosomes (**Fig. 21A-C**). However, compared to direct inhibition of Tat-mediated LTR transactivation by the mutant (**Fig. 21C**), exosomes from cells expressing both Tat and the mutant showed much less inhibitory effects on Tat-mediated LTR transactivation (**Fig. 21D**). These results indicate that Tat interaction with biological membranes may not be involved in Tat trafficking to the endocytic system and exosome biogenesis apparatus. On the other hand, studies have shown that neutralizing the positive charges of Tat basic domain do not abolish the interaction of Tat with membranes [386] and that hydrophobic domains of Tat (aa 36-47) are capable of forming

bonds with lipid bilayers [284]. It is clear that additional studies are needed to determine the role of other Tat domains such as the hydrophobic domain in Tat traffic to the MVB.

Lack of detection of exosomal Tat in proteomics studies

It is interesting to note that two recent proteomic studies on exosomes from HIV-1 infected T cells have failed to detect Tat protein but have detected either known Tat-interacting cellular proteins such as CD38 and ANAXA5, and other viral components such as Gag, Env, and TAR miRNA in exosomes using the highly sensitive liquid chromatography-linked tandem mass spectrometry (LC-MS/MS) [264, 387]. However, lack of detection of Tat in exosomes from the infected cells in these two studies cannot simply be interpreted as absence of the protein. LC-MS/MS has not detected Tat protein in HIV-producing CD4 T cells [388-390] and in sera of HIV-infected patients [391]. Only one study has detected Tat protein in purified HIV using LC-MS/MS in combination with micro-capillary reversed phase liquid chromatography (μRPLC) [392], which has been shown to improve detection of low-abundant proteins such as Tat [393]. These findings suggest that LC-MS/MS alone is not sufficiently sensitive to detect trace amount of highly basic proteins such as Tat [394]. In addition, since Tat is not packaged into HIV, the Tat protein detected in the purified virus preparation above is likely derived from exosomes that were co-fractionated with HIV.

Advantages of Tat exosomal incorporation for viral pathogenesis

Viral proteins and nucleic acids and intact viruses have been shown to be present in exosomes from infected cells. In case of HIV, intact HIV, Gag protein, unspliced HIV-1 RNA, and HIV-derived microRNA have been detected in exosomes from HIV-infected cells [262-265]. Thus, exosomes from HIV-infected cells could contribute to transmission of the virus or work as a mechanism of defense against the virus. In this study, we showed that a fraction of HIV-1 Tat protein is released in the form of exosomes and is biologically active. Incorporation of Tat into exosomes can be considered advantageous for HIV-1 pathogenicity. The majority of Tat protein has been shown to secrete outside the infected cell while a trace amount of the protein remains in the nucleus to ensure efficient transcription of the viral genome [395]. Therefore, exosomal secretion of Tat will not negatively affect the life cycle of HIV-1. On the other hand, the non-discriminative nature of exosome uptake could afford access of exosome-associated Tat to diverse cell types and therefore enhance the adverse effects of HIV-1 infection. In the CNS, exosomes produced from HIV-infected microglia/macrophages and astrocytes can potentially improve the stability of Tat by protecting the protein from degradation, and expand the efficient delivery of Tat to other cells in the CNS including neurons. A recent study has shown that Tat is persistently expressed in the CNS in the era of combination antiretroviral therapy [37]. Thus, additional studies on therapeutic interventions targeted at exosome-associated Tat protein are warranted and may help mitigate the symptoms of HIV/neuroAIDS.

Tat phosphorylation of CREB

HIV-1 Tat damages the dendritic arbor, shortens neurites and reduces synaptic protein levels [64, 65, 68]. Widespread expression and secretion of this protein in the CNS of the HIV-infected population despite HAART [37] is strongly correlated with synaptodendritic damage, the hallmark of pathology in HAND [61, 396]. The reversible nature [346] of Tat's deleterious effects on dendritic integrity warrant a deeper understanding of the potential molecular events that connect Tat to the regulation of synaptodendritic plasticity.

We demonstrated that miR-132 induction was likely due to Tat's ability to induce phosphorylation of CREB (**Fig. 29**) and subsequent binding of phosphorylated CREB to CREB-responsive elements within the transcriptional control locus of miR-132 [364]. CREB phosphorylation also promotes the binding of phosphorylated CREB to CBP, which leads to the transactivation of the miR-132 loci containing CREB-responsive elements [326]. Tat expression leads to phosphorylation of CREB at Ser^{133} through several pathways [322-325]. Alternatively, Tat directly binds CBP, recruiting the histone acetyltransferase to the CRE [327]. Both CREB phosphorylation and CBP binding activities of Tat have been shown to be dependent on the basic domain of this protein [328, 329]. Our data showed complete abrogation of CREB phosphorylation and lack of miR-132 induction following transfection with basic-domain deleted Tat (**Fig. 29A & B**), further supporting Tat effects on CREB phosphorylation and the requirement of Tat basic domain for this effect. Despite a comparable level of Tat-induced CREB phosphorylation in both astrocytes (**Fig. 29C**) and neurons (**Fig. 29D**), the basal levels of total CREB and

phosphorylated CREB in neurons were higher than those in astrocytes. Greater involvement of CREB in neuronal responses has been noted in multiple processes related to development, survival, and synapse formation [397]. On the other hand, astrocytes employ fewer pathways of CREB activation in comparison to neurons. For instance, unlike neurons, astrocytes do not utilize calcium signaling pathways for CREB activation [398] and they lack B-raf kinase which mediates MAPK-dependent phosphorylation of CREB [399].

Basal expression levels of miR-132

We showed that HIV-1 Tat protein significantly upregulated miR-132 in astrocytes and neurons (**Fig. 23**). Unlike an early report [400], our data did not show a difference in the basal expression levels of this microRNA between the two cell types. Following Tat expression, however, astrocytes showed significantly higher fold changes in miR-132 compared to neurons. This might in part be due to the well documented activity-dependent nature of miR-132 expression in neurons which happens rapidly and in a transient fashion [401]. On the other hand, Tat transfection of neuronal cells was less efficient compared with astrocytes as supported by our immunoblotting results which showed a lower level of Tat expression in neurons.

Different outcomes of miR-132 target repression

miR-132 plays a crucial role in the development of neurons by regulating two targets in charge of controlling neurite outgrowth; MecP2, which is a potentiating factor of neurite

growth, and p250GAP which inhibits the outgrowth of neurites [321, 369]. The question is then which direction miR-132 expression takes the neurons in regards to neurite growth while this microRNA represses both an enhancer and an inhibitor of neurite outgrowth. The different temporal expression of p250GAP and MecP2 in development may likely provide the key. p250GAP is involved in neuronal differentiation and is expressed prior to MecP2 [402]. In fact, the studies that discovered p250GAP as a target of miR-132, only found repression of this target in immature neurons [364] and showed that miR-132 overexpression led to the enhancement of neurite outgrowth due to the repression of p250GAP. Studies performed on adult neurons however, showed the complete opposite; overexpressing miR-132 in adult neurons leads to a significant decrease in dendritic growth [403], which is due to MecP2 repression. MecP2 is expressed starting at the 10th gestational week and is required for the maintenance of adult neurons [404]. Our data are in agreement with these findings indicating the repression of MecP2 in fully differentiated neuronal cells while p250GAP levels are unchanged (**Fig. 28**). p250GAP expression in adult neurons has been found to be activity dependent and controlled by NMDA receptor signaling events [402].

Regulatory axis between miR-132, MecP2, and BDNF

MecP2 has significant roles in neurogenesis, neuronal differentiation, and proper development of dendritic arbor [305, 307]. This major target of miR-132 in the CNS has been found to be dysregulated in HAND [308]. BDNF, another important regulator of

dendritic growth [309, 310] and synaptic function [312, 313] which shows notable reduction in the brain and serum of HIV-infected subjects [314, 315], is directly and positively regulated by MecP2 [405]. In fact, an axis of regulation exists in the brain involving BDNF, miR-132, and MecP2 [317], in which BDNF induces miR-132 through phosphorylation of CREB [318, 319]. As a target of miR-132, MecP2 is ultimately repressed, leading to the repression of BDNF due to the negative regulatory feedback nature of this axis. Improper timing or duration of miR-132 expression has been shown to be neurotoxic, indicating the delicate balance in the regulation of this axis [320]. Rett syndrome, an autism spectrum disorder resulting from genetic mutation in the MecP2 gene [406], shares striking similarities in neuropathology with HAND. MecP2 is essential for the proper outgrowth of dendrites and formation of synapses [307]. The activity-dependent expression of this protein starts prior to synaptogenesis in development and is tightly controlled in most adult neurons [407]. Reduced size and branching of dendrites inflicted by the lack of MecP2 expression in the developing brain result in microcephaly and mental retardation. Interestingly, RNA levels of MecP2 do not differ in fetal and adult brains while its expression is not similar in different neuronal populations [408]. This is indicative of post-transcriptional control of MecP2 by miRNA and is in agreement with our data that failed to find changes in MecP2 mRNA but showed significant reduction in MecP2 protein and consequently BDNF, the transcription of which depends on MecP2 (**Fig. 26 & 27**).

Differentiating the effects of exosomal Tat from miR-132

To discern the direct detrimental effects of Tat on neurons from miR-132 overexpression, we employed synthetic miR-132 inhibitor in our experiments. We confirmed that miR-132 inhibitor transfection efficiently antagonized miR-132 (data not shown). Next, we showed that miR-132 overexpression was at least in part responsible for Tat neurotoxicity (**Fig. 31**). Antagonizing miR-132 expression also led to reduced exosomal levels of miR-132 (**Fig. 32**). In our previous study, we reported exosome-associated Tat release from Tat-expressing and HIV-1 infected cells [376]. With miR-132 inhibitor expression, we were able to conclude that overexpression of miR-132 was responsible for neurite shortening in neurons treated with exosomes from Tat-expressing astrocytes (**Fig. 33**), as antagonizing miR-132 improved neurite lengths even in presence of Tat-containing exosomes. Similarly, we also showed that exosomal miR-132 contributes to neurotoxicity (**Fig. 33D**). Although miR-132 inhibitor expression consistently negated the Tat-induced down-modulation of MecP2 in astrocytes (**Fig. 26 & 27**) and neurons (**Fig. 28**), its effects on rescuing BDNF levels were not consistent across cell types. Only primary human astrocytes (**Fig. 26**) showed improved BDNF levels with miR-132i transfection, while primary mouse astrocytes (**Fig. 27**) and neurons (**Fig. 28**) did not show such an effect. This might be due to the temporal difference that exists in MecP2-induced BDNF expression. Antagonizing miR-132 in presence of Tat rescues MecP2 levels as the direct target of miR-132. This process rapidly improves BDNF mRNA levels, while this improvement is not reflected in protein levels of BDNF as rapidly.

The role of miR-132 in synapse formation and functionality

miR-132 has been shown to increase the width of dendritic spines, which are storage sites for post synaptic density, contain glutamate receptors, and increase the contact points between neurons [403]. These protrusions also establish contact with synaptic terminals containing synaptophysin [409]. Therefore, it has been suggested that miR-132 may affect the strength of excitatory synapses [410]. Our analysis of synaptic protein levels in cortical neurons treated with exosomes derived from Tat-expressing astrocytes (+DOX-miR-132i/+DOX+miR-132i) reduced both SYP and PSD-95. Moreover, reducing miR-132 levels in exosomes did not change the significant loss of these proteins (**Fig. 34A-C**). Western blotting data from these neurons also showed consistent reduction in both SYP and PSD-95 and although there was no change in PSD-95 with miR-132i, SYP levels showed improvement with reduced exosomal miR-132 (**Fig. 34D**). However, lack of consistency between the effects of miR-132 inhibition on the two proteins and reduction in protein levels of neurons treated with WT exosomes prevent us from concluding that miR-132 affected synaptic protein levels or synapse formation. MAP-2 protein levels were consistent with the miR-132-dependent reduction in neurite lengths by Tat and increase in neurite lengths by miR-132 inhibition despite of Tat expression. These results are in agreement with Tat's direct involvement in the reduction of post-synaptic proteins followed by negative feedback [64, 66] on pre-synaptic proteins.

PERSPECTIVES

Neurodegenerative processes that trail HIV-1 infection in the CNS can lead to dementia and other cognitive and motor disorders [411-415]. Although currently greater than 50 percent of HIV patients suffer neurological consequences of the infection, anti-retroviral therapy's success in controlling the replication of the virus in the periphery has reduced the viral burden in the CNS and led to dramatic reduction in severity of neurocognitive disorders that accompany the infection. This is evident by the reversion of the most severe symptoms of HIV associated dementia within weeks of starting cART [45, 49, 416].

Presence of the virus in glia and infiltrating immune cells but not neurons is indicative of indirect mechanisms of neuronal injury which have been attributed to the production of soluble viral proteins and pro-inflammatory mediators by glial cells. Other than microglia which fully support the replication of HIV-1 and production of its components, astrocytes are implicated as major contributors to injury in the CNS; they do not support replication of the virus but are restrictively and latently infected and produce soluble neurotoxic proteins such as Tat and inflammatory cytokines and chemokines. On the other hand, astrocytosis as a result of virus presence in astrocytes leads to the dysfunction of these significant regulators of homeostasis in the CNS, further intoxicating the delicate balance of this environment [222, 417-422].

Tat is a soluble protein of HIV-1 and a potent neurotoxin [299]. As an early protein of the virus which is not affected by the protease inhibitors in cART, it is produced and released

from infected cells in CNS and elicits both direct and indirect damage to neuronal cells. This is evident by the detection of Tat in CSF and brain of patients who receive cART and have undetectable virus RNA [37]. Chronic presence of Tat protein in the CNS is strongly correlated with one of the prominent pathological hallmarks of neuroAIDS, widespread synaptodendritic injury [61] and in vitro treatment of neuronal cells with Tat and in vivo injection of the protein into rodent brains both demonstrate the damaging effect of Tat on neurites and dendritic processes [1, 423]. The molecular mechanisms of Tat release in the CNS and its neurite shortening effect however have not been yet elucidated. Uncovering these mechanisms is crucial for better understanding HIV pathogenesis in the brain and for seeking potentially novel therapies for controlling the negative impacts of the virus on the affected population.

This work contributes to the much needed knowledge on the molecular basis of Tat's direct and indirect toxicity to neurons and other CNS cells and introduces mechanisms that explain the amplified detrimental effects of Tat on the nervous system through astrocytes, exosomes and microRNA. Until complete removal of the provirus is possible from astrocyte reservoirs, interventions that minimize Tat secretion in exosomes and at the same time inhibit miR-132 overexpression can provide neuroprotection and potentially reduce HIV-associated neurological symptoms.

Identification of other domains of Tat with potential involvement in exosomal sorting

In the first part of my dissertation, we provide evidence for a previously unrecognized mechanism of Tat secretion, exosomal release. Incorporation of Tat inside exosomes released from infected cells, including astrocytes, is consistent with the widespread presence, reach, and persistence of this protein within the CNS [299]. Protection inside exosomal membranes makes extracellular Tat more stable and more efficient in inducing damage to by stander cells. Considering the significance of exosomes in intercellular communications within the CNS [347], and the proven role of exosomes in spreading pathological components of infectious agents [424], therapeutic interventions targeted at exosome-associated Tat protein are warranted and may help mitigate the symptoms of HIV/neuroAIDS. Further studies in uncovering the specific domain (s) of Tat which offer this protein access to the endocytic membranes and ultimately MVB are needed. We rejected our hypothesis that the basic domain of Tat could be responsible for this access by detecting basic-domain deleted Tat mutant in exosomal fractions. Investigating domains with hydrophobic nature are important since they might provide a better explanation of Tat's interaction with endocytic membranes. For this purpose, mutants of Tat that have deficient or modified hydrophobic domains need to be constructed and analyzed for presence or lack of presence in exosomal compartments. Considering the importance of exosomes in glia-neuron communications and the proven exploitation of this pathway by viruses, inhibition of exosomal production by astrocytes as a means of reducing toxic insults of exosome-incorporated viral proteins should also be investigated. Our results

indicate that ceramide inhibition is an efficient method of reducing exosome production and its effects need to be further investigated.

Demonstrating the direct role of CREB phosphorylation in Tat-induced miR-132 expression

In the second part of my dissertation, we provide evidence of Tat's induction of miR-132, a brain enriched microRNA which regulates dendritic plasticity. The crucial roles of this miRNA in neuronal differentiation and continued maintenance of these cells have been identified in the context of Rett syndrome, at autism spectrum disorder with mutations in an important target of miR-132, MecP2 [404]. There are significant similarities between brain pathologies in Rett and neuroAIDS in terms of dendritic pruning and brain volume. We show that Tat can upregulate this microRNA by activating CREB and probably stabilizing the interaction of p-CREB with CREB-binding protein. In normal situations, miR-132 expression is activity dependent and short term and it works in an important regulatory access with bidirectional control on BDNF expression [425]. Consistent expression of Tat in the CNS however, extends the expression of miR-132, leading to neurite shortening and neurotoxicity, an effect that has been previously observed by introducing exogenous miR-132 into neurons [403]. These data provide new mechanistic insights of Tat's injury to dendritic arbor and identify novel pathways that potentially contribute to Tat neurotoxicity. Further studies in the future are required to determine directly the CREB dependent mechanism of miR-132 expression by Tat since our conclusions are based on the dependence of miR-132 induction on CREB phosphorylation and the established role of Tat in CREB activation. A more direct approach would employ

the use of genetic miR-132 constructs with mutations in CREB responsive elements within the transcriptional control loci of this microRNA.

Investigating other target genes of miR-132 in the brain

Each miRNA has the potential to bind several mRNA targets. In the case of miR-132, a total of 17 validated targets have been identified [369]. Our work on Tat-induced neurite shortening only focuses on relevant regulators of neuronal dendritic plasticity that are controlled by miR-132, a microRNA with established and significant roles in altering the dendritic arbor throughout development and adult life [320], which has also been shown to be upregulated in the context of HIV infection in the brain [292]. However, there are other targets of miR-132 that have important functions in the CNS and need to be further investigated in the context of Tat induction; these include acetylcholinesterase (AChE) and matrix metalloproteinase 9 (MMP9). AChE inhibition leads to impediments in neurotransmission at the neuromuscular junction especially in the motor neurons [426]. It is important to investigate whether Tat's induction of miR-132 leads to the suppression of AChE, and if this process is involved in the motor dysfunction associated with HIV/neuroAIDS. MMP9 has been shown to be induced by HIV-1 and contributes to the disruption of BBB [427]. Repression of MMP9 by miR-132 has been shown to be involved in the regulation of dendritic spine structure [428]. Characterizing the effect of Tat and miR-132 on this important tissue remodeling protein is further needed. Future experiments need to be considered in order to measure RNA and protein levels of both AChE and MMP9 in neurons and astrocytes following Tat expression or exposure in these cells.

Studying the potential benefits of BDNF replacement in HIV/neuroAIDS

BDNF is a required factor in survival, growth, and synaptogenesis of neurons [429] and its deficit has been documented in several diseases including Rett syndrome [430] and in HIV patients with cognitive impairment [431]. Our findings on Tat-induced miR-132 expression in neurons and astrocytes show that BDNF is significantly reduced following Tat expression. We confirmed Tat and miR-132 specific nature of this reduction by showing that inhibiting miR-132 induction abolishes BDNF loss. We also argued that loss of BDNF is secondary to MecP2 loss since MecP2 directly and positively regulates BDNF transcription. These results indicate the potential of HIV-1 Tat protein in reducing BDNF levels in the context of HIV infection. The next important step for future experiments would then be to measure plasma and CSF levels of BDNF by ELISA in our iTat mouse model following Tat expression. If our assumptions are correct, we should expect to see reduced levels of BDNF similar to HIV patients because of the established relevance of our mouse model to the molecular pathology of HIV-associated neurocognitive disorders. After confirming reduced BDNF levels, we need to study the effects of BDNF replacement therapy in our mouse model. This is because in mouse models of Rett which show incredible similarities in neuropathology to rodent models of HIV, providing exogenous BDNF has virtually reversed the shortening of dendrites and loss of synapses and has led to the rescue of behavioral phenotypes [306]. Having discovered the novel exosomal secretion of Tat in CNS, we can conduct studies that combine simultaneous inhibition of exosome production with exogenous BDNF replacement therapy. Reducing exosome biogenesis in mice can be done safely and specifically in astrocytes by feeding the mice a

statin regimen. Statins have been shown to induce the autophagy pathway in primary mouse astrocytes [432]. Because of the delicate and opposite balance of autophagy and exosome biogenesis in cells [433], inducing autophagy will result in the reduction of exosomes and exosomal Tat burden in the CNS. Delivery of BDNF is challenging due to the short half-life of recombinant BDNF and the fact that BDNF has very low BBB permeability. Several studies have attempted various methods of BDNF delivery in mouse models of Huntington with partial success. These include direct rBDNF administration through indwelling osmotic mini-pumps in the brain [434], and adenoviral delivery of BDNF gene [435]. Nanoparticle delivery of BDNF has been shown to be the most efficient method since it eliminates the risk of BDNF expiry before reaching the target tissue while ensuring facilitated crossing of BBB through receptor mediated transcytosis [436].

The plastic nature of neuronal viability and synaptodendritic integrity warrant the investigation of the effects of BDNF replacement therapy in our iTat mouse model and can lead to the establishment of significant and novel interventions that reduce Tat-mediated assaults in the CNS.

REFERENCES

1. Kim, B.O., et al., *Neuropathologies in transgenic mice expressing human immunodeficiency virus type 1 Tat protein under the regulation of the astrocyte-specific glial fibrillary acidic protein promoter and doxycycline.* Am J Pathol, 2003. **162**(5): p. 1693-707.
2. Sepkowitz, K.A., *AIDS--the first 20 years.* N Engl J Med, 2001. **344**(23): p. 1764-72.
3. Do, P.H., E. Caumes, and F. Bricaire, *[Emerging and re-emerging infectious diseases--a challenge for public health].* Praxis (Bern 1994), 2000. **89**(4): p. 125-32.
4. Piot, P., et al., *The global impact of HIV/AIDS.* Nature, 2001. **410**(6831): p. 968-73.
5. Gilbert, P.B., et al., *Comparison of HIV-1 and HIV-2 infectivity from a prospective cohort study in Senegal.* Stat Med, 2003. **22**(4): p. 573-93.
6. UNAIDS. *UNAIDS Fact Sheet 2015*. 2015 [cited 2015 December 18]; Available from: http://www.unaids.org/en/resources/campaigns/HowAIDSchangedeverything/factsheet.
7. Maartens, G., C. Celum, and S.R. Lewin, *HIV infection: epidemiology, pathogenesis, treatment, and prevention.* Lancet, 2014. **384**(9939): p. 258-71.
8. WHO, *WHO case definitions of HIV for surveillance and revised clinical staging and immunological classification of HIV-related disease in adults and children*. 2007.
9. Hicks, C.B., C. Gay, and G. Ferrari, *Acute HIV infection: the impact of anti-retroviral treatment on cellular immune responses.* Clin Exp Immunol, 2007. **149**(2): p. 211-6.
10. Wu, L. and V.N. KewalRamani, *Dendritic-cell interactions with HIV: infection and viral dissemination.* Nat Rev Immunol, 2006. **6**(11): p. 859-68.
11. Serrano-Villar, S., et al., *The CD4/CD8 ratio in HIV-infected subjects is independently associated with T-cell activation despite long-term viral suppression.* J Infect, 2013. **66**(1): p. 57-66.
12. Nyamweya, S., et al., *Comparing HIV-1 and HIV-2 infection: Lessons for viral immunopathogenesis.* Rev Med Virol, 2013. **23**(4): p. 221-40.
13. Cunningham, P.H., et al., *Evidence for independent development of resistance to HIV-1 reverse transcriptase inhibitors in the cerebrospinal fluid.* AIDS, 2000. **14**(13): p. 1949-54.
14. Kramer-Hammerle, S., et al., *Cells of the central nervous system as targets and reservoirs of the human immunodeficiency virus.* Virus Res, 2005. **111**(2): p. 194-213.
15. Liu, Y., et al., *Analysis of human immunodeficiency virus type 1 gp160 sequences from a patient with HIV dementia: evidence for monocyte trafficking into brain.* J Neurovirol, 2000. **6 Suppl 1**: p. S70-81.

16. Albright, A.V., S.S. Soldan, and F. Gonzalez-Scarano, *Pathogenesis of human immunodeficiency virus-induced neurological disease.* J Neurovirol, 2003. **9**(2): p. 222-7.
17. Marcondes, M.C., et al., *Highly activated CD8(+) T cells in the brain correlate with early central nervous system dysfunction in simian immunodeficiency virus infection.* J Immunol, 2001. **167**(9): p. 5429-38.
18. Petito, C.K., et al., *CD4+ and CD8+ cells accumulate in the brains of acquired immunodeficiency syndrome patients with human immunodeficiency virus encephalitis.* J Neurovirol, 2003. **9**(1): p. 36-44.
19. Choi, S.S., et al., *Human astrocytes: secretome profiles of cytokines and chemokines.* PLoS One, 2014. **9**(4): p. e92325.
20. Ballabh, P., A. Braun, and M. Nedergaard, *The blood-brain barrier: an overview: structure, regulation, and clinical implications.* Neurobiol Dis, 2004. **16**(1): p. 1-13.
21. Engelhardt, B. and L. Sorokin, *The blood-brain and the blood-cerebrospinal fluid barriers: function and dysfunction.* Semin Immunopathol, 2009. **31**(4): p. 497-511.
22. Williams, D.W., et al., *Monocyte maturation, HIV susceptibility, and transmigration across the blood brain barrier are critical in HIV neuropathogenesis.* J Leukoc Biol, 2012. **91**(3): p. 401-15.
23. Kanmogne, G.D., R.C. Kennedy, and P. Grammas, *HIV-1 gp120 proteins and gp160 peptides are toxic to brain endothelial cells and neurons: possible pathway for HIV entry into the brain and HIV-associated dementia.* J Neuropathol Exp Neurol, 2002. **61**(11): p. 992-1000.
24. Kim, T.A., et al., *HIV-1 Tat-mediated apoptosis in human brain microvascular endothelial cells.* J Immunol, 2003. **170**(5): p. 2629-37.
25. Pomerantz, R.J., *Effects of HIV-1 Vpr on neuroinvasion and neuropathogenesis.* DNA Cell Biol, 2004. **23**(4): p. 227-38.
26. Ritter, M.R., et al., *Myeloid progenitors differentiate into microglia and promote vascular repair in a model of ischemic retinopathy.* J Clin Invest, 2006. **116**(12): p. 3266-76.
27. Aloisi, F., *Immune function of microglia.* Glia, 2001. **36**(2): p. 165-79.
28. Ladeby, R., et al., *Microglial cell population dynamics in the injured adult central nervous system.* Brain Res Brain Res Rev, 2005. **48**(2): p. 196-206.
29. Walker, P.A., et al., *Intravenous multipotent adult progenitor cell therapy after traumatic brain injury: modulation of the resident microglia population.* J Neuroinflammation, 2012. **9**: p. 228.
30. Joseph, S.B., et al., *HIV-1 target cells in the CNS.* J Neurovirol, 2015. **21**(3): p. 276-89.
31. Walsh, J.G., et al., *Rapid inflammasome activation in microglia contributes to brain disease in HIV/AIDS.* Retrovirology, 2014. **11**: p. 35.
32. Trillo-Pazos, G., et al., *Detection of HIV-1 DNA in microglia/macrophages, astrocytes and neurons isolated from brain tissue with HIV-1 encephalitis by laser capture microdissection.* Brain Pathol, 2003. **13**(2): p. 144-54.

33. Churchill, M.J., et al., *Extensive astrocyte infection is prominent in human immunodeficiency virus-associated dementia.* Ann Neurol, 2009. **66**(2): p. 253-8.
34. Messam, C.A. and E.O. Major, *Stages of restricted HIV-1 infection in astrocyte cultures derived from human fetal brain tissue.* J Neurovirol, 2000. **6 Suppl 1**: p. S90-4.
35. Gorry, P.R., et al., *Astrocyte infection by HIV-1: mechanisms of restricted virus replication, and role in the pathogenesis of HIV-1-associated dementia.* Curr HIV Res, 2003. **1**(4): p. 463-73.
36. Chauhan, A., et al., *Intracellular human immunodeficiency virus Tat expression in astrocytes promotes astrocyte survival but induces potent neurotoxicity at distant sites via axonal transport.* J Biol Chem, 2003. **278**(15): p. 13512-9.
37. Johnson, T.P., et al., *Induction of IL-17 and nonclassical T-cell activation by HIV-Tat protein.* Proc Natl Acad Sci U S A, 2013. **110**(33): p. 13588-93.
38. Deiva, K., et al., *CCR5-, DC-SIGN-dependent endocytosis and delayed reverse transcription after human immunodeficiency virus type 1 infection in human astrocytes.* AIDS Res Hum Retroviruses, 2006. **22**(11): p. 1152-61.
39. Liu, Y., et al., *CD4-Independent Infection of Astrocytes by Human Immunodeficiency Virus Type 1: Requirement for the Human Mannose Receptor.* J Virol, 2004. **78**(8): p. 4120-4133.
40. Churchill, M. and A. Nath, *Where does HIV hide? A focus on the central nervous system.* Curr Opin HIV AIDS, 2013. **8**(3): p. 165-9.
41. Banerjee, A., R. Benjamin, and S. Banerjee, *Impact of viral factors on subcellular distribution and RNA export activity of HIV-1 rev in astrocytes 1321N1.* PLoS One, 2013. **8**(9): p. e72905.
42. Li, J., et al., *Expression of exogenous Sam68, the 68-kilodalton SRC-associated protein in mitosis, is able to alleviate impaired Rev function in astrocytes.* J Virol, 2002. **76**(9): p. 4526-35.
43. Brennan, T.P., et al., *Analysis of human immunodeficiency virus type 1 viremia and provirus in resting CD4+ T cells reveals a novel source of residual viremia in patients on antiretroviral therapy.* J Virol, 2009. **83**(17): p. 8470-81.
44. Narasipura, S.D., S. Kim, and L. Al-Harthi, *Epigenetic regulation of HIV-1 latency in astrocytes.* J Virol, 2014. **88**(5): p. 3031-8.
45. Kaul, M., G.A. Garden, and S.A. Lipton, *Pathways to neuronal injury and apoptosis in HIV-associated dementia.* Nature, 2001. **410**(6831): p. 988-94.
46. Valcour, V., et al., *Central nervous system viral invasion and inflammation during acute HIV infection.* J Infect Dis, 2012. **206**(2): p. 275-82.
47. Power, C. and B.J. Brew, *Editorial: HIV-1 infection and the nervous system: a shifting target.* Curr Opin HIV AIDS, 2014. **9**(6): p. 515-6.
48. Gelman, B.B., et al., *The National NeuroAIDS Tissue Consortium brain gene array: two types of HIV-associated neurocognitive impairment.* PLoS One, 2012. **7**(9): p. e46178.
49. Kaul, M., et al., *HIV-1 infection and AIDS: consequences for the central nervous system.* Cell Death Differ, 2005. **12 Suppl 1**: p. 878-92.
50. Brew, B.J. and P. Chan, *Update on HIV dementia and HIV-associated neurocognitive disorders.* Curr Neurol Neurosci Rep, 2014. **14**(8): p. 468.

51. Sanmarti, *HIV-associated neurocognitive disorders.* Journal of Molecular Psychiatry, 2014. **2**(1): p. 1-10.
52. Heaton, R.K., et al., *HIV-associated neurocognitive disorders persist in the era of potent antiretroviral therapy: CHARTER Study.* Neurology, 2010. **75**(23): p. 2087-96.
53. Ghafouri, M., et al., *HIV-1 associated dementia: symptoms and causes.* Retrovirology, 2006. **3**: p. 28.
54. An, S.F., et al., *Axonal damage revealed by accumulation of beta-APP in HIV-positive individuals without AIDS.* J Neuropathol Exp Neurol, 1997. **56**(11): p. 1262-8.
55. Kamat, R., et al., *Neurobehavioral Disturbances During Acute and Early HIV Infection.* Cogn Behav Neurol, 2016. **29**(1): p. 1-10.
56. Gray, F. and M.C. Lescs, *HIV-related demyelinating disease.* Eur J Med, 1993. **2**(2): p. 89-96.
57. Smith, D.B., P. Simmonds, and J.E. Bell, *Brain viral burden, neuroinflammation and neurodegeneration in HAART-treated HIV positive injecting drug users.* J Neurovirol, 2014. **20**(1): p. 28-38.
58. Moore, D.J., et al., *Cortical and subcortical neurodegeneration is associated with HIV neurocognitive impairment.* AIDS, 2006. **20**(6): p. 879-87.
59. Masliah, E., et al., *Spectrum of human immunodeficiency virus-associated neocortical damage.* Ann Neurol, 1992. **32**(3): p. 321-9.
60. Adle-Biassette, H., et al., *Neuronal apoptosis does not correlate with dementia in HIV infection but is related to microglial activation and axonal damage.* Neuropathol Appl Neurobiol, 1999. **25**(2): p. 123-33.
61. Masliah, E., et al., *Dendritic injury is a pathological substrate for human immunodeficiency virus-related cognitive disorders. HNRC Group. The HIV Neurobehavioral Research Center.* Ann Neurol, 1997. **42**(6): p. 963-72.
62. Rao, J.S., et al., *Neuroinflammation and synaptic loss.* Neurochem Res, 2012. **37**(5): p. 903-10.
63. Rao, J.S., et al., *Increased neuroinflammatory and arachidonic acid cascade markers, and reduced synaptic proteins, in brain of HIV-1 transgenic rats.* J Neuroinflammation, 2011. **8**: p. 101.
64. Hargus, N.J. and S.A. Thayer, *Human immunodeficiency virus-1 Tat protein increases the number of inhibitory synapses between hippocampal neurons in culture.* J Neurosci, 2013. **33**(45): p. 17908-20.
65. Kim, H.J., K.A. Martemyanov, and S.A. Thayer, *Human immunodeficiency virus protein Tat induces synapse loss via a reversible process that is distinct from cell death.* J Neurosci, 2008. **28**(48): p. 12604-13.
66. Shin, A.H. and S.A. Thayer, *Human immunodeficiency virus-1 protein Tat induces excitotoxic loss of presynaptic terminals in hippocampal cultures.* Mol Cell Neurosci, 2013. **54**: p. 22-9.
67. Fitting, S., et al., *Synaptic dysfunction in the hippocampus accompanies learning and memory deficits in human immunodeficiency virus type-1 Tat transgenic mice.* Biol Psychiatry, 2013. **73**(5): p. 443-53.
68. Bertrand, S.J., et al., *HIV-1 Tat protein variants: critical role for the cysteine region in synaptodendritic injury.* Exp Neurol, 2013. **248**: p. 228-35.

69. Tornatore, C., et al., *HIV-1 infection of subcortical astrocytes in the pediatric central nervous system.* Neurology, 1994. **44**(3 Pt 1): p. 481-7.
70. Schweighardt, B. and W.J. Atwood, *HIV type 1 infection of human astrocytes is restricted by inefficient viral entry.* AIDS Res Hum Retroviruses, 2001. **17**(12): p. 1133-42.
71. Gorry, P., et al., *Restricted HIV-1 infection of human astrocytes: potential role of nef in the regulation of virus replication.* J Neurovirol, 1998. **4**(4): p. 377-86.
72. Saito, Y., et al., *Overexpression of nef as a marker for restricted HIV-1 infection of astrocytes in postmortem pediatric central nervous tissues.* Neurology, 1994. **44**(3 Pt 1): p. 474-81.
73. Gartner, S., *HIV infection and dementia.* Science, 2000. **287**(5453): p. 602-4.
74. Anderson, E., et al., *HIV-1-associated dementia: a metabolic encephalopathy perpetrated by virus-infected and immune-competent mononuclear phagocytes.* J Acquir Immune Defic Syndr, 2002. **31 Suppl 2**: p. S43-54.
75. Bukrinsky, M.I., et al., *Regulation of nitric oxide synthase activity in human immunodeficiency virus type 1 (HIV-1)-infected monocytes: implications for HIV-associated neurological disease.* J Exp Med, 1995. **181**(2): p. 735-45.
76. Stanley, L.C., et al., *Glial cytokines as neuropathogenic factors in HIV infection: pathogenic similarities to Alzheimer's disease.* J Neuropathol Exp Neurol, 1994. **53**(3): p. 231-8.
77. Price, T.O., et al., *A novel antioxidant N-acetylcysteine amide prevents gp120- and Tat-induced oxidative stress in brain endothelial cells.* Exp Neurol, 2006. **201**(1): p. 193-202.
78. Rao, V.R., A.P. Ruiz, and V.R. Prasad, *Viral and cellular factors underlying neuropathogenesis in HIV associated neurocognitive disorders (HAND).* AIDS Res Ther, 2014. **11**: p. 13.
79. Ensoli, B., et al., *Release, uptake, and effects of extracellular human immunodeficiency virus type 1 Tat protein on cell growth and viral transactivation.* J Virol, 1993. **67**(1): p. 277-87.
80. Bardi, G., et al., *Human immunodeficiency virus gp120-induced apoptosis of human neuroblastoma cells in the absence of CXCR4 internalization.* J Neurovirol, 2006. **12**(3): p. 211-8.
81. Choi, D.W., *Glutamate receptors and the induction of excitotoxic neuronal death.* Prog Brain Res, 1994. **100**: p. 47-51.
82. Ton, H. and H. Xiong, *Astrocyte Dysfunctions and HIV-1 Neurotoxicity.* J AIDS Clin Res, 2013. **4**(11): p. 255.
83. Conant, K., et al., *Induction of monocyte chemoattractant protein-1 in HIV-1 Tat-stimulated astrocytes and elevation in AIDS dementia.* Proc Natl Acad Sci U S A, 1998. **95**(6): p. 3117-21.
84. Nath, A., et al., *Transient exposure to HIV-1 Tat protein results in cytokine production in macrophages and astrocytes. A hit and run phenomenon.* J Biol Chem, 1999. **274**(24): p. 17098-102.
85. El-Hage, N., et al., *Synergistic increases in intracellular Ca2+, and the release of MCP-1, RANTES, and IL-6 by astrocytes treated with opiates and HIV-1 Tat.* Glia, 2005. **50**(2): p. 91-106.

86. Williams, R., et al., *HIV-1 Tat co-operates with IFN-gamma and TNF-alpha to increase CXCL10 in human astrocytes.* PLoS One, 2009. **4**(5): p. e5709.
87. Vitkovic, L. and A. da Cunha, *Role for astrocytosis in HIV-1-associated dementia.* Curr Top Microbiol Immunol, 1995. **202**: p. 105-16.
88. Tripathi, S., et al., *Glial alterations in tuberculous and cryptococcal meningitis and their relation to HIV co-infection--a study on human brains.* J Infect Dev Ctries, 2014. **8**(11): p. 1421-43.
89. Sierra, S., B. Kupfer, and R. Kaiser, *Basics of the virology of HIV-1 and its replication.* J Clin Virol, 2005. **34**(4): p. 233-44.
90. Gelderblom, H.R., *Assembly and morphology of HIV: potential effect of structure on viral function.* AIDS, 1991. **5**(6): p. 617-37.
91. Hirsch MS, C.J., *Human immunodeficiency viruses*. Virology. 4th ed. 1990.: Philadelphia: Lippincott-Raven Publishers. 195375.
92. Gatignol, A., et al., *Characterization of a human TAR RNA-binding protein that activates the HIV-1 LTR.* Science, 1991. **251**(5001): p. 1597-600.
93. Starcich, B., et al., *Characterization of long terminal repeat sequences of HTLV-III.* Science, 1985. **227**(4686): p. 538-40.
94. Moss, J.A., *HIV/AIDS Review.* Radiol Technol, 2013. **84**(3): p. 247-67; quiz p 268-70.
95. Emerman, M. and M.H. Malim, *HIV-1 regulatory/accessory genes: keys to unraveling viral and host cell biology.* Science, 1998. **280**(5371): p. 1880-4.
96. Strebel, K., *HIV accessory proteins versus host restriction factors.* Curr Opin Virol, 2013. **3**(6): p. 692-9.
97. Kulberg, A.J., *Structural homology between HIV-1 tat protein and various human proteins.* AIDS Res Hum Retroviruses, 1990. **6**(9): p. 1059-60.
98. Wei, P., et al., *A novel CDK9-associated C-type cyclin interacts directly with HIV-1 Tat and mediates its high-affinity, loop-specific binding to TAR RNA.* Cell, 1998. **92**(4): p. 451-62.
99. Wei, Q. and P.N. Fultz, *Extensive diversification of human immunodeficiency virus type 1 subtype B strains during dual infection of a chimpanzee that progressed to AIDS.* J Virol, 1998. **72**(4): p. 3005-17.
100. Gu, J., et al., *Crystal structure of HIV-1 Tat complexed with human P-TEFb and AFF4.* Cell Cycle, 2014. **13**(11): p. 1788-97.
101. Hottiger, M.O. and G.J. Nabel, *Interaction of human immunodeficiency virus type 1 Tat with the transcriptional coactivators p300 and CREB binding protein.* J Virol, 1998. **72**(10): p. 8252-6.
102. Kamine, J., et al., *Identification of a cellular protein that specifically interacts with the essential cysteine region of the HIV-1 Tat transactivator.* Virology, 1996. **216**(2): p. 357-66.
103. Veschambre, P., P. Simard, and P. Jalinot, *Evidence for functional interaction between the HIV-1 Tat transactivator and the TATA box binding protein in vivo.* J Mol Biol, 1995. **250**(2): p. 169-80.
104. Weeks, B.S., et al., *Identification of a novel cell attachment domain in the HIV-1 Tat protein and its 90-kDa cell surface binding protein.* J Biol Chem, 1993. **268**(7): p. 5279-84.

105. Xiao, H., et al., *A cofactor, TIP30, specifically enhances HIV-1 Tat-activated transcription.* Proc Natl Acad Sci U S A, 1998. **95**(5): p. 2146-51.
106. Colin, L., E. Verdin, and C. Van Lint, *HIV-1 chromatin, transcription, and the regulatory protein Tat.* Methods Mol Biol, 2014. **1087**: p. 85-101.
107. Rice, A.P. and F. Carlotti, *Structural analysis of wild-type and mutant human immunodeficiency virus type 1 Tat proteins.* J Virol, 1990. **64**(12): p. 6018-26.
108. Sodroski, J., et al., *Trans-acting transcriptional regulation of human T-cell leukemia virus type III long terminal repeat.* Science, 1985. **227**(4683): p. 171-3.
109. Bayer, P., et al., *Structural studies of HIV-1 Tat protein.* J Mol Biol, 1995. **247**(4): p. 529-35.
110. Koken, S.E., et al., *Intracellular analysis of in vitro modified HIV Tat protein.* J Biol Chem, 1994. **269**(11): p. 8366-75.
111. Henderson, L.J., et al., *Human immunodeficiency virus type 1 (HIV-1) transactivator of transcription through its intact core and cysteine-rich domains inhibits Wnt/beta-catenin signaling in astrocytes: relevance to HIV neuropathogenesis.* J Neurosci, 2012. **32**(46): p. 16306-13.
112. Churcher, M.J., et al., *High affinity binding of TAR RNA by the human immunodeficiency virus type-1 tat protein requires base-pairs in the RNA stem and amino acid residues flanking the basic region.* J Mol Biol, 1993. **230**(1): p. 90-110.
113. Luo, Y., et al., *Functional analysis of interactions between Tat and the trans-activation response element of human immunodeficiency virus type 1 in cells.* J Virol, 1993. **67**(9): p. 5617-22.
114. Lin, M.H., et al., *A mutant tat protein inhibits HIV-1 reverse transcription by targeting the reverse transcription complex.* J Virol, 2015. **89**(9): p. 4827-36.
115. Brake, D.A., C. Debouck, and G. Biesecker, *Identification of an Arg-Gly-Asp (RGD) cell adhesion site in human immunodeficiency virus type 1 transactivation protein, tat.* J Cell Biol, 1990. **111**(3): p. 1275-81.
116. Monini, P., et al., *HIV-1 tat promotes integrin-mediated HIV transmission to dendritic cells by binding Env spikes and competes neutralization by anti-HIV antibodies.* PLoS One, 2012. **7**(11): p. e48781.
117. Debaisieux, S., et al., *The ins and outs of HIV-1 Tat.* Traffic, 2012. **13**(3): p. 355-63.
118. Westendorp, M.O., et al., *Sensitization of T cells to CD95-mediated apoptosis by HIV-1 Tat and gp120.* Nature, 1995. **375**(6531): p. 497-500.
119. Xiao, H., et al., *Selective CXCR4 antagonism by Tat: implications for in vivo expansion of coreceptor use by HIV-1.* Proc Natl Acad Sci U S A, 2000. **97**(21): p. 11466-71.
120. Ensoli, B., et al., *Tat protein of HIV-1 stimulates growth of cells derived from Kaposi's sarcoma lesions of AIDS patients.* Nature, 1990. **345**(6270): p. 84-6.
121. Chang, H.C., et al., *HIV-1 Tat protein exits from cells via a leaderless secretory pathway and binds to extracellular matrix-associated heparan sulfate proteoglycans through its basic region.* Aids, 1997. **11**(12): p. 1421-31.
122. Morgavi, P., et al., *The association of HIV-1 Tat with nuclei is regulated by Ca2+ ions and cytosolic factors.* J Biol Chem, 1997. **272**(17): p. 11256-60.

123. Albini, A., et al., *HIV-1 Tat protein mimicry of chemokines.* Proc Natl Acad Sci U S A, 1998. **95**(22): p. 13153-8.
124. Milani, D., et al., *Influence of the human immunodeficiency virus type 1 Tat protein on the proliferation and differentiation of PC12 rat pheochromocytoma cells.* J Gen Virol, 1993. **74**(Pt 12): p. 2587-94.
125. Zauli, G., et al., *Human immunodeficiency virus type 1 Tat protein protects lymphoid, epithelial, and neuronal cell lines from death by apoptosis.* Cancer Res, 1993. **53**(19): p. 4481-5.
126. Zauli, G., et al., *An autocrine loop of HIV type-1 Tat protein responsible for the improved survival/proliferation capacity of permanently Tat-transfected cells and required for optimal HIV-1 LTR transactivating activity.* J Acquir Immune Defic Syndr Hum Retrovirol, 1995. **10**(3): p. 306-16.
127. Zeitler, M., et al., *HIV-Tat Protein Forms Phosphoinositide-dependent Membrane Pores Implicated in Unconventional Protein Secretion.* J Biol Chem, 2015. **290**(36): p. 21976-84.
128. Finzi, D. and R.F. Siliciano, *Viral dynamics in HIV-1 infection.* Cell, 1998. **93**(5): p. 665-71.
129. Steinaa, L., et al., *Antibody to HIV-1 Tat protein inhibits the replication of virus in culture.* Arch Virol, 1994. **139**(3-4): p. 263-71.
130. Frankel, A.D. and C.O. Pabo, *Cellular uptake of the tat protein from human immunodeficiency virus.* Cell, 1988. **55**(6): p. 1189-93.
131. Green, M., M. Ishino, and P.M. Loewenstein, *Mutational analysis of HIV-1 Tat minimal domain peptides: identification of trans-dominant mutants that suppress HIV-LTR-driven gene expression.* Cell, 1989. **58**(1): p. 215-23.
132. Liu, Y., et al., *Uptake of HIV-1 tat protein mediated by low-density lipoprotein receptor-related protein disrupts the neuronal metabolic balance of the receptor ligands.* Nat Med, 2000. **6**(12): p. 1380-7.
133. Fawell, S., et al., *Tat-mediated delivery of heterologous proteins into cells.* Proc Natl Acad Sci U S A, 1994. **91**(2): p. 664-8.
134. Schwarze, S.R., et al., *In vivo protein transduction: delivery of a biologically active protein into the mouse.* Science, 1999. **285**(5433): p. 1569-72.
135. Vives, E., P. Brodin, and B. Lebleu, *A truncated HIV-1 Tat protein basic domain rapidly translocates through the plasma membrane and accumulates in the cell nucleus.* J Biol Chem, 1997. **272**(25): p. 16010-7.
136. Rizzuti, M., et al., *Therapeutic applications of the cell-penetrating HIV-1 Tat peptide.* Drug Discov Today, 2015. **20**(1): p. 76-85.
137. Bodor, N., et al., *Novel, cell-penetrating molecular transporters with flexible backbones and permanently charged side-chains.* J Pharm Pharmacol, 2007. **59**(8): p. 1065-76.
138. Rayne, F., et al., *Detecting HIV-1 Tat in Cell Culture Supernatants by ELISA or Western Blot.* Methods Mol Biol, 2016. **1354**: p. 329-42.
139. Gibellini, D., et al., *Recombinant human immunodeficiency virus type-1 (HIV-1) Tat protein sequentially up-regulates IL-6 and TGF-beta 1 mRNA expression and protein synthesis in peripheral blood monocytes.* Br J Haematol, 1994. **88**(2): p. 261-7.

140. Nabell, L.M., et al., *Human immunodeficiency virus 1 Tat stimulates transcription of the transforming growth factor alpha gene in an epidermal growth factor- dependent manner.* Cell Growth Differ, 1994. **5**(1): p. 87-93.
141. Cupp, C., et al., *Evidence for stimulation of the transforming growth factor beta 1 promoter by HIV-1 Tat in cells derived from CNS.* Oncogene, 1993. **8**(8): p. 2231-6.
142. Sastry, K.J., et al., *HIV-1 tat gene induces tumor necrosis factor-beta (lymphotoxin) in a human B-lymphoblastoid cell line.* J Biol Chem, 1990. **265**(33): p. 20091-3.
143. Ganju, R.K., et al., *Human immunodeficiency virus tat modulates the Flk-1/KDR receptor, mitogen-activated protein kinases, and components of focal adhesion in Kaposi's sarcoma cells.* J Virol, 1998. **72**(7): p. 6131-7.
144. Pocsik, E., M. Higuchi, and B.B. Aggarwal, *Down-modulation of cell surface expression of p80 form of the tumor necrosis factor receptor by human immunodeficiency virus-1 tat gene.* Lymphokine Cytokine Res, 1992. **11**(6): p. 317-25.
145. Puri, R.K. and B.B. Aggarwal, *Human immunodeficiency virus type 1 tat gene up-regulates interleukin 4 receptors on a human B-lymphoblastoid cell line.* Cancer Res, 1992. **52**(13): p. 3787-90.
146. Albini, A., et al., *The angiogenesis induced by HIV-1 tat protein is mediated by the Flk- 1/KDR receptor on vascular endothelial cells.* Nat Med, 1996. **2**(12): p. 1371-5.
147. Singhal, P.C., P. Sharma, and P. Garg, *HIV-1 gp160 protein-macrophage interactions modulate mesangial cell proliferation and matrix synthesis.* Am J Pathol, 1995. **147**(6): p. 1780-9.
148. Albini, A., et al., *HIV-1 tat protein mimicry of chemokines [In Process Citation].* Proc Natl Acad Sci U S A, 1998. **95**(22): p. 13153-8.
149. Huang, L., et al., *Tat protein induces human immunodeficiency virus type 1 (HIV-1) coreceptors and promotes infection with both macrophage-tropic and T- lymphotropic HIV-1 strains [In Process Citation].* J Virol, 1998. **72**(11): p. 8952-60.
150. Albini, A., et al., *Angiogenic properties of human immunodeficiency virus type 1 Tat protein.* Proc Natl Acad Sci U S A, 1995. **92**(11): p. 4838-42.
151. Corallini, A., et al., *Promotion of tumour metastases and induction of angiogenesis by native HIV-1 Tat protein from BK virus/tat transgenic mice.* Aids, 1996. **10**(7): p. 701-10.
152. Albini, A., et al., *Angiogenic potential in vivo by Kaposi's sarcoma cell-free supernatants and HIV-1 tat product: inhibition of KS-like lesions by tissue inhibitor of metalloproteinase-2.* Aids, 1994. **8**(9): p. 1237-44.
153. Albini, A., et al., *HIV-tat protein is a heparin-binding angiogenic growth factor.* Oncogene, 1996. **12**(2): p. 289-97.
154. Barbanti-Brodano, G., et al., *HIV-1 tat acts as a growth factor and induces angiogenic activity in BK virus/tat transgenic mice.* Antibiot Chemother, 1994. **46**: p. 88-101.

155. Schuurman, H.J., et al., *Epitopes of human immunodeficiency virus regulatory proteins tat, nef and rev are expressed in skin in atopic dermatitis.* Int Arch Allergy Immunol, 1993. **100**(2): p. 107-14.
156. Li, C.J., et al., *Induction of apoptosis in uninfected lymphocytes by HIV-1 Tat protein.* Science, 1995. **268**(5209): p. 429-31.
157. Dunne, A.L., et al., *HIV replication in chronically infected macrophages is not inhibited by the Tat inhibitors Ro-5-3335 and Ro-24-7429.* J Leukoc Biol, 1994. **56**(3): p. 369-73.
158. Kundu, M., et al., *HIV-1 Tat elongates the G1 phase and indirectly promotes HIV-1 gene expression in cells of glial origin.* J Biol Chem, 1998. **273**(14): p. 8130-6.
159. Barton, C.H., et al., *The human immunodeficiency virus type 1 regulatory protein Tat inhibits interferon-induced iNos activity in a murine macrophage cell line.* J Gen Virol, 1996. **77 (Pt 8)**: p. 1643-7.
160. Carroll, R., B.M. Peterlin, and D. Derse, *Inhibition of human immunodeficiency virus type 1 Tat activity by coexpression of heterologous trans activators.* J Virol, 1992. **66**(4): p. 2000-7.
161. Caldwell, R.L., B.S. Egan, and V.L. Shepherd, *HIV-1 Tat represses transcription from the mannose receptor promoter.* J Immunol, 2000. **165**(12): p. 7035-41.
162. Ito, M., et al., *HIV type 1 Tat protein inhibits interleukin 12 production by human peripheral blood mononuclear cells.* AIDS Res Hum Retroviruses, 1998. **14**(10): p. 845-9.
163. Kim, Y.S. and R. Risser, *TAR-independent transactivation of the murine cytomegalovirus major immediate-early promoter by the Tat protein.* J Virol, 1993. **67**(1): p. 239-48.
164. Chowdhury, M., et al., *Evidence that a sequence similar to TAR is important for induction of the JC virus late promoter by human immunodeficiency virus type 1 Tat.* J Virol, 1992. **66**(12): p. 7355-61.
165. Chowdhury, M., et al., *Regulation of the human neurotropic virus promoter by JCV-T antigen and HIV-1 tat protein.* Oncogene, 1990. **5**(12): p. 1737-42.
166. Tada, H., et al., *Trans-activation of the JC virus late promoter by the tat protein of type 1 human immunodeficiency virus in glial cells.* Proc Natl Acad Sci U S A, 1990. **87**(9): p. 3479-83.
167. Hudson, L., et al., *Detection of the human immunodeficiency virus regulatory protein tat in CNS tissues.* J Neurovirol, 2000. **6**(2): p. 145-55.
168. Chen, L.L., et al., *Increased cellular uptake of the human immunodeficiency virus-1 Tat protein after modification with biotin.* Anal Biochem, 1995. **227**(1): p. 168-75.
169. Banks, W.A., S.M. Robinson, and A. Nath, *Permeability of the blood-brain barrier to HIV-1 Tat.* Exp Neurol, 2005. **193**(1): p. 218-27.
170. Bratanich, A.C., et al., *Brain-derived HIV-1 tat sequences from AIDS patients with dementia show increased molecular heterogeneity.* J Neurovirol, 1998. **4**(4): p. 387-93.
171. Aprea, S., et al., *Tubulin-mediated binding of human immunodeficiency virus-1 Tat to the cytoskeleton causes proteasomal-dependent degradation of*

microtubule-associated protein 2 and neuronal damage. J Neurosci, 2006. **26**(15): p. 4054-62.
172. Caporello, E., et al., *The immunophilin ligand GPI1046 protects neurons from the lethal effects of the HIV-1 proteins gp120 and Tat by modulating endoplasmic reticulum calcium load.* J Neurochem, 2006. **98**(1): p. 146-55.
173. Norman, J.P., et al., *HIV-1 trans activator of transcription protein elicits mitochondrial hyperpolarization and respiratory deficit, with dysregulation of complex IV and nicotinamide adenine dinucleotide homeostasis in cortical neurons.* J Immunol, 2007. **178**(2): p. 869-76.
174. Brailoiu, E., et al., *Acute exposure to ethanol potentiates human immunodeficiency virus type 1 Tat-induced Ca(2+) overload and neuronal death in cultured rat cortical neurons.* J Neurovirol, 2006. **12**(1): p. 17-24.
175. Kruman, II, A. Nath, and M.P. Mattson, *HIV-1 protein Tat induces apoptosis of hippocampal neurons by a mechanism involving caspase activation, calcium overload, and oxidative stress.* Exp Neurol, 1998. **154**(2): p. 276-88.
176. Orsini, M.J., et al., *Extracellular human immunodeficiency virus type 1 Tat protein promotes aggregation and adhesion of cerebellar neurons.* J Neurosci, 1996. **16**(8): p. 2546-52.
177. Haughey, N.J., et al., *HIV-1 Tat through phosphorylation of NMDA receptors potentiates glutamate excitotoxicity.* J Neurochem, 2001. **78**(3): p. 457-67.
178. Perez, A., et al., *Evaluation of HIV-1 Tat induced neurotoxicity in rat cortical cell culture.* J Neurovirol, 2001. **7**(1): p. 1-10.
179. Brailoiu, G.C., et al., *Excitatory effects of human immunodeficiency virus 1 Tat on cultured rat cerebral cortical neurons.* Neuroscience, 2008. **151**(3): p. 701-10.
180. Philippon, V., et al., *The basic domain of the lentiviral Tat protein is responsible for damages in mouse brain: involvement of cytokines.* Virology, 1994. **205**(2): p. 519-29.
181. Eugenin, E.A., et al., *HIV-1 tat protein induces a migratory phenotype in human fetal microglia by a CCL2 (MCP-1)-dependent mechanism: possible role in NeuroAIDS.* Glia, 2005. **49**(4): p. 501-10.
182. El-Hage, N., et al., *HIV-1 Tat and opiate-induced changes in astrocytes promote chemotaxis of microglia through the expression of MCP-1 and alternative chemokines.* Glia, 2006. **53**(2): p. 132-46.
183. Shi, B., et al., *Neuronal apoptosis induced by HIV-1 Tat protein and TNF-alpha: potentiation of neurotoxicity mediated by oxidative stress and implications for HIV-1 dementia.* J Neurovirol, 1998. **4**(3): p. 281-90.
184. Eddleston, M. and L. Mucke, *Molecular profile of reactive astrocytes--implications for their role in neurologic disease.* Neuroscience, 1993. **54**(1): p. 15-36.
185. da Cunha, A., et al., *Control of astrocytosis by interleukin-1 and transforming growth factor-beta 1 in human brain.* Brain Res, 1993. **631**(1): p. 39-45.
186. Mennerick, S. and C.F. Zorumski, *Glial contributions to excitatory neurotransmission in cultured hippocampal cells.* Nature, 1994. **368**(6466): p. 59-62.

187. Cornell-Bell, A.H., et al., *Glutamate induces calcium waves in cultured astrocytes: long-range glial signaling.* Science, 1990. **247**(4941): p. 470-3.
188. Kleinschmidt, A., et al., *Restricted expression of HIV1 in human astrocytes: molecular basis for viral persistence in the CNS.* Res Virol, 1994. **145**(3-4): p. 147-53.
189. Tornatore, C., et al., *Persistent human immunodeficiency virus type 1 infection in human fetal glial cells reactivated by T-cell factor(s) or by the cytokines tumor necrosis factor alpha and interleukin-1 beta.* J Virol, 1991. **65**(11): p. 6094-100.
190. Brenner, M., et al., *GFAP promoter directs astrocyte-specific expression in transgenic mice.* J Neurosci, 1994. **14**(3 Pt 1): p. 1030-7.
191. Eng, L.F., R.S. Ghirnikar, and Y.L. Lee, *Glial fibrillary acidic protein: GFAP-thirty-one years (1969-2000).* Neurochem Res, 2000. **25**(9-10): p. 1439-51.
192. Norenburg, M., *Astrocytes pathophysiology in disorders of the central nervous system.*, in *Astrocytes: in Brain Aging and Neurodegeneration.*, H. Schipper, Editor. 1997, Landes Bioscience: Austin.
193. Coulombe, P.A. and P. Wong, *Cytoplasmic intermediate filaments revealed as dynamic and multipurpose scaffolds.* Nat Cell Biol, 2004. **6**(8): p. 699-706.
194. Herrmann, H., et al., *Intermediate filaments: from cell architecture to nanomechanics.* Nat Rev Mol Cell Biol, 2007. **8**(7): p. 562-73.
195. Ding, M., et al., *Altered taurine release following hypotonic stress in astrocytes from mice deficient for GFAP and vimentin.* Brain Res Mol Brain Res, 1998. **62**(1): p. 77-81.
196. Pekny, M., et al., *Abnormal reaction to central nervous system injury in mice lacking glial fibrillary acidic protein and vimentin.* J Cell Biol, 1999. **145**(3): p. 503-14.
197. Sullivan, S.M., et al., *Cytoskeletal anchoring of GLAST determines susceptibility to brain damage: an identified role for GFAP.* J Biol Chem, 2007. **282**(40): p. 29414-23.
198. McCall, M.A., et al., *Targeted deletion in astrocyte intermediate filament (Gfap) alters neuronal physiology.* Proc Natl Acad Sci U S A, 1996. **93**(13): p. 6361-6.
199. Pekny, M., *Astrocytic intermediate filaments: lessons from GFAP and vimentin knock-out mice.* Prog Brain Res, 2001. **132**: p. 23-30.
200. Liedtke, W., et al., *GFAP is necessary for the integrity of CNS white matter architecture and long-term maintenance of myelination.* Neuron, 1996. **17**(4): p. 607-15.
201. Pekny, M., et al., *GFAP-deficient astrocytes are capable of stellation in vitro when cocultured with neurons and exhibit a reduced amount of intermediate filaments and an increased cell saturation density.* Exp Cell Res, 1998. **239**(2): p. 332-43.
202. Aksenov, M.Y., et al., *Temporal relationships between HIV-1 Tat-induced neuronal degeneration, OX-42 immunoreactivity, reactive astrocytosis, and protein oxidation in the rat striatum.* Brain Res, 2003. **987**(1): p. 1-9.
203. Zhou, B.Y., et al., *Astrocyte activation and dysfunction and neuron death by HIV-1 Tat expression in astrocytes.* Mol Cell Neurosci, 2004. **27**(3): p. 296-305.

204. Zou, W., et al., *Involvement of p300 in constitutive and HIV-1 Tat-activated expression of glial fibrillary acidic protein in astrocytes.* Glia, 2010. **58**(13): p. 1640-8.
205. Fan, Y., et al., *Activation of Egr-1 expression in astrocytes by HIV-1 Tat: new insights into astrocyte-mediated Tat neurotoxicity.* J Neuroimmune Pharmacol, 2011. **6**(1): p. 121-9.
206. Fan, Y., K.A. Timani, and J.J. He, *STAT3 and its phosphorylation are involved in HIV-1 Tat-induced transactivation of glial fibrillary acidic protein.* Curr HIV Res, 2015. **13**(1): p. 55-63.
207. Biancone, L., et al., *Motility induced by human immunodeficiency virus-1 Tat on Kaposi's sarcoma cells requires platelet-activating factor synthesis.* Am J Pathol, 1999. **155**(5): p. 1731-9.
208. Del Sorbo, L., et al., *The synthesis of platelet-activating factor modulates chemotaxis of monocytes induced by HIV-1 Tat.* Eur J Immunol, 1999. **29**(5): p. 1513-21.
209. Xiong, H., et al., *HIV-1 infected mononuclear phagocyte secretory products affect neuronal physiology leading to cellular demise: relevance for HIV-1-associated dementia.* J Neurovirol, 2000. **6 Suppl 1**: p. S14-23.
210. Johnston, J.B., et al., *HIV-1 Tat neurotoxicity is prevented by matrix metalloproteinase inhibitors.* Ann Neurol, 2001. **49**(2): p. 230-41.
211. Perry, S.W., et al., *Platelet-activating factor receptor activation. An initiator step in HIV-1 neuropathogenesis.* J Biol Chem, 1998. **273**(28): p. 17660-4.
212. Bennett, S.A., et al., *Platelet activating factor receptor expression is associated with neuronal apoptosis in an in vivo model of excitotoxicity.* Cell Death Differ, 1998. **5**(10): p. 867-75.
213. Kolb, S.A., et al., *Matrix metalloproteinases and tissue inhibitors of metalloproteinases in viral meningitis: upregulation of MMP-9 and TIMP-1 in cerebrospinal fluid.* J Neuroimmunol, 1998. **84**(2): p. 143-50.
214. Sporer, B., et al., *Presence of matrix metalloproteinase-9 activity in the cerebrospinal fluid of human immunodeficiency virus-infected patients.* J Infect Dis, 1998. **178**(3): p. 854-7.
215. Xu, R., et al., *HIV-1 Tat protein increases the permeability of brain endothelial cells by both inhibiting occludin expression and cleaving occludin via matrix metalloproteinase-9.* Brain Res, 2012. **1436**: p. 13-9.
216. Andras, I.E., et al., *Signaling mechanisms of HIV-1 Tat-induced alterations of claudin-5 expression in brain endothelial cells.* J Cereb Blood Flow Metab, 2005. **25**(9): p. 1159-70.
217. Mishra, R. and S.K. Singh, *HIV-1 Tat C phosphorylates VE-cadherin complex and increases human brain microvascular endothelial cell permeability.* BMC Neurosci, 2014. **15**: p. 80.
218. Cohen, O.J., A. Kinter, and A.S. Fauci, *Host factors in the pathogenesis of HIV disease.* Immunol Rev, 1997. **159**: p. 31-48.
219. Wesselingh, S.L., et al., *Detection of cytokine mRNA in astrocyte cultures using the polymerase chain reaction.* Lymphokine Res, 1990. **9**(2): p. 177-85.

220. Talley, A.K., et al., *Tumor necrosis factor alpha-induced apoptosis in human neuronal cells: protection by the antioxidant N-acetylcysteine and the genes bcl-2 and crmA.* Mol Cell Biol, 1995. **15**(5): p. 2359-66.
221. Fine, S.M., et al., *Tumor necrosis factor alpha inhibits glutamate uptake by primary human astrocytes. Implications for pathogenesis of HIV-1 dementia.* J Biol Chem, 1996. **271**(26): p. 15303-6.
222. Vallieres, L., et al., *Reduced hippocampal neurogenesis in adult transgenic mice with chronic astrocytic production of interleukin-6.* J Neurosci, 2002. **22**(2): p. 486-92.
223. Nakanishi, M., et al., *Microglia-derived interleukin-6 and leukaemia inhibitory factor promote astrocytic differentiation of neural stem/progenitor cells.* Eur J Neurosci, 2007. **25**(3): p. 649-58.
224. Weiss, J.M., et al., *HIV-1 Tat induces monocyte chemoattractant protein-1-mediated monocyte transmigration across a model of the human blood-brain barrier and up-regulates CCR5 expression on human monocytes.* J Immunol, 1999. **163**(5): p. 2953-9.
225. Sui, Y., et al., *CXCL10-induced cell death in neurons: role of calcium dysregulation.* Eur J Neurosci, 2006. **23**(4): p. 957-64.
226. Cinque, P., et al., *Cerebrospinal fluid interferon-gamma-inducible protein 10 (IP-10, CXCL10) in HIV-1 infection.* J Neuroimmunol, 2005. **168**(1-2): p. 154-63.
227. Xia, M.Q., et al., *Expression of the chemokine receptor CXCR3 on neurons and the elevated expression of its ligand IP-10 in reactive astrocytes: in vitro ERK1/2 activation and role in Alzheimer's disease.* J Neuroimmunol, 2000. **108**(1-2): p. 227-35.
228. Butterfield, D.A., et al., *Evidence of oxidative damage in Alzheimer's disease brain: central role for amyloid beta-peptide.* Trends Mol Med, 2001. **7**(12): p. 548-54.
229. Turchan, J., et al., *Oxidative stress in HIV demented patients and protection ex vivo with novel antioxidants.* Neurology, 2003. **60**(2): p. 307-14.
230. Price, T.O., et al., *HIV-1 viral proteins gp120 and Tat induce oxidative stress in brain endothelial cells.* Brain Res, 2005. **1045**(1-2): p. 57-63.
231. Aksenov, M.Y., et al., *Oxidative damage induced by the injection of HIV-1 Tat protein in the rat striatum.* Neurosci Lett, 2001. **305**(1): p. 5-8.
232. Hu, J., A. Ferreira, and L.J. Van Eldik, *S100beta induces neuronal cell death through nitric oxide release from astrocytes.* J Neurochem, 1997. **69**(6): p. 2294-301.
233. Choi, D.S., et al., *Proteomics of extracellular vesicles: Exosomes and ectosomes.* Mass Spectrom Rev, 2014.
234. Cocucci, E., G. Racchetti, and J. Meldolesi, *Shedding microvesicles: artefacts no more.* Trends Cell Biol, 2009. **19**(2): p. 43-51.
235. Mathivanan, R.J.S.a.S., *Extracellular Microvesicles: The Need for Internationally Recognised*

Nomenclature and Stringent Purification Criteria. J Proteomics Bioinform, 2012. **5**.
236. Simons, M. and G. Raposo, *Exosomes--vesicular carriers for intercellular communication.* Curr Opin Cell Biol, 2009. **21**(4): p. 575-81.

237. Corrado, C., et al., *Exosomes as intercellular signaling organelles involved in health and disease: basic science and clinical applications.* Int J Mol Sci, 2013. **14**(3): p. 5338-66.
238. Bellingham, S.A., et al., *Exosomes: vehicles for the transfer of toxic proteins associated with neurodegenerative diseases?* Front Physiol, 2012. **3**: p. 124.
239. Raposo, G. and W. Stoorvogel, *Extracellular vesicles: exosomes, microvesicles, and friends.* J Cell Biol, 2013. **200**(4): p. 373-83.
240. Colombo, M., G. Raposo, and C. Thery, *Biogenesis, secretion, and intercellular interactions of exosomes and other extracellular vesicles.* Annu Rev Cell Dev Biol, 2014. **30**: p. 255-89.
241. Tanaka, N., M. Kyuuma, and K. Sugamura, *Endosomal sorting complex required for transport proteins in cancer pathogenesis, vesicular transport, and non-endosomal functions.* Cancer Sci, 2008. **99**(7): p. 1293-303.
242. Trajkovic, K., et al., *Ceramide triggers budding of exosome vesicles into multivesicular endosomes.* Science, 2008. **319**(5867): p. 1244-7.
243. Megha and E. London, *Ceramide selectively displaces cholesterol from ordered lipid domains (rafts): implications for lipid raft structure and function.* J Biol Chem, 2004. **279**(11): p. 9997-10004.
244. Théry, C., L. Zitvogel, and S. Amigorena, *Exosomes: composition, biogenesis and function.* Nature Reviews Immunology, 2002. **2**(8): p. 569-579.
245. Record, M., et al., *Exosomes as new vesicular lipid transporters involved in cell–cell communication and various pathophysiologies.* Biochimica et Biophysica Acta (BBA)-Molecular and Cell Biology of Lipids, 2014. **1841**(1): p. 108-120.
246. Nichols, B.J., et al., *Rapid cycling of lipid raft markers between the cell surface and Golgi complex.* The Journal of cell biology, 2001. **153**(3): p. 529-542.
247. Pols, M.S. and J. Klumperman, *Trafficking and function of the tetraspanin CD63.* Exp Cell Res, 2009. **315**(9): p. 1584-92.
248. Hicks, D., et al., *Membrane targeting, shedding and protein interactions of brain acetylcholinesterase.* J Neurochem, 2011. **116**(5): p. 742-6.
249. Kerem, A., et al., *Interrelations between assembly and secretion of recombinant human acetylcholinesterase.* J Biol Chem, 1993. **268**(1): p. 180-4.
250. Schweitzer, E.S., *Regulated and constitutive secretion of distinct molecular forms of acetylcholinesterase from PC12 cells.* J Cell Sci, 1993. **106 (Pt 3)**: p. 731-40.
251. Johnstone, R., *Maturation of reticulocytes: formation of exosomes as a mechanism for shedding membrane proteins.* Biochemistry and Cell Biology, 1992. **70**(3-4): p. 179-190.
252. Mathivanan, S., H. Ji, and R.J. Simpson, *Exosomes: extracellular organelles important in intercellular communication.* J Proteomics, 2010. **73**(10): p. 1907-20.
253. Vlassov, A.V., et al., *Exosomes: current knowledge of their composition, biological functions, and diagnostic and therapeutic potentials.* Biochim Biophys Acta, 2012. **1820**(7): p. 940-8.
254. Urbanelli, L., et al., *Signaling pathways in exosomes biogenesis, secretion and fate.* Genes (Basel), 2013. **4**(2): p. 152-70.

255. ExoCarta. *database of exosomal proteins, RNA and lipids*. [cited 2013 12/12/13]; Available from: http://www.exocarta.org.
256. Ramakrishnaiah, V. and L.J. Van Der Laan, *Hepatitis virus hijacks shuttle: Exosome-like vehicles provide protection against neutralizing antibodies.* Hepatology, 2013.
257. Klohn, P.C., R. Castro-Seoane, and J. Collinge, *Exosome release from infected dendritic cells: a clue for a fast spread of prions in the periphery?* J Infect, 2013. **67**(5): p. 359-68.
258. Ramakrishnaiah, V., et al., *Exosome-mediated transmission of hepatitis C virus between human hepatoma Huh7.5 cells.* Proc Natl Acad Sci U S A, 2013. **110**(32): p. 13109-13.
259. Verweij, F.J., et al., *Analysis of viral microRNA exchange via exosomes in vitro and in vivo.* Methods Mol Biol, 2013. **1024**: p. 53-68.
260. Schorey, J.S. and S. Bhatnagar, *Exosome function: from tumor immunology to pathogen biology.* Traffic, 2008. **9**(6): p. 871-81.
261. Mignot, G., et al., *Prospects for exosomes in immunotherapy of cancer.* J Cell Mol Med, 2006. **10**(2): p. 376-88.
262. Fang, Y., et al., *Higher-order oligomerization targets plasma membrane proteins and HIV gag to exosomes.* PLoS Biol, 2007. **5**(6): p. e158.
263. Columba Cabezas, S. and M. Federico, *Sequences within RNA coding for HIV-1 Gag p17 are efficiently targeted to exosomes.* Cell Microbiol, 2013. **15**(3): p. 412-29.
264. Narayanan, A., et al., *Exosomes derived from HIV-1-infected cells contain trans-activation response element RNA.* J Biol Chem, 2013. **288**(27): p. 20014-33.
265. Wiley, R.D. and S. Gummuluru, *Immature dendritic cell-derived exosomes can mediate HIV-1 trans infection.* Proc Natl Acad Sci U S A, 2006. **103**(3): p. 738-43.
266. Kadiu, I., et al., *Biochemical and biologic characterization of exosomes and microvesicles as facilitators of HIV-1 infection in macrophages.* J Immunol, 2012. **189**(2): p. 744-54.
267. Cantin, R., et al., *Discrimination between exosomes and HIV-1: purification of both vesicles from cell-free supernatants.* J Immunol Methods, 2008. **338**(1-2): p. 21-30.
268. Zi, Y., et al., *Circulating MicroRNA as Potential Source for Neurodegenerative Diseases Biomarkers.* Mol Neurobiol, 2015. **52**(3): p. 1494-503.
269. Lin, S. and R.I. Gregory, *MicroRNA biogenesis pathways in cancer.* Nat Rev Cancer, 2015. **15**(6): p. 321-33.
270. Vrijens, K., V. Bollati, and T.S. Nawrot, *MicroRNAs as potential signatures of environmental exposure or effect: a systematic review.* Environ Health Perspect, 2015. **123**(5): p. 399-411.
271. Jin, X.-F., et al., *Circulating microRNAs: a novel class of potential biomarkers for diagnosing and prognosing central nervous system diseases.* Cellular and molecular neurobiology, 2013. **33**(5): p. 601-613.
272. Iorio, M.V. and C.M. Croce, *MicroRNA dysregulation in cancer: diagnostics, monitoring and therapeutics. A comprehensive review.* EMBO Mol Med, 2012. **4**(3): p. 143-59.

273. Tyagi, M.G., *MicroRNAs in health and disease; a review of its multifaceted roles*. 2016. Vol. 5. 2016.
274. Fowler, L. and N.K. Saksena, *Micro-RNA: new players in HIV-pathogenesis, diagnosis, prognosis and antiviral therapy.* AIDS Rev, 2013. **15**(1): p. 3-14.
275. Wang, X., et al., *Cellular microRNA expression correlates with susceptibility of monocytes/macrophages to HIV-1 infection.* Blood, 2009. **113**(3): p. 671-4.
276. Triboulet, R., et al., *Suppression of microRNA-silencing pathway by HIV-1 during virus replication.* Science, 2007. **315**(5818): p. 1579-82.
277. Houzet, L., et al., *MicroRNA profile changes in human immunodeficiency virus type 1 (HIV-1) seropositive individuals.* Retrovirology, 2008. **5**: p. 118.
278. Hayes, A.M., et al., *Tat RNA silencing suppressor activity contributes to perturbation of lymphocyte miRNA by HIV-1.* Retrovirology, 2011. **8**: p. 36.
279. Chang, J.R., et al., *HIV-1 Tat protein promotes neuronal dysfunction through disruption of microRNAs.* J Biol Chem, 2011. **286**(47): p. 41125-34.
280. Bagashev, A., et al., *Involvement of miR-196a in HIV-associated neurocognitive disorders.* Apoptosis, 2014. **19**(8): p. 1202-14.
281. Houzet, L., et al., *MicroRNA profile changes in human immunodeficiency virus type 1 (HIV-1) seropositive individuals.* Retrovirology, 2008. **5**(1): p. 118.
282. Munshi, S.U., et al., *MicroRNA-150 is a potential biomarker of HIV/AIDS disease progression and therapy.* PLoS One, 2014. **9**(5): p. e95920.
283. Witwer, K.W., et al., *Relationships of PBMC microRNA expression, plasma viral load, and CD4+ T-cell count in HIV-1-infected elite suppressors and viremic patients.* Retrovirology, 2012. **9**(5): p. 1-15.
284. Swaminathan, S., et al., *Differential regulation of the Let-7 family of microRNAs in CD4+ T cells alters IL-10 expression.* The Journal of Immunology, 2012. **188**(12): p. 6238-6246.
285. Duskova, K., et al., *MicroRNA regulation and its effects on cellular transcriptome in human immunodeficiency virus-1 (HIV-1) infected individuals with distinct viral load and CD4 cell counts.* BMC infectious diseases, 2013. **13**(1): p. 250.
286. Bennasser, Y. and K.-T. Jeang, *HIV-1 Tat interaction with Dicer: requirement for RNA.* Retrovirology, 2006. **3**(1): p. 95.
287. Hayes, A.M., et al., *Tat RNA silencing suppressor activity contributes to perturbation of lymphocyte miRNA by HIV-1.* Retrovirology, 2011. **8**(1): p. 36.
288. Coley, W., et al., *Absence of DICER in monocytes and its regulation by HIV-1.* Journal of Biological Chemistry, 2010. **285**(42): p. 31930-31943.
289. Zhou, L., et al., *A parallel genome-wide mRNA and microRNA profiling of the frontal cortex of HIV patients with and without HIV-associated dementia shows the role of axon guidance and downstream pathways in HIV-mediated neurodegeneration.* BMC Genomics, 2012. **13**: p. 677.
290. Noorbakhsh, F., et al., *MicroRNA profiling reveals new aspects of HIV neurodegeneration: caspase-6 regulates astrocyte survival.* The FASEB Journal, 2010. **24**(6): p. 1799-1812.
291. Kadri, F., et al., *Defining Plasma MicroRNAs Associated With Cognitive Impairment in Hiv - Infected Patients.* Journal of cellular physiology, 2015.

292. Pacifici, M., et al., *Cerebrospinal fluid miRNA profile in HIV - encephalitis.* Journal of cellular physiology, 2013. **228**(5): p. 1070-1075.
293. Berezikov, E., et al., *Diversity of microRNAs in human and chimpanzee brain.* Nat Genet, 2006. **38**(12): p. 1375-7.
294. Krichevsky, A.M., et al., *A microRNA array reveals extensive regulation of microRNAs during brain development.* RNA, 2003. **9**(10): p. 1274-81.
295. Le, M.T., et al., *MicroRNA-125b promotes neuronal differentiation in human cells by repressing multiple targets.* Mol Cell Biol, 2009. **29**(19): p. 5290-305.
296. Johnston, R.J. and O. Hobert, *A microRNA controlling left/right neuronal asymmetry in Caenorhabditis elegans.* Nature, 2003. **426**(6968): p. 845-9.
297. Schratt, G.M., et al., *A brain-specific microRNA regulates dendritic spine development.* Nature, 2006. **439**(7074): p. 283-9.
298. Yu, J.Y., et al., *MicroRNA miR-124 regulates neurite outgrowth during neuronal differentiation.* Exp Cell Res, 2008. **314**(14): p. 2618-33.
299. Bagashev, A. and B.E. Sawaya, *Roles and functions of HIV-1 Tat protein in the CNS: an overview.* Virol J, 2013. **10**: p. 358.
300. Kadri, F., et al., *Defining Plasma MicroRNAs Associated With Cognitive Impairment in Hiv-Infected Patients.* J Cell Physiol, 2015.
301. Noorbakhsh, F., et al., *MicroRNA profiling reveals new aspects of HIV neurodegeneration: caspase-6 regulates astrocyte survival.* FASEB J, 2010. **24**(6): p. 1799-812.
302. Hernandez-Rapp, J., et al., *Memory formation and retention are affected in adult miR-132/212 knockout mice.* Behavioural brain research, 2015. **287**: p. 15-26.
303. Smith, P.Y., et al., *miR-132/212 deficiency impairs tau metabolism and promotes pathological aggregation in vivo.* Human Molecular Genetics, 2015: p. ddv377.
304. Chiang, K., H. Liu, and A.P. Rice, *miR-132 enhances HIV-1 replication.* Virology, 2013. **438**(1): p. 1-4.
305. Guy, J., et al., *The role of MeCP2 in the brain.* Annu Rev Cell Dev Biol, 2011. **27**: p. 631-52.
306. Robinson, L., et al., *Morphological and functional reversal of phenotypes in a mouse model of Rett syndrome.* Brain, 2012. **135**(Pt 9): p. 2699-710.
307. Jugloff, D.G., et al., *Increased dendritic complexity and axonal length in cultured mouse cortical neurons overexpressing methyl-CpG-binding protein MeCP2.* Neurobiol Dis, 2005. **19**(1-2): p. 18-27.
308. Desplats, P., et al., *Molecular and pathologic insights from latent HIV-1 infection in the human brain.* Neurology, 2013. **80**(15): p. 1415-23.
309. Jin, X., et al., *Brain-derived neurotrophic factor mediates activity-dependent dendritic growth in nonpyramidal neocortical interneurons in developing organotypic cultures.* J Neurosci, 2003. **23**(13): p. 5662-73.
310. Gorski, J.A., et al., *Brain-derived neurotrophic factor is required for the maintenance of cortical dendrites.* J Neurosci, 2003. **23**(17): p. 6856-65.
311. McDole, B., et al., *BDNF over-expression increases olfactory bulb granule cell dendritic spine density in vivo.* Neuroscience, 2015. **304**: p. 146-160.

312. Bamji, S.X., et al., *BDNF mobilizes synaptic vesicles and enhances synapse formation by disrupting cadherin-beta-catenin interactions.* J Cell Biol, 2006. **174**(2): p. 289-99.
313. Park, S.W., et al., *p11 mediates the BDNF-protective effects in dendritic outgrowth and spine formation in B27-deprived primary hippocampal cells.* J Affect Disord, 2016. **196**: p. 1-10.
314. Albrecht, D., et al., *Trophic factors in cerebrospinal fluid and spinal cord of patients with tropical spastic paraparesis, HIV, and Creutzfeldt-Jakob disease.* AIDS Res Hum Retroviruses, 2006. **22**(3): p. 248-54.
315. Fields, J., et al., *Role of neurotrophic factor alterations in the neurodegenerative process in HIV associated neurocognitive disorders.* J Neuroimmune Pharmacol, 2014. **9**(2): p. 102-16.
316. Su, M., et al., *MeCP2 controls hippocampal brain-derived neurotrophic factor expression via homeostatic interactions with microRNA-132 in rats with depression.* Molecular medicine reports, 2015. **12**(4): p. 5399-5406.
317. Klein, M.E., et al., *Homeostatic regulation of MeCP2 expression by a CREB-induced microRNA.* Nat Neurosci, 2007. **10**(12): p. 1513-4.
318. Impey, S., et al., *Defining the CREB regulon: a genome-wide analysis of transcription factor regulatory regions.* Cell, 2004. **119**(7): p. 1041-54.
319. Yi, L.-T., et al., *BDNF–ERK–CREB signalling mediates the role of miR-132 in the regulation of the effects of oleanolic acid in male mice.* Journal of psychiatry & neuroscience: JPN, 2014. **39**(5): p. 348.
320. Pathania, M., et al., *miR-132 enhances dendritic morphogenesis, spine density, synaptic integration, and survival of newborn olfactory bulb neurons.* PloS one, 2012. **7**(5): p. e38174.
321. Nakazawa, T., et al., *Regulation of dendritic spine morphology by an NMDA receptor-associated Rho GTPase-activating protein, p250GAP.* J Neurochem, 2008. **105**(4): p. 1384-93.
322. Gee, K., et al., *IL-10 regulation by HIV-Tat in primary human monocytic cells: involvement of calmodulin/calmodulin-dependent protein kinase-activated p38 MAPK and Sp-1 and CREB-1 transcription factors.* J Immunol, 2007. **178**(2): p. 798-807.
323. Zhong, Y., et al., *HIV-1 Tat triggers nuclear localization of ZO-1 via Rho signaling and cAMP response element-binding protein activation.* J Neurosci, 2012. **32**(1): p. 143-50.
324. Gibellini, D., et al., *Extracellular HIV-1 Tat protein induces the rapid Ser133 phosphorylation and activation of CREB transcription factor in both Jurkat lymphoblastoid T cells and primary peripheral blood mononuclear cells.* The Journal of Immunology, 1998. **160**(8): p. 3891-3898.
325. Zauli, G., et al., *HIV-1 Tat protein down-regulates CREB transcription factor expression in PC12 neuronal cells through a phosphatidylinositol 3-kinase/AKT/cyclic nucleoside phosphodiesterase pathway.* FASEB J, 2001. **15**(2): p. 483-91.
326. Cardinaux, J.R., et al., *Recruitment of CREB binding protein is sufficient for CREB-mediated gene activation.* Mol Cell Biol, 2000. **20**(5): p. 1546-52.

327. Wong, K., et al., *HIV-1 Tat interactions with p300 and PCAF transcriptional coactivators inhibit histone acetylation and neurotrophin signaling through CREB.* J Biol Chem, 2005. **280**(10): p. 9390-9.
328. Wu, R.F., et al., *HIV-1 Tat activates dual Nox pathways leading to independent activation of ERK and JNK MAP kinases.* J Biol Chem, 2007. **282**(52): p. 37412-9.
329. Marzio, G., et al., *HIV-1 tat transactivator recruits p300 and CREB-binding protein histone acetyltransferases to the viral promoter.* Proceedings of the National Academy of Sciences, 1998. **95**(23): p. 13519-13524.
330. Hatziioannou, T. and D.T. Evans, *Animal models for HIV/AIDS research.* Nat Rev Microbiol, 2012. **10**(12): p. 852-67.
331. Gorantla, S., L. Poluektova, and H.E. Gendelman, *Rodent models for HIV-associated neurocognitive disorders.* Trends Neurosci, 2012. **35**(3): p. 197-208.
332. Zou, W., et al., *Protection against human immunodeficiency virus type 1 Tat neurotoxicity by Ginkgo biloba extract EGb 761 involving glial fibrillary acidic protein.* Am J Pathol, 2007. **171**(6): p. 1923-35.
333. Fan, Y.T., A., He, J.J., *STAT3 and its phosphorylation are involved in HIV-1 Tat-induced transactivation of glial fibrillary acidic protein.* Current HIV Research, 2015. **In Press**.
334. Zhou, B.Y. and J.J. He, *Proliferation inhibition of astrocytes, neurons, and non-glial cells by intracellularly expressed human immunodeficiency virus type 1 (HIV-1) Tat protein.* Neurosci Lett, 2004. **359**(3): p. 155-8.
335. Kim, B.O., et al., *Induction of C chemokine XCL1 (lymphotactin/single C motif-1 alpha/activation-induced, T cell-derived and chemokine-related cytokine) expression by HIV-1 Tat protein.* J Immunol, 2004. **172**(3): p. 1888-95.
336. Giunta, B., et al., *HIV-1 Tat contributes to Alzheimer's disease-like pathology in PSAPP mice.* Int J Clin Exp Pathol, 2009. **2**(5): p. 433-43.
337. Fields, J., et al., *HIV-1 Tat alters neuronal autophagy by modulating autophagosome fusion to the lysosome: implications for HIV-associated neurocognitive disorders.* J Neurosci, 2015. **35**(5): p. 1921-38.
338. Paris, J.J., et al., *Anxiety-like behavior of mice produced by conditional central expression of the HIV-1 regulatory protein, Tat.* Psychopharmacology (Berl), 2014. **231**(11): p. 2349-60.
339. Paris, J.J., J. Fenwick, and J.P. McLaughlin, *Progesterone protects normative anxiety-like responding among ovariectomized female mice that conditionally express the HIV-1 regulatory protein, Tat, in the CNS.* Horm Behav, 2014. **65**(5): p. 445-53.
340. Paris, J.J., et al., *Effects of conditional central expression of HIV-1 tat protein to potentiate cocaine-mediated psychostimulation and reward among male mice.* Neuropsychopharmacology, 2014. **39**(2): p. 380-8.
341. Cooper, D.A., *Life and death in the cART era.* Lancet, 2008. **372**(9635): p. 266-7.
342. Van Vaerenbergh, K., *Study of the impact of HIV genotypic drug resistance testing on therapy efficacy.* Verh K Acad Geneeskd Belg, 2001. **63**(5): p. 447-73.

343. Chun, T.W., et al., *HIV-infected individuals receiving effective antiviral therapy for extended periods of time continually replenish their viral reservoir.* J Clin Invest, 2005. **115**(11): p. 3250-5.
344. Cummins, N.W. and A.D. Badley, *Mechanisms of HIV-associated lymphocyte apoptosis: 2010.* Cell Death Dis, 2010. **1**: p. e99.
345. Wong, J.K., et al., *Recovery of replication-competent HIV despite prolonged suppression of plasma viremia.* Science, 1997. **278**(5341): p. 1291-5.
346. Bertrand, S.J., et al., *Synaptodendritic recovery following HIV Tat exposure: neurorestoration by phytoestrogens.* J Neurochem, 2014. **128**(1): p. 140-51.
347. Fruhbeis, C., D. Frohlich, and E.M. Kramer-Albers, *Emerging roles of exosomes in neuron-glia communication.* Front Physiol, 2012. **3**: p. 119.
348. Chesebro, B., et al., *Macrophage-tropic human immunodeficiency virus isolates from different patients exhibit unusual V3 envelope sequence homogeneity in comparison with T-cell-tropic isolates: definition of critical amino acids involved in cell tropism.* J Virol, 1992. **66**(11): p. 6547-54.
349. Harada, S., Y. Koyanagi, and N. Yamamoto, *Infection of HTLV-III/LAV in HTLV-I-carrying cells MT-2 and MT-4 and application in a plaque assay.* Science, 1985. **229**(4713): p. 563-6.
350. Wei, X., et al., *Emergence of resistant human immunodeficiency virus type 1 in patients receiving fusion inhibitor (T-20) monotherapy.* Antimicrob Agents Chemother, 2002. **46**(6): p. 1896-905.
351. Schwartz, L., et al., *Evidence of human immunodeficiency virus type 1 infection of nestin-positive neural progenitors in archival pediatric brain tissue.* J Neurovirol, 2007. **13**(3): p. 274-83.
352. Ipas, H., A. Guttin, and J.P. Issartel, *Exosomal MicroRNAs in Tumoral U87 MG Versus Normal Astrocyte Cells.* Microrna, 2015. **4**(2): p. 131-45.
353. Takeuchi, Y., M.O. McClure, and M. Pizzato, *Identification of gammaretroviruses constitutively released from cell lines used for human immunodeficiency virus research.* J Virol, 2008. **82**(24): p. 12585-8.
354. Spiegel, S., *Cautionary note on the use of the B subunit of cholera toxin as a ganglioside GM1 probe: detection of cholera toxin A subunit in B subunit preparations by a sensitive adenylate cyclase assay.* J Cell Biochem, 1990. **42**(3): p. 143-52.
355. Subra, C., *Dendritic Cells Pulsed with HIV-1 Release Exosomes that Promote Apoptosis in Cd4+ T Lymphocytes.* Journal of Clinical & Cellular Immunology, 2013. **04**(01): p. 2.
356. Van Deun, J., et al., *The impact of disparate isolation methods for extracellular vesicles on downstream RNA profiling.* J Extracell Vesicles, 2014. **3**.
357. Luo, X., et al., *Exosomes are unlikely involved in intercellular Nef transfer.* PLoS One, 2015. **10**(4): p. e0124436.
358. Singh, I.N., et al., *Differential involvement of p38 and JNK MAP kinases in HIV-1 Tat and gp120-induced apoptosis and neurite degeneration in striatal neurons.* Neuroscience, 2005. **135**(3): p. 781-90.
359. Hui, L., et al., *Role of endolysosomes in HIV-1 Tat-induced neurotoxicity.* ASN Neuro, 2012. **4**(4): p. 243-52.

360. Roy, S., et al., *A bulge structure in HIV-1 TAR RNA is required for Tat binding and Tat-mediated trans-activation.* Genes Dev, 1990. **4**(8): p. 1365-73.
361. Fraisier, C., et al., *Inhibition of Tat-mediated transactivation and HIV replication with Tat mutant and repressor domain fusion proteins.* Gene Ther, 1998. **5**(7): p. 946-54.
362. Meredith, L.W., et al., *Potent inhibition of HIV-1 replication by a Tat mutant.* PLoS One, 2009. **4**(11): p. e7769.
363. Orsini, M.J. and C.M. Debouck, *Inhibition of human immunodeficiency virus type 1 and type 2 Tat function by transdominant Tat protein localized to both the nucleus and cytoplasm.* J Virol, 1996. **70**(11): p. 8055-63.
364. Vo, N., et al., *A cAMP-response element binding protein-induced microRNA regulates neuronal morphogenesis.* Proc Natl Acad Sci U S A, 2005. **102**(45): p. 16426-31.
365. Gee, K., et al., *Intracellular HIV-Tat expression induces IL-10 synthesis by the CREB-1 transcription factor through Ser133 phosphorylation and its regulation by the ERK1/2 MAPK in human monocytic cells.* J Biol Chem, 2006. **281**(42): p. 31647-58.
366. Gibellini, D., et al., *Extracellular HIV-1 Tat protein induces the rapid Ser133 phosphorylation and activation of CREB transcription factor in both Jurkat lymphoblastoid T cells and primary peripheral blood mononuclear cells.* J Immunol, 1998. **160**(8): p. 3891-8.
367. Marzio, G., et al., *HIV-1 tat transactivator recruits p300 and CREB-binding protein histone acetyltransferases to the viral promoter.* Proc Natl Acad Sci U S A, 1998. **95**(23): p. 13519-24.
368. Krol, J., I. Loedige, and W. Filipowicz, *The widespread regulation of microRNA biogenesis, function and decay.* Nat Rev Genet, 2010. **11**(9): p. 597-610.
369. Wanet, A., et al., *miR-212/132 expression and functions: within and beyond the neuronal compartment.* Nucleic Acids Res, 2012. **40**(11): p. 4742-53.
370. Conaco, C., et al., *Reciprocal actions of REST and a microRNA promote neuronal identity.* Proc Natl Acad Sci U S A, 2006. **103**(7): p. 2422-7.
371. Remenyi, J., et al., *Regulation of the miR-212/132 locus by MSK1 and CREB in response to neurotrophins.* Biochem J, 2010. **428**(2): p. 281-91.
372. Zhou, B.Y., et al., *Astrocyte activation and dysfunction and neuron death by HIV-1 Tat expression in astrocytes.* Molecular and Cellular Neuroscience, 2004. **27**(3): p. 296-305.
373. Conant, K., et al., *Induction of monocyte chemoattractant protein-1 in HIV-1 Tat-stimulated astrocytes and elevation in AIDS dementia.* Proceedings of the National Academy of Sciences, 1998. **95**(6): p. 3117-3121.
374. El - Hage, N., et al., *Synergistic increases in intracellular Ca2+, and the release of MCP - 1, RANTES, and IL - 6 by astrocytes treated with opiates and HIV - 1 Tat.* Glia, 2005. **50**(2): p. 91-106.
375. Chen, P., et al., *The Tat Protein of HIV-1 Induces Tumor Necrosis Factor-α Production IMPLICATIONS FOR HIV-1-ASSOCIATED NEUROLOGICAL DISEASES.* Journal of Biological Chemistry, 1997. **272**(36): p. 22385-22388.

376. Rahimian, P. and J.J. He, *Exosome-associated release, uptake, and neurotoxicity of HIV-1 Tat protein.* J Neurovirol, 2016.
377. Lewis, S., *Glia: Transporting cargo from A to B.* Nat Rev Neurosci, 2013. **14**(9): p. 589.
378. Boon, R.A. and K.C. Vickers, *Intercellular transport of microRNAs.* Arterioscler Thromb Vasc Biol, 2013. **33**(2): p. 186-92.
379. Blázquez, C., et al., *The AMP-activated protein kinase prevents ceramide synthesis de novo and apoptosis in astrocytes.* FEBS letters, 2001. **489**(2): p. 149-153.
380. Wang, G., et al., *Astrocytes secrete exosomes enriched with proapoptotic ceramide and prostate apoptosis response 4 (PAR-4): potential mechanism of apoptosis induction in Alzheimer disease (AD).* J Biol Chem, 2012. **287**(25): p. 21384-95.
381. Rayne, F., et al., *HIV-1 Tat is unconventionally secreted through the plasma membrane.* Cell Biol Int, 2010. **34**(4): p. 409-13.
382. Akabori, K., et al., *HIV-1 Tat membrane interactions probed using X-ray and neutron scattering, CD spectroscopy and MD simulations.* Biochim Biophys Acta, 2014. **1838**(12): p. 3078-87.
383. Xie, X., et al., *The basic domain of HIV-tat transactivating protein is essential for its targeting to lipid rafts and regulating fibroblast growth factor-2 signaling in podocytes isolated from children with HIV-1-associated nephropathy.* J Am Soc Nephrol, 2014. **25**(8): p. 1800-13.
384. Futaki, S., et al., *Arginine-rich peptides An abundant source of membrane-permeable peptides having potential as carriers for intracellular protein delivery.* Journal of Biological Chemistry, 2001. **276**(8): p. 5836-5840.
385. Tyagi, M., et al., *Internalization of HIV-1 tat requires cell surface heparan sulfate proteoglycans.* Journal of Biological Chemistry, 2001. **276**(5): p. 3254-3261.
386. Rusnati, M., et al., *The basic domain in HIV-1 Tat protein as a target for polysulfonated heparin-mimicking extracellular Tat antagonists.* J Biol Chem, 1998. **273**(26): p. 16027-37.
387. Li, M., et al., *Quantitative proteomic analysis of exosomes from HIV-1-infected lymphocytic cells.* Proteomics, 2012. **12**(13): p. 2203-11.
388. Santos, S., et al., *Virus-producing cells determine the host protein profiles of HIV-1 virion cores.* Retrovirology, 2012. **9**: p. 65.
389. Saphire, A.C., P.A. Gallay, and S.J. Bark, *Proteomic analysis of human immunodeficiency virus using liquid chromatography/tandem mass spectrometry effectively distinguishes specific incorporated host proteins.* J Proteome Res, 2006. **5**(3): p. 530-8.
390. Li, M., *Proteomics in the investigation of HIV-1 interactions with host proteins.* Proteomics Clin Appl, 2015. **9**(1-2): p. 221-34.
391. Donnelly, M.R. and P. Ciborowski, *Proteomics, biomarkers, and HIV-1: A current perspective.* Proteomics Clin Appl, 2016. **10**(2): p. 110-25.
392. Chertova, E., et al., *Proteomic and biochemical analysis of purified human immunodeficiency virus type 1 produced from infected monocyte-derived macrophages.* J Virol, 2006. **80**(18): p. 9039-52.

393. Tomlinson, A.J. and R.M. Chicz, *Microcapillary liquid chromatography/tandem mass spectrometry using alkaline pH mobile phases and positive ion detection.* Rapid Commun Mass Spectrom, 2003. **17**(9): p. 909-16.
394. Ott, D.E., *Cellular proteins detected in HIV-1.* Rev Med Virol, 2008. **18**(3): p. 159-75.
395. Rayne, F., et al., *Phosphatidylinositol-(4,5)-bisphosphate enables efficient secretion of HIV-1 Tat by infected T-cells.* EMBO J, 2010. **29**(8): p. 1348-62.
396. Everall, I.P., et al., *Cortical synaptic density is reduced in mild to moderate human immunodeficiency virus neurocognitive disorder. HNRC Group. HIV Neurobehavioral Research Center.* Brain Pathol, 1999. **9**(2): p. 209-17.
397. Barco, A. and H. Marie, *Genetic approaches to investigate the role of CREB in neuronal plasticity and memory.* Mol Neurobiol, 2011. **44**(3): p. 330-49.
398. Murray, P.D., T.J. Kingsbury, and B.K. Krueger, *Failure of Ca2+-activated, CREB-dependent transcription in astrocytes.* Glia, 2009. **57**(8): p. 828-34.
399. Dugan, L.L., et al., *Differential effects of cAMP in neurons and astrocytes. Role of B-raf.* J Biol Chem, 1999. **274**(36): p. 25842-8.
400. Numakawa, T., et al., *Growth factors stimulate expression of neuronal and glial miR-132.* Neurosci Lett, 2011. **505**(3): p. 242-7.
401. Nudelman, A.S., et al., *Neuronal activity rapidly induces transcription of the CREB - regulated microRNA - 132, in vivo.* Hippocampus, 2010. **20**(4): p. 492-498.
402. Nakazawa, T., et al., *p250GAP, a novel brain-enriched GTPase-activating protein for Rho family GTPases, is involved in the N-methyl-d-aspartate receptor signaling.* Mol Biol Cell, 2003. **14**(7): p. 2921-34.
403. Edbauer, D., et al., *Regulation of synaptic structure and function by FMRP-associated microRNAs miR-125b and miR-132.* Neuron, 2010. **65**(3): p. 373-84.
404. Armstrong, D.D., K. Deguchi, and B. Antallfy, *Survey of MeCP2 in the Rett syndrome and the non-Rett syndrome brain.* J Child Neurol, 2003. **18**(10): p. 683-7.
405. !!! INVALID CITATION !!! .
406. Amir, R.E., et al., *Rett syndrome is caused by mutations in X-linked MECP2, encoding methyl-CpG-binding protein 2.* Nat Genet, 1999. **23**(2): p. 185-8.
407. Kaufmann, W.E., S. Naidu, and S. Budden, *Abnormal expression of microtubule-associated protein 2 (MAP-2) in neocortex in Rett syndrome.* Neuropediatrics, 1995. **26**(2): p. 109-13.
408. Shahbazian, M.D., et al., *Insight into Rett syndrome: MeCP2 levels display tissue- and cell-specific differences and correlate with neuronal maturation.* Hum Mol Genet, 2002. **11**(2): p. 115-24.
409. Korkotian, E. and M. Segal, *Regulation of dendritic spine motility in cultured hippocampal neurons.* J Neurosci, 2001. **21**(16): p. 6115-24.
410. Luikart, B.W., et al., *miR-132 mediates the integration of newborn neurons into the adult dentate gyrus.* PloS one, 2011. **6**(5): p. e19077-e19077.
411. Dube, B., et al., *Neuropsychiatric manifestations of HIV infection and AIDS.* J Psychiatry Neurosci, 2005. **30**(4): p. 237-46.

412. Durvasula, R.S., et al., *Predictors of neuropsychological performance in HIV positive women.* J Clin Exp Neuropsychol, 2001. **23**(2): p. 149-63.
413. Valcour, V.G., et al., *Cognitive impairment in older HIV-1-seropositive individuals: prevalence and potential mechanisms.* Aids, 2004. **18 Suppl 1**: p. S79-86.
414. Epstein, L.G., et al., *Neurologic Manifestations of human immunodeficiency virus infection in children.* Pediatrics, 1986. **78**: p. 678-687.
415. Gabuzda, D.H., et al., *Immunohistochemical identification of HTLV-III antigen in brains of patients with AIDS.* Ann Neurol, 1986. **20**(3): p. 289-95.
416. Ellis, R.J., et al., *Neurocognitive impairment is an independent risk factor for death in HIV infection. San Diego HIV Neurobehavioral Research Center Group.* Arch Neurol, 1997. **54**(4): p. 416-24.
417. Iosif, R.E., et al., *Tumor necrosis factor receptor 1 is a negative regulator of progenitor proliferation in adult hippocampal neurogenesis.* J Neurosci, 2006. **26**(38): p. 9703-12.
418. Lee, J., W. Duan, and M.P. Mattson, *Evidence that brain-derived neurotrophic factor is required for basal neurogenesis and mediates, in part, the enhancement of neurogenesis by dietary restriction in the hippocampus of adult mice.* J Neurochem, 2002. **82**(6): p. 1367-75.
419. Sairanen, M., et al., *Brain-derived neurotrophic factor and antidepressant drugs have different but coordinated effects on neuronal turnover, proliferation, and survival in the adult dentate gyrus.* J Neurosci, 2005. **25**(5): p. 1089-94.
420. Yoshimura, S., et al., *FGF-2 regulation of neurogenesis in adult hippocampus after brain injury.* Proc Natl Acad Sci U S A, 2001. **98**(10): p. 5874-9.
421. Yoshimura, S., et al., *FGF-2 regulates neurogenesis and degeneration in the dentate gyrus after traumatic brain injury in mice.* J Clin Invest, 2003. **112**(8): p. 1202-10.
422. Peng, H., et al., *HIV-1-infected and/or immune-activated macrophage-secreted TNF-alpha affects human fetal cortical neural progenitor cell proliferation and differentiation.* Glia, 2008. **56**(8): p. 903-16.
423. Lu, S.-M., et al., *HIV-1 Tat-induced microgliosis and synaptic damage via interactions between peripheral and central myeloid cells.* PloS one, 2011. **6**(9): p. e23915.
424. Schorey, J.S., et al., *Exosomes and other extracellular vesicles in host-pathogen interactions.* EMBO Rep, 2015. **16**(1): p. 24-43.
425. Nudelman, A.S., et al., *Neuronal activity rapidly induces transcription of the CREB-regulated microRNA-132, in vivo.* Hippocampus, 2010. **20**(4): p. 492-8.
426. Colovic, M.B., et al., *Acetylcholinesterase inhibitors: pharmacology and toxicology.* Curr Neuropharmacol, 2013. **11**(3): p. 315-35.
427. Huang, W., et al., *PPARalpha and PPARgamma protect against HIV-1-induced MMP-9 overexpression via caveolae-associated ERK and Akt signaling.* FASEB J, 2011. **25**(11): p. 3979-88.
428. Jasinska, M., et al., *miR-132 Regulates Dendritic Spine Structure by Direct Targeting of Matrix Metalloproteinase 9 mRNA.* Mol Neurobiol, 2015.

429. Murray, P.S. and P.V. Holmes, *An overview of brain-derived neurotrophic factor and implications for excitotoxic vulnerability in the hippocampus.* Int J Pept, 2011. **2011**: p. 654085.
430. Sun, Y.E. and H. Wu, *The ups and downs of BDNF in Rett syndrome.* Neuron, 2006. **49**(3): p. 321-3.
431. Avdoshina, V., et al., *HIV-1 decreases the levels of neurotrophins in human lymphocytes.* AIDS, 2011. **25**(8): p. 1126-8.
432. Son, S.M., et al., *Statins induce insulin-degrading enzyme secretion from astrocytes via an autophagy-based unconventional secretory pathway.* Mol Neurodegener, 2015. **10**: p. 56.
433. Baixauli, F., C. Lopez-Otin, and M. Mittelbrunn, *Exosomes and autophagy: coordinated mechanisms for the maintenance of cellular fitness.* Front Immunol, 2014. **5**: p. 403.
434. Giampa, C., et al., *Systemic delivery of recombinant brain derived neurotrophic factor (BDNF) in the R6/2 mouse model of Huntington's disease.* PLoS One, 2013. **8**(5): p. e64037.
435. Benraiss, A. and S.A. Goldman, *Cellular therapy and induced neuronal replacement for Huntington's disease.* Neurotherapeutics, 2011. **8**(4): p. 577-90.
436. Khalin, I., et al., *Brain-derived neurotrophic factor delivered to the brain using poly (lactide-co-glycolide) nanoparticles improves neurological and cognitive outcome in mice with traumatic brain injury.* Drug Deliv, 2016: p. 1-9.

CURRICULUM VITAE

EDUCATION:

Aug. 2011- Aug 2016

Graduate Research Assistant, UNT Health Science Center Fort Worth TX
Neurobiology of aging fellow (NIH T32 training grant, UNTHSC department of pharmacology and neuroscience's Institute for healthy aging)
Successfully defended doctoral dissertation with distinction on June 15, 2016

Aug 2005- Dec 2006

University of Texas Southwestern Medical Center, Dallas Texas
Post Baccalaureate certificate in Medical Technology

Aug 2000- June 2004

Azad University of Tehran North Branch, Tehran Iran.
Bachelor of Science in Microbiology

EMPLOYMENT:

2010-2016

MedFusion Clin-Labs Clin-Trials, Lewisville TX

Medical Technologist, Infectious diseases department

2006-2011

ProPath Services, Dallas TX

Medical Technologist, Molecular Pathology department

2009-2010

Baylor University Medical Center, Dallas TX

Medical Technologist, Microbiology and Virology departments

2006-2009

St. Paul Hospital, Dallas TX

Medical Technologist, Microbiology department

AWARDS:

- NIH T32 training grant in Neurobiology of Aging, Apr 2015-Apr 2016, UNTHSC
- GSBS Student affairs Scholarship, July 2015, UNTHSC
- Research Achievement Award, Cell Biology and Immunology department, Apr 2016, UNTHSC
- Robert J. Wordinger's Excellence in Virology Research, Apr 2016, UNTHSC
- GSBS Travel Award, Apr 2016, UNTHSC
- GSA Travel Award, May 2016, UNTHSC

PUBLICATIONS:

Rahimian, Pejman, and Johnny J. He. "Exosome-associated release, uptake, and neurotoxicity of HIV-1 Tat protein." Journal of NeuroVirology (2016): 1-15.

Rahimian, Pejman, and Johnny J. He. "HIV/neuroAIDS biomarkers." Progress in Neurobiology (2016).

Rahimian Pejman, and Johnny J. He. "HIV-1 Tat shortened neurite outgrowth through regulation of miR-132 and its target gene expression." Submitted to Journal of Neuroinflammation